



UNIVERSITÀ
DEGLI STUDI
DI PADOVA

Sede Amministrativa: Università degli Studi di Padova

Dipartimento di Scienze Chimiche

SCUOLA DI DOTTORATO DI RICERCA IN : Studio e Conservazione dei Beni Archeologici e Architettonici

INDIRIZZO: Scienze e Tecnologie per i Beni Archeologici e Architettonici

CICLO XXV

Dosimetric dating techniques applied to desert prehistoric pottery

Direttore della Scuola : Ch.mo Prof. Giovanni Leonardi

Coordinatore d'indirizzo: Ch.mo Prof. Giuseppe Salemi

Supervisore: Ch.mo Prof. Renzo Bertoncetto

Co-supervisore: Ch.ma Prof.sa Marina Brustolon

Dottorando: Claudia Bortolussi

Dosimetric dating techniques applied to desert prehistoric pottery

Claudia Bortolussi

Ph.D. Thesis – University of Padova

Printed in Padova – January 2013

Contents

Summary (English)	1
Summary (Italiano)	2
Introduction	5
1 Overview of The Radiation Effect Dating Techniques	11
1.1 Radiation effect dating	13
1.1.1 Radioactive decay: the physical basis for dating	13
1.1.2 Radioactivity and dating of archaeological findings . .	18
2 Luminescence and EPR Dating	21
2.1 Defects	22
2.1.1 Lifetime of defects	24
2.2 Age equation	25
2.3 Precision and accuracy	27
2.4 Assumptions	28
2.5 Quartz	29
2.5.1 TL emission spectra	30
2.5.2 OSL emission spectra	32
2.5.3 EPR spectra	33
3 Methods in Luminescence and EPR dating	37
3.1 Equivalent dose determination methods	37
3.1.1 Multiple Aliquot Additive Dose (MAAD)	37
3.1.2 Single Aliquot Regenerative Dose Protocol (SAR) . . .	38
3.2 Thermoluminescence (TL)	40
3.2.1 Fine grain and Quartz inclusion techniques	40
3.3 Optically Stimulated Luminescence (OSL)	41

3.3.1	Principles of OSL dating	41
3.3.2	OSL of heated materials	42
3.4	Electron Paramagnetic Resonance (EPR)	43
3.4.1	EPR dating	43
3.4.2	Principles of EPR	44
3.4.3	CWEPR and Echo Detected EPR	45
3.5	Annual dose	48
3.5.1	Effect of moisture	49
3.5.2	Radioisotopes contribution	49
4	Pottery in archaeology	51
4.1	The role of pottery in archaeology	51
4.2	Origin of pottery	53
4.3	Dating pottery	55
5	The <i>El Salha Archaeological Project: rescue excavation in central Sudan</i>	59
5.1	Actual environment and palaeoenvironment along the White Nile	62
5.1.1	El Salha	64
5.2	The excavation at site 16-D-5, Al Khiday 1	65
5.2.1	Pottery assemblages at 16-D-5	66
6	Materials and Methods	69
6.1	Description of the samples	69
6.2	Annual dose determination	73
6.3	Samples preparation	73
6.3.1	Fine grain	73
6.3.2	EPR	73
6.3.3	Quartz separation	74
6.4	TL measurements and artificial irradiation	74
6.5	OSL measurements	75
6.6	EPR measurements	76
6.7	XRF analysis	78
7	Results and discussion	79
7.1	Annual doses	79
7.2	TL	79
7.2.1	TL MAAD	79
7.2.2	TL SAR	80
7.3	OSL	83

7.4	Comparison between luminescence ages	85
7.5	Petrographic analysis	88
7.5.1	Optical Microscopy	88
7.5.2	Digital Image Analysis (DIA)	96
7.6	EPR	102
7.6.1	CWEPR	102
7.6.2	Echo Detected EPR	104
7.7	Comparison between EDEPR spectra and petrographic analysis	107
7.8	Quartz extracted from pottery matrix	110
8	Conclusions	115

Summary (English)

Archaeological sites in arid and semi-arid environments have mostly suffered from strong erosion that results in the removal of the anthropic deposits incorporating artifacts produced and discarded by human beings. Artifacts, after this process, accumulate on the surface representing the only witness of human activities. The principal issue for an archaeologist, in this context, is establishing which moment in the past these artifacts had been produced by human beings to be able, afterwards, to try inferring on more general aspects of the economic and social sphere. Thermoluminescence has been used in different occasions in Saharan Africa for dating fragments of pottery found in surface contexts, disturbed ones or where nothing else could be used to apply the more common radiocarbon dating technique. The results have always been highly debated as they usual appeared incongruent and problems inherent to the thermoluminescence technique itself not entirely tackled. It seemed, for this reason, appropriate to resume work on this technique as well as to compare different protocols (Multiple Aliquot Additive Dose, MAAD and Single Aliquot Regenerative dose, SAR) of dating techniques for the measurement of prehistoric pottery coming from a desert environment. These methods are based on the accumulation of charges in the defects present in crystals of some minerals, like quartz, as a consequence of the natural radioactivity. The number of defect centers depends on the time elapsed from the starting moment of the irradiation, thus the radiation dose absorbed by the materials is directly proportional to the age of the potsherd. The techniques of luminescence (TL: Thermoluminescence, OSL: Optically Stimulated Luminescence) and of EPR spectrometry (Electron Paramagnetic Resonance) are methods of dosimetric dating and have been applied in this work with different aims. In the case of luminescence, the goal was to select a protocol in order to obtain the highest precision. In fact, the dating of prehistoric pottery by luminescence is generally affected by a substantial error

if compared to other methods. On the other hand, while the radiocarbon technique is more precise but applicable only to the organic material found together with the potsherd, the luminescence analyzes the intrinsic characteristics of the material. Moreover, the majority of the potsherds found in desert environments undergo erosive processes that irreparably alter the stratigraphy. In these situations where it is not possible to collect information about the relative chronology, the dating by luminescence allows a first chronological framework. For this reason the research work was focused on the optimization of the experimental protocols to reduce the error associated to the results. In the case of EPR spectrometry, the goal was to evaluate its potential as a method for dating recent materials as pottery. EPR spectrometry is in fact widely used in geology and palaeontology, but its application in archaeology is still experimental. An important advantage of EPR is the repeatability of the measurements, because the spectrum acquisition does not reset the signal as occurs in the luminescence procedure. The employ of the pulsed technique (EchoEPR) allowed isolating the signals of the defects induced by the irradiation that are not visible with the traditional method of continuous wave (CWEPR) due to the strong signal of iron present in all potsherds. The study is also supported by a petrographic characterization of the materials, with particular attention for inclusion grain size, a parameter that was demonstrated to be crucial for the dosimetry.

The potsherds analyzed for this project were selected on the basis of their provenance from an undisturbed stratigraphy, as well as for the simple ceramic fabrics. They have a limited typology of inclusions, thus minimizing variables which could negatively influence dosimetric studies. Samples come from the 16D5 site at Al Khiday (Omdurman, central Sudan), excavated by the Italian archaeological mission directed by D. Usai and co-directed by S. Salvatori (Centro Studi Sudanese e Sub-Sahariani and Istituto Italiano per l'Africa e l'Oriente). The site presents a rare case in a semi-desert environment of a preserved stratigraphy. The selected samples come from radiocarbon dated stratigraphic units, whose determinations are a necessary reference for the comparison with the experimental results. Moreover, the high quartz content characterizing these potsherds is a suitable feature for applying dosimetric dating techniques.

The luminescence dating was performed at the Archaeometry Laboratory at the Department of Material Sciences of the University of Milan Bicocca; the study by EPR spectroscopy and the petrographic analysis at the University of Padua, at the Departments of Chemical Sciences and Geosciences respectively.

Summary (Italiano)

I siti archeologici in ambienti aridi e semi-aridi sono soggetti ad una forte erosione che comporta la rimozione dei depositi antropici in cui si trovano i manufatti prodotti e scartati dall'uomo. I reperti si trovano perciò in superficie, privi di stratigrafia, come unica testimonianza dell'attività umana. In questo contesto, la questione principale che un archeologo deve affrontare è stabilire in quale momento del passato tali manufatti siano stati prodotti, per poter poi essere in grado di ricavare informazioni generali legate alla sfera economica e sociale. In diverse occasioni si è ricorsi alla termoluminescenza per la datazione di materiali provenienti dall'Africa sahariana. Si tratta di ceramica rinvenuta in superficie, in contesti disturbati o in assenza di condizioni ideali per l'impiego di altre tecniche, come la più comune datazione al radiocarbonio. I risultati sono sempre stati molto discussi e spesso considerati incongruenti, ma le problematiche relative alla tecnica non sono state affrontate pienamente. Per questo motivo si è considerato di primaria importanza approfondire le tematiche legate a questa tecnica, in particolare con il confronto di diversi protocolli di misura (Multiple Aliquot Additive Dose, MAAD e Single Aliquot Regenerative dose, SAR) con diversi metodi dosimetrici finalizzati alla datazione di ceramica preistorica proveniente da ambiente desertico. Questi metodi si basano sull'accumulo di cariche nei difetti presenti nei cristalli di alcuni minerali (come ad esempio il quarzo) per effetto della radioattività naturale. Il numero dei centri difettivi dipende dal tempo trascorso dall'inizio dell'irraggiamento, perciò la dose di radiazione assorbita dai materiali è direttamente proporzionale all'età del reperto ceramico. Le tecniche di luminescenza (TL: Thermoluminescence, OSL: Optically Stimulated Luminescence) e la spettroscopia EPR (Electron Paramagnetic Resonance) sono metodi di datazione dosimetrica e sono qui impiegati con diversi scopi. Nel caso della luminescenza, si tratta di individuare un protocollo di misura che consenta di ottenere la maggiore precisione possibile.

Infatti, la datazione di materiale ceramico preistorico mediante luminescenza è affetta in genere da un elevato errore rispetto ad altri metodi. Tuttavia, rispetto alla tecnica del radiocarbonio che è più precisa, ma applicabile solo a sostanze organiche trovate in associazione al reperto, analizza caratteristiche intrinseche del materiale. Inoltre, i materiali rinvenuti in ambiente desertico sono nella maggior parte affetti da processi erosivi che disturbano irrimediabilmente la stratigrafia. In tali situazioni di mancanza di caratteri utili alla costruzione di cronologie relative, la datazione con le tecniche di luminescenza fornisce un primo inquadramento cronologico. Per questo motivo il lavoro di ricerca mira all'ottimizzazione dei protocolli sperimentali per ridurre l'errore associato alle datazioni. Nel caso della spettroscopia EPR, invece, l'obiettivo è quello di valutarne le potenzialità applicative per la datazione di un materiale recente come la ceramica. La spettroscopia EPR è utilizzata ampiamente in campo geologico e paleontologico, ma è ancora in fase sperimentale in archeologia. Un vantaggio notevole dell'EPR è la ripetibilità della misura, poichè l'acquisizione dello spettro non comporta la cancellazione del segnale, che invece viene azzerato dalla procedura di datazione con la luminescenza. L'impiego della tecnica impulsata (EchoEPR) ha permesso di isolare i segnali dei difetti indotti da irraggiamento, che con il metodo tradizionale in onda continua (CWEPR) non sono visibili a causa del forte segnale del ferro contenuto in tutte le ceramiche. Lo studio è anche supportato da una caratterizzazione petrografica dei materiali, con particolare attenzione per la granulometria degli inclusi, che si è rivelata un parametro importante per lo studio dosimetrico.

Le ceramiche analizzate in questo progetto sono state selezionate per l'appartenenza ad una serie stratigrafica non disturbata, nonchè per la semplicità degli impasti. Questi infatti hanno un numero molto limitato di tipologie di inclusi, minimizzando eventuali variabili che influiscono negativamente sullo studio dosimetrico. I materiali ceramici provengono dal sito 16D5 di Al Khiday (Omdurman, Sudan centrale), scavato dalla missione archeologica italiana diretta dalla dott.ssa D. Usai e co-diretta dal dott. S. Salvatori (Centro Studi Sudanesi e Sub-Sahariani ed Istituto Italiano per l'Africa e l'Oriente). Il sito rappresenta un raro caso di stratigrafia preservata in ambiente desertico. I materiali qui analizzati provengono da unità stratigrafiche datate al radiocarbonio, le cui età rappresentano un necessario ed assoluto riferimento per il confronto dei risultati sperimentali. Inoltre, l'elevato contenuto in quarzo che caratterizza questi campioni li rende particolarmente adatti per testare le tecniche di datazione dosimetrica.

La datazione con le tecniche di luminescenza è stata realizzata presso il laboratorio di Archeometria del Dipartimento di Scienze dei Materiali dell'Università di Milano Bicocca; lo studio con Risonanza di Spin Elettronico

e la caratterizzazione petrografica presso l'Università di Padova rispettivamente nei dipartimenti di Scienze Chimiche e Geoscienze.

Introduction

The field of archaeological research concerns the knowledge of human past through the study of materials and cultural remains. An archaeological excavation should be generally undertaken after surface field survey and preliminary studies of the area that allow for the selection of the most promising site, being it a settlement, a cemetery or loci intended for specific activities. For the most part, archaeological sites are made by superimposed layers testifying each one a specific moment in time with the lower deposited first and those overlying in closely related chronological relationship. However, either human or natural post-depositional processes can mix or affect the expected sequence of stratigraphy. This is a common situation in the desert, where the traditional archaeological practices not always can be performed. Regions characterized by desert landscape at the present time, underwent strong climatic changes in the past. The archaeological record is now found in a context very different from the one of its formation and environmental events as well as animal and anthropic disturbances influence its survival and the general burial conditions. A good understanding of site formation processes is necessary in order to lay at deliberate or accidental human activities or at natural phenomena each specific archaeological context. The stratification which in general provides a relative chronological sequence is rare in areas affected by strong wind and water erosion and with incoherent sediments as sand. Detailed surface survey and systematic sampling are used to deal with the generally poor preservation of sites due to anthropic or natural disturbances. Sampling enables the evaluation of the archaeological potential of a site but it is difficult to understand the significance of these artefacts without knowing their correlation to human activities and natural events and their chronological setting. Test trenches are usually performed in order to understand chronological trends. The excavation is usually made by test trenches and proceed by recognition of each anthropic deposit and if none is

preserved, by artificial cuts. In highly disturbed contexts, vertical and lateral moving of the materials may be high and resulting in a mix of tools, pottery, bones and in situ findings are not so frequent. Furthermore, the absence of structural remains at prehistoric sites due both to the poor preservation of anthropic deposits and the very light structures usually associated to highly mobile human groups, makes the archaeological investigation more difficult when dealing with hunter-gatherer societies. In prehistoric times there were no written records so materials are the only source of information to document the cultures of the past. For all these reasons, the development of an absolute dating protocol of findings is a viable alternative for the interpretation of materials from unstratified deposit. This is of relevance not only for the Nile Valley archaeology, but for prehistoric archaeology in any part of the world.

Dealing with the terminology used in the present work we have to underlay that cultural labels like Mesolithic and Neolithic apply the first to early Holocene more or less complex societies with a subsistence economy based on hunting, gathering and fishing, the second to middle Holocene food producing communities. This economically based meaning of old cultural labels originally based on a restricted range of material traits like *Mesolithic* and *Neolithic* is nowadays generally accepted.

The attention of the present work is focused on pottery. Traditional methods of creating relative or absolute chronologies are difficult to apply to ceramic found in the desert, in surface sites. The combination of relative and absolute dating would help in the chronological arrangement of potsherds even if found without their original stratigraphic context. New approaches are here proposed based on the application of different protocols of measurements of traditional luminescence dating technique and the evaluation of the Electron Paramagnetic Resonance (EPR) as a possible new dating method for pottery. Thermoluminescence (TL) is almost a standard pottery dating method but its application on prehistoric materials is still affected by large errors in age determination. Optical Stimulated Luminescence (OSL) has its main use in geology but recently it has been extended for studying heated materials. Similarly, the potential of EPR dating is demonstrated for different materials as sediments and teeth, with the development of specific protocols and the field of application has grown to include materials from a few thousand years ago to several million years ago. Compared to luminescence technique, EPR has the big advantage of not erasing the signal during measurements, allowing the use of small fraction of the object that has to be dated. While TL is more reliable for recent materials, EPR is suitable especially for geological chronologies but it is for this reason a fundamental tool for all the situations in which the ages exceed the radiocarbon limit. In the

majority of cases, a cross-calibration is required, as it will be tested in this study. The possibility of trying to date prehistoric desert pottery by means of all these techniques that have in common the same physical bases (radiation induced defects) but different experimental requirements and limits is very challenging.

Overview of The Radiation Effect Dating Techniques

In studying natural and human events, the dating techniques are useful to answer the question “when?”. Physical anthropology, geology and archaeology are some of the fields in which the construction of a chronology of the past events is essential. Dating methods can be divided into two types: relative and absolute. While in the first case it is possible just to establish a relationship between the objects or the events to reconstruct their chronological order/sequence, the absolute dating is able to assign an age. It is important to underline the difference between the terms *age* and *date*. The age is expressed as a number representing the years passed from the moment that has to be dated and the time of the measurements. This expression is suitable only for very ancient events, since the age increases every year and it is inappropriate for recent materials in which more precision is needed. In these cases it is better to use the calendar date, given in years before or after Christ (BC or AD) since it is independent of the time of measurements. An absolute dating technique must be based on a physical or chemical phenomenon with a time dependence constant over the period of interest of the event to be dated. Furthermore, the event and the phenomenon must start at the same time. The radioactivity is a process suitable for dating purposes since the radioisotopes decay has an unchanging rate and it is not affected by external factors as, for example, environmental conditions. The best-known method exploiting radioactivity is radiocarbon (^{14}C), however other dating techniques are based on decay, exploiting its effect on matter [1]. The ionizing radiation arising from the decay process is responsible for the production of free charges in some minerals in which the particular crystal structure allows the trapping of electrons at lattice defects sites. The number of trapped charges (called centers) is proportional to the radiation received by the sam-

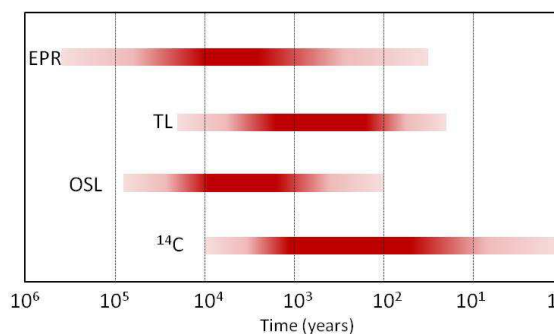


Figure 1.1: Time intervals covered by different absolute dating methods.

ple. Since the decay is time dependent, the quantification of these centers can be linked to the age of the material. Physical techniques able to quantify radiation induced defects could be in principle considered as dating methods. Luminescence methods as Thermoluminescence (TL) and Optically Stimulated Luminescence (OSL) belong to this category as well as Electron Paramagnetic Resonance (EPR) and they form the so called *dosimetric dating techniques*. Although radioactivity is independent from external conditions, its effect on materials is strongly influenced by the environment and by the mineralogical composition of the sample. For example, the humidity is an important parameter to be taken into account because water absorbs part of the radiation and acts as a screen for the sample. Radiation induced defects dating is limited to those materials (natural or artificial) containing minerals as feldspar and quartz in which lattice defects are able to trap free charges for a long time. The events that can be dated are the ones that erase the previous signals accumulated in the sample material. For example, the high temperature reached during the firing of pottery is able to reset the geological signal of raw materials for TL studies, while the end of the light exposure is functional to OSL measurements. The time range covered by the different methods (Figure 1.1) depends on the lifetime of the defects, the saturation of the signals and the sensitivity of the instruments. Not all the archaeological findings, even corresponding to the assumption of radiometric techniques, can be dated. Care must be taken in sampling artifacts, because a considerably high amount of material is required. The mineral composition, the shape and the conservation conditions must be checked before the measurements and it is important to note that dating techniques are destructive methods.

The dating techniques need continual review of both theoretical and laboratory considerations. Physical phenomena involved in the generation of

signals are not yet fully understood and some limitations in dating application still remain unsolved [1].

1.1 Radiation effect dating

Radioactive elements emit alpha and beta particles and gamma rays producing atomic or electronic defects in solids. The radiation interacts with non-conductive solids forming pairs of electrons and positively charged holes. Electrons and holes move throughout the crystal, some of them recombining rapidly, others being trapped at the defect lattice sites, as impurities and vacancies. Electrons can be trapped for millions of years, forming the so called *radiation induced centers*. Dating materials is possible by observing the accumulated centers produced in crystals as a consequence of irradiation. Any physical technique able to detect and quantify radiation induced defect centers can be in principle applied as a dating method. Belong to this category:

- Luminescence dating (TL, OSL)
- Electron Paramagnetic Resonance (EPR).

In general, in EPR and luminescence dating of archaeological materials the aim is to determine the dose to which the sample was exposed over its burial period. The exposure time and thereby the age, are determined by comparing the accumulated dose to the average annual dose rate. Materials suitable for dating purpose are insulators which exhibit trapped charges with a lifetime considerably longer than the time of exposure.

1.1.1 Radioactive decay: the physical basis for dating

The physical phenomena involved in the interaction between radiation and matter are briefly explained in order to understand the principles of radiometric dating. Natural radioactivity is present everywhere at low doses, due to the transformation of unstable nuclei (radioactive isotopes) which emit ionizing radiation. A neutral atom is characterized by the atomic number (Z) and by the mass number (A). Z is the number of protons of the nucleus while A is the sum of protons and neutrons. The notation is: A_zX

Isotopes are nuclides of the same element ($=Z$) with a different number of neutrons ($\neq A$), thus they have the same chemical behavior but different physical properties and nuclear stability. Isotopes can be stable or unstable. In the second case, the isotope decays spontaneously without any external

stimulation into a nuclide of a different element, called radiogenic daughter that may be radioactive itself. If there is a series of radioactive daughters, a decay chain is formed and it ends when a stable isotope is achieved. Radioactivity is a statistical process. It is not possible to predict the moment in which a decay will occur; it is a stochastic process whose quantification requires a sufficient number of nuclides N . The activity of a radionuclide is measured in Becquerel (Bq, s^{-1} : number of decay per time unit) and it is defined as the fraction dN of the initial nuclide number N disintegrating within the time dt :

$$A = \frac{dN}{dt} = -\lambda N \quad (1.1)$$

where λ is the decay constant (the probability that a nucleus decays per time unit). By integration:

$$\frac{N}{N_0} = e^{-\lambda t} \quad (1.2)$$

$$N = N_0 e^{-\lambda t} \quad (1.3)$$

N : number of atoms

N_0 : number of atoms at time zero ($t=0$)

Another constant characterizing the activity is the mean lifetime (τ) which is the lifetime of the radioactive particle (average time in which no decay occurs). It can be demonstrated that: $\tau=1/\lambda$

Often, another quantity is used that is the half life $t_{1/2}$, the time required for half the atoms in a given sample to undergo radioactive decay. Imposing $N(t_{1/2})=N_0/2$:

$$t_{1/2} = \ln 2 \cdot \tau = \frac{\ln 2}{\lambda} \quad (1.4)$$

Three types of decay are possible, alpha, beta and gamma. Alpha particles are helium nuclei, beta rays are electrons and gamma rays are high energy electromagnetic radiation. The production defect efficiency depends, at the same dose, on the nature of the ionizing radiation and on the density of the material. The energy involved is on the order of several MeV (10^6 eV).

In alpha decay an atomic nucleus with atomic number Z and mass A , emits an alpha particle transforming into an atom with mass number $(A-4)$ and atomic number $(Z-2)$ (Figure 1.2).

For example

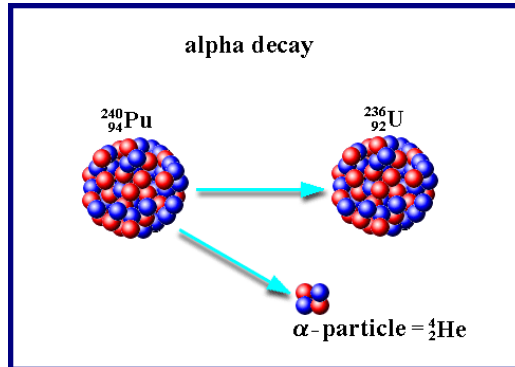
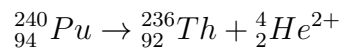


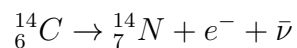
Figure 1.2: Schematic representation of the alpha decay.



Alpha particles have quite a large mass and +2 electric charge. When the alpha particle interacts with matter an orbital electron of the atoms in the material can be raised to a higher shell (excitation) or it can be directly removed from the atom (ionization). The energy necessary for these events is removed from the primary incident particles which thus loses velocity. For one interaction, the alpha particle loses about 1/500 of its energy per nucleon: before being stopped it will undergo several interactions that will result in a continuous energy loss. This kind of interactions does not change significantly the direction of the particles, and the path is quite straight. The heavy damage caused by alpha rays is responsible of the rapid recombination of most of the electrons and holes produced, thus only a small fraction of electrons remains trapped as stable centers.

Beta decay is the emission of an electron (beta minus β^-) or a positron (beta plus β^+) (Figure 1.3).

For example:



Compared with heavy charged particles as alpha particles, electrons lose their energy at a lower rate and following a much more tortuous path inside

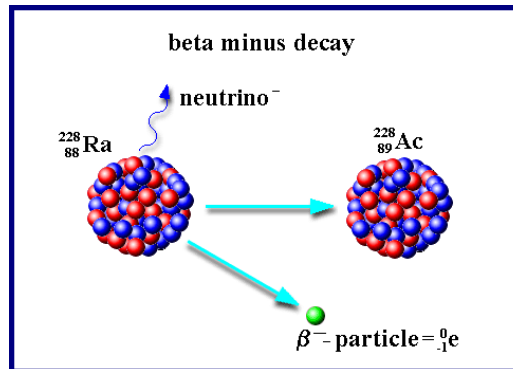


Figure 1.3: Schematic representation of beta decay.

the matter, due to the fact that their mass is equal to the one of the orbital electrons with which interacts and this makes possible also large energy transfer in single events.

Gamma rays are produced by decay of high energy states in atomic nuclei. When a nucleus emits an α or β particle, the daughter nucleus is usually left in an excited state. It can then move to a lower energy state by emitting a gamma ray (Figure 1.4).

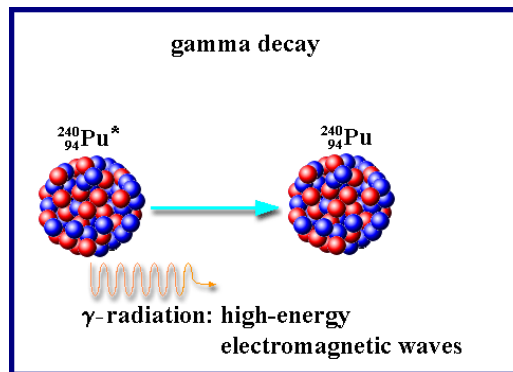
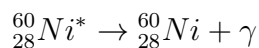


Figure 1.4: Schematic representation of gamma decay.

For example:





The energy loss of gamma radiation in matter leads to the partial or total energy transfer to an electron of the medium, resulting in the total disappearance of the gamma ray or in its scattering with lower energy. At intermediate energies (as for example the ones of the gamma radiation emitted by the radioisotopes) the most probable interaction of the gamma rays in matter is the Compton effect, that is a scattering process between the gamma rays and the electrons present in the absorber, both free or bound to the atoms. The electron is put in motion and the gamma ray undergoes loss of energy and change of direction.

Different types of radiation, in particular charged and uncharged, undergo different interaction in crossing matter. The charged particles continuously interact with the electrons of the atoms that constitute the medium where they pass, via the Coulomb force. The uncharged radiations such as gamma rays and neutrons are not subject to this force, thus they interact following other mechanisms, and their energy deposition in matter occurs through secondary charged radiation. An important concept related to the loss of energy of charged radiation in matter is the range, that can be described through a simple experiment. A collimated source of monoenergetic charged particles is counted by a detector after passing different thicknesses of absorbing material. When the thickness is small, all the particles are transmitted, and no attenuation of the beam is observed until the thickness reaches the length of the shortest track in the material. Increasing the thickness a higher number of particles is stopped until no particles reach the detector. The mean range is defined as the absorber thickness that reduces the particle count to one-half of the initial value. In Table 1.1 the ranges of alpha and beta particles in quartz, the mineral of interest for dating applications are reported.

In a transmission experiment performed with a beam of monoenergetic

Table 1.1: Ranges in quartz of alpha and beta particles at the indicated energies.

	Energy (MeV)	Range
Alpha	4.0-5.0	15.0-20.0 μm
Beta	0.5-1.0	0.9-2.2 mm

gamma rays, the probability of absorption in the medium is given by the sum of the cross section of the three described processes, which is called linear attenuation coefficient μ . The number of transmitted photons I is:

$$\frac{I}{I_0} = e^{-\mu t} \quad (1.5)$$

where I_0 is the initial number of photons and t is the crossed thickness. The linear mean free path λ is the average distance traveled in the absorber before an interaction takes place, it is equal to $1/\mu$ and it is expressed in cm. In order to take into account also the effect of the density of the material (ρ), that affects the linear mean free path, another quantity is often used: the mass attenuation coefficient, equal to μ/ρ and expressed in cm^2/g . The mass attenuation coefficient of 1 MeV photons for SiO_2 is $0.0278 \text{ cm}^2/\text{g}$ [2].

The described processes of radiation interaction in matter lead to a transfer of the energy of the incoming particle/photon to the absorbing material. The most important quantity to be calculated for the purposes of this work is the absorbed dose, defined as the mean energy imparted by an ionizing radiation to a material of unit mass. It is expressed by a specific unit called gray (Gy): Joule/kg.

1.1.2 Radioactivity and dating of archaeological findings

In the most common situation, the radiation induced defects are produced by the natural radioactivity not depending on human activity. The background radiation has two components, cosmic radiation and radionuclides present in the earth crust. The cosmic rays come from the sun and from the outside of the solar system and they are composed mainly by protons and high energetic alpha particles. They are absorbed by the atmosphere, where cosmogenic radionuclides (as for example ^{14}C) are formed. Gamma rays pass through the atmosphere reaching the earth surface. The use of radioactivity for age determination of archaeological findings presupposes that neither the parent nor the daughter nuclide are lost or gained except through the decay processes. These are the conditions that define a closed system. The removal of the outer 2 mm of pottery samples is proven to be an adequate procedure to avoid the influence of the surrounding soil. The absorbed dose for materials buried in sediment must be treated separately for alpha, beta and gamma rays considering their ranges and the sample size (Figure 1.5).

The thermoluminescence contribution from beta and alpha particles arises from radioisotopes within the sample and in the soil, whereas the thermo-

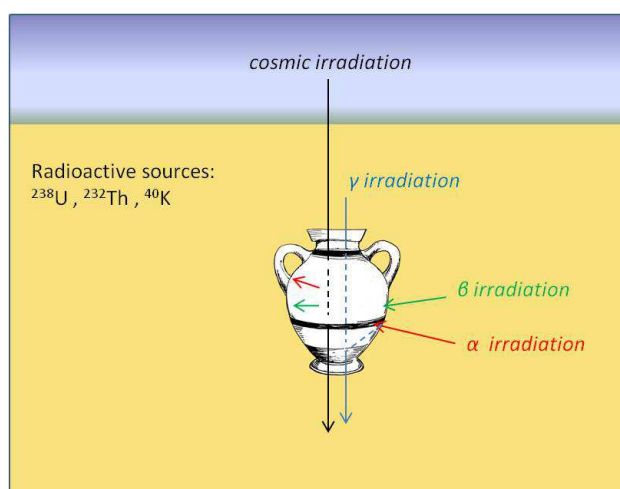


Figure 1.5: Alpha beta and gamma contribution for a buried archaeological sample.

luminescence from gamma radiation is almost entirely from the soil. The gamma irradiation comes from a sphere of 0.3 m radius centered on pottery.

Among the radioactive elements, the isotopes of ^{238}U , ^{232}Th (and their decay products) and ^{40}K are responsible approximately in equal parts of the energy absorption by the crystals. Only few percent of the absorbed dose is provided by cosmic rays (0.2 mGy/year). The contribution of thorium and uranium depends on their radioactive series with the emission of alpha, beta and gamma radiations. The radioactivity of potassium comes from the isotope ^{40}K which has a natural abundance of 0.0117% and emits beta particles and gamma radiation.

Luminescence and EPR Dating

EPR and luminescence dating methods are based on the effects of ionizing radiation interacting with crystals. Luminescence techniques are able to determine the time elapsed since the last heating (TL) or the last light exposure (OSL), on the basis of a similar physical mechanism. It consists in the trapping of electron charges by some minerals as quartz and feldspar as a consequence of the interaction with ionizing radiation. When samples are heated or illuminated for the measurement, a light emission occurs, due to the recombination of the electrons (set free from their traps) with the holes.

The radiation emitted in the decay of radioactive nuclides present in the sample and in the local external surroundings is responsible of the creation of the defects in crystalline lattices. The high energetic radiation produces positively charged holes and free electrons in non-conductive solids. The free charges move throughout the crystalline lattice and two processes may occur. Most of the negative and positive charges recombine rapidly, while a few are trapped at lattice defects, forming paramagnetic centers. Some of these centers are stable over a long period and are useful for dating purpose, since it is verified the principle: the more trapped charges, the older the material is. The stability of the radiation induced centers could be of millions of years, but not all the electrons stay in the traps over a time interval longer than the age of the material that must be dated. The lifetime of the centers is finite and for dating purpose it is necessary to select and quantify only those traps for which a sufficient stability is proven.

The number of radiation induced defects could be related to the age if it was zero for a sample of zero age. For this reason it is required an annealing treatment (bleaching) which erases any irradiation memory from the dosimetric minerals in the material, thus setting the clock time to zero for the event to be dated. For example, the firing of pottery is an event able to reset defects in raw materials accumulated over a geological time. A new

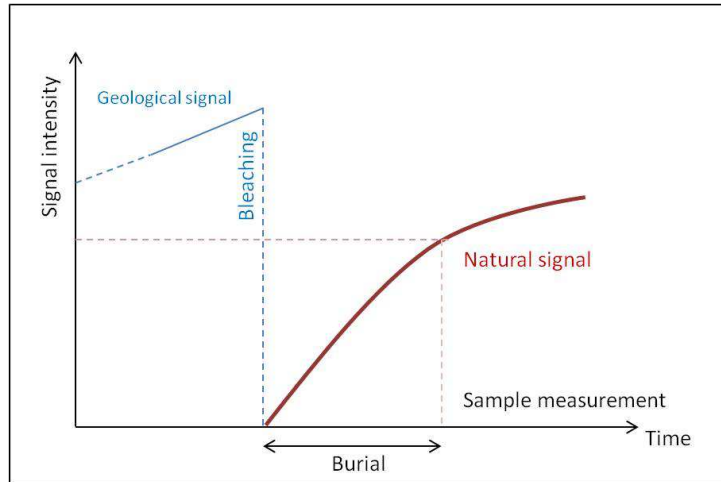


Figure 2.1: Basics concepts of dosimetric dating.

accumulation of radiation induced defects starts and it ends at the moment of the measurement in laboratory, when the natural signal is recorded (Figure 2.1).

2.1 Defects

A crystal lattice is characterized by a periodic arrangement of atoms according to specific symmetries. In natural minerals deviations from this regular pattern are always present, forming lattice defects. Many types of defects can be recognized, but only the point defects are relevant for dating purpose (Figure 2.2). They are localized around lattice points and they are not extended in space. They can be divided in:

1. Intrinsic defects, due to an irregular arrangement of the crystal atoms
 - Vacancies: empty spaces where an atom should be, but is missing
 - Interstitial ion: an extra atom in a non proper lattice site
2. Extrinsic defects, related to impurities
 - Substitutional ion: an atom of a different type than the bulk ones, which has replaced one of the bulk atoms in the lattice.

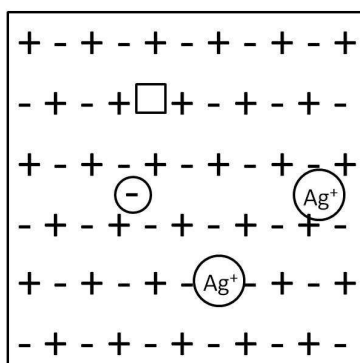


Figure 2.2: Representation of defects in the crystalline lattice of an ionic crystal (vacancy, interstitial ion, interstitial impurity and substitutional ion).

- Interstitial impurity: an atom of a different type than the bulk ones fits into the open space between the bulk atoms of the lattice structure

The classification of the point defects can be based also on their electronic configuration. Defects having unpaired electrons are paramagnetic, the others are diamagnetic. This distinction is important for the detection of point defects by EPR spectroscopy, which is able to record just species with unpaired electrons.

A representation explaining the trapping of the electrons and the luminescence production is the so called *energy band model* (Figure 2.3). In insulating minerals there are two energy levels at which electrons may stay. The lower energy level is the valence band, where electrons are found at the equilibrium state. The valence band is separated from the higher energy level (conduction band) by a forbidden zone (band gap).

In an ideal crystal, within the energetic gap there are no levels at which electrons may be found. In real crystals, the presence of lattice defects allows metastable energy levels in the forbidden region which are able to trap electrons moving through the crystal. At the starting point, as after a resetting event, all the electrons are in the ground state. The ionizing radiation coming from the radioactive decay of unstable isotopes causes the transition of the electrons from the valence band to the conduction band. Then, in returning to the equilibrium state, they can recombine or get trapped at lattice defects. If the traps are thermally and/or optically stable, electrons are not released until external energy stimulation is given to the mineral. The ionization creates also negative charge deficit (called hole) acting as a

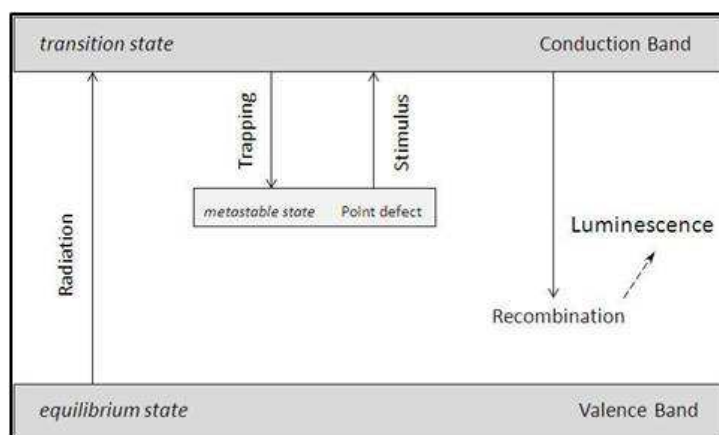


Figure 2.3: Energy band model representation of luminescence.

recombination centre since it attracts electrons freed from their traps. When an electron is evicted from its trap it is rapidly re-trapped or it recombines with a hole. When the recombination occurs, energy is released. This energy is emitted as a photon, and the ions at which radiative recombination takes place are called luminescence centers [3]. This is the way in which TL and OSL signals are generated, in relation to heat or light as a source of stimulation for de-trapping electrons. The amount of emitted light expressed in number of photons is proportional to the trapped electrons and thus to the radiation dose absorbed by the sample. Non-radiative centers and thermally unstable traps are not useful for dating purpose.

A similar description is applicable to EPR dating, except that there is not the eviction of the electrons from the traps. EPR is able to measure trapped (unpaired) electrons by exposing the sample to a magnetic field and recording their absorption of microwaves, without the necessity of their recombination with the holes. Unlike luminescence techniques, for EPR dating applications a preliminary step of characterization of defects is required, in order to select just signals showing a dose dependence and a sufficient stability over long times.

2.1.1 Lifetime of defects

The electrons remain trapped in the defects until the temperature is not raised or the material undergoes light exposure. However, there is a probability of escape even at room temperature, therefore the lifetime of an electron in a trap is finite. For deep traps this probability is very low below 400°C at

which eviction occurs, but it rises very rapidly with increasing temperature. It is important to note that in any crystal there are different types of traps with different characteristic temperatures of eviction. For very shallow traps lifetime could be of few hours. In dating procedure is fundamental to select only centers having lifetimes of tens of thousands of years. Lifetime (τ) is related to the trap depth defined as the energy difference (E , eV) between the conduction band and the trap level:

$$\tau = \frac{1}{s} e^{-\frac{E}{kT}} \quad (2.1)$$

where s is the frequency factor representing the attempts to escape per second of the electron from the trap (10^{10} - 10^{12} s^{-1}) and it depends on lattice vibrations, and k is the Boltzmann's constant: ($8.52 \cdot 10^{-5}$ eV/K).

2.2 Age equation

In radiometric dating the age is calculated according to the equation:

$$age = \frac{palaeodose(Gy)}{annualdose(Gy/year)} \quad (2.2)$$

The palaeodose is the radiation dose to which the sample has been exposed, due to the presence of naturally occurring radionuclides within the pottery and the surrounding sediments since the event of zeroing. The annual dose is the radiation dose received by the sample per year.

The palaeodose, or archaeological dose, is also called *equivalent dose* because it is the amount of radiation in terms of absorbed dose required to produce a luminescence signal corresponding to the natural one measured on the sample. Typical values of absorbed dose in ceramic range between a few Gy and a few tents of Gy. The annual dose is not a directly measurable quantity but has to be estimated. The dose rate is generated from an internal component coming from the sample and an external component from the environment, both constituted by short ranged alpha and beta radiation, long ranged gamma rays and cosmic radiation. The annual dose rate ranges from 1 mGy/y to 10 mGy/y in pottery. This estimation not only depends on the direct interaction between radiation and minerals, but also on factors as the spatial distribution of radioactivity and the presence of water. Humidity absorbs part of the radiation which does not arrive to the sample thus affecting the effective annual dose rate. In order to quantify the dose rate during the burial period, measurements of radioactivity in situ at the

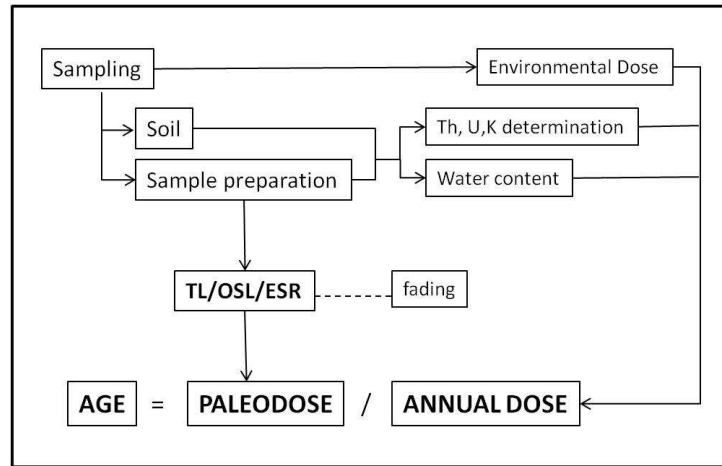


Figure 2.4: The dating procedure with the steps for the estimation of the palaeodose and the annual dose.

moment of sampling, when possible, should be performed. Any changes occurred during the history of the sample must be taken into account. Annual dose rates are not constant, however, being the half-lives of the major sources (^{40}K , ^{238}U and ^{232}Th) of the order of millions or billions years, the irradiation and therefore the annual dose rate can be assumed constant over historical or archaeological times (hundreds or thousands years). For these reasons radiation induced dating is meaningful only for objects whose period of use is negligible compared with the burial period.

In the age equation it is necessary to consider the different interaction of alpha particles with matter in respect to the beta and gamma rays. The thermoluminescence per Gray for alpha radiation is less than for beta and gamma radiation, being lower by a factor (a-value) depending on the substance. The age equation becomes:

$$age = \frac{ED\beta}{aD\alpha + D\beta + D\gamma} \quad (2.3)$$

$ED\beta$: artificial beta dose required to produce the natural signal

$aD\alpha$, $D\beta$, $D\gamma = \alpha$, β , γ components of annual dose.

$a = 0.05-0.5$

In Figure 2.4 the main steps of dosimetric dating method for the evaluation of the palaeodose and the annual dose are summarized.

During the archaeological excavation, in addition to environmental radioactivity measurements, it is also required the collection of the soil surrounding the samples, preferably from the same stratigraphic unit. Data

from radioactivity of soils and environment are directed to the calculation of the external dose. The internal contribution is obtained by measuring the radioactivity of the sample matrix. The water content of the sample completes the data useful for annual dose estimation. The palaeodose is achieved from TL, OSL and EPR signals, with the possibility of applying different protocols and experimental settings.

2.3 Precision and accuracy

The ages obtained by the experimental dating procedure, must be reported with their uncertainty. The typical error limit of a single measurement is 10% but the value could decrease to 5% by dating groups of supposed coeval samples. Uncertainties are proportional to the age of the sample, thus limiting for dating very ancient materials. Systematic and random errors affect the dating procedure [4]. The systematic uncertainty comes from the calibration of the radiation sources and from the measurements procedures. Errors affect all the samples measurements reducing the accuracy of the results. The term accuracy indicates the closeness of a measurement with the true value of the quantity under measurement. Random errors are different from sample to sample (for example caused by non homogeneities of the material) and can be reduced by averaging the results for a number of contemporary samples. This type of error determines the precision of the measurement, which refers to its reproducibility.

In dosimetric dating, many parameters are needed to calculate the equivalent dose and the annual dose rates, introducing several uncertainties. The precision that can be achieved depends primarily on the sampling context and on the sample features. The best condition is achieved when a homogeneous soil surround the samples within a 30 cm radius, because this is the approximate penetration limit of gamma rays in soil. Unfortunately, the variability is relevant from region to region and sometimes also from site to site. The calculation of the annual dose rate requires in situ and laboratory measurements but they are both based on present day conditions. In order to reduce errors in age estimation, it is necessary to reconstruct the history of deposition and take into account possible relevant events occurred during the burial period. The influence of water content is of particular concern in dating procedure. For this reason, climate and environmental changes must be considered in annual dose rate estimation. Furthermore, less precision affects the dating of samples removed from their burial context for long times, for which it is not possible to conduct in situ dosimetry measurements. Two methods have been recently tested to estimate the external dose in such con-

ditions. The first is based on average data of natural dosimetry collected throughout the world, the second on geochemical studies of environments comparable with those of the provenance of the materials. The latter starts from the assumption that the soil is identical to the pottery clay matrix and thus it is applicable only when the sample and the environment are very similar [5]. The attainable accuracy does not always satisfy chronological demands of archaeology, but the luminescence method offers meaningful and advantageous solutions despite the low precision.

2.4 Assumptions

In radiation induced defect methods, some requirements must be satisfied in order to obtain meaningful ages. First of all, it is possible to date only the materials containing crystalline inclusions acting as a dosimeter. Quartz and feldspars are the main natural dosimeters and they are at the base of luminescence dating. Pottery almost always contains in its matrix these minerals (deliberately added or naturally present in clay used as a raw material) thus in general it is a suitable material for dosimetric dating applications. Quartz is also well characterized by EPR spectroscopy and different paramagnetic centers are induced by ionizing radiation.

EPR signals and luminescence emissions useful to reconstruct the chronology, should be zero at the time of the event to be dated. It is necessary a complete zeroing process, which evicts all the electron trapped until the event of interest, for example the firing process in dating of pottery. Partial bleaching of the signal may prevent the age determination of the sample.

Another condition concerns the irradiation. Artificial doses must be administered to the sample in order to determine the equivalent dose and to calibrate the signal. The natural signal is the result of a mixture of alpha, beta and gamma irradiation and it is essential that artificial dose truly mimics the natural processes. Laboratory irradiation can introduce unstable signals, which need to be removed before measuring the absorbed dose by preheating the sample.

Also the lifetime of the defects is important, to ensure that the signal has not faded during the burial period. Specific tests must be performed if there is the suspect that this phenomenon is affecting the sample. Signals must be stable over the period of interest, in archaeological time scale for pottery or geological time scale for sediments. For this reason a so called plateau test is performed. At low temperatures, the ratio of the natural signal divided by the artificial irradiated signal is very small. As the temperature increases, so too does this ratio, until above some temperature, typically 300°C, a

plateau is observed. The observation of a plateau confirms that above this temperature range the traps are sufficiently stable to accurately record the radiation dose acquired over time.

The assessment of the age of a sample is strictly related to its history of use and deposition because the irradiation comes from the material but also from the surrounding, as burial soil. Water content plays an important role in determining the dose received by the sample. In general, it is not possible to be certain of the conservation conditions over long times, therefore for dating purposes all the information about environment, climate changes and history of sites are of primary interest.

2.5 Quartz

Silicates are the most common class of minerals composing the earth crust. The most widespread rock forming mineral is quartz (SiO_2) which is also the most important crystal showing luminescence. It is present not only in rocks and soils, but also in artificial materials as pottery. Quartz is formed by a silicon atom inside four oxygen atoms forming a tetrahedral structure. The three dimensional lattice is obtained by the sharing of the four oxygen atoms with neighboring. The composition of quartz is very close to 100% SiO_2 . Small amounts of others ions are present in the crystals as substitutional ions replacing Si^{4+} , mostly Al^{3+} and Ti^{4+} but also Fe^{3+} and Ge^{4+} , and interstitial ions as Li^+ and Na^+ which cause changes in the lattices. These kinds of imperfections may also be precursors for radiation induced centers, functioning as a trap or recombination sites. Another type of defect recognized in quartz is due to oxygen vacancies which cause the break of the bond between Si and O.

The technological importance of SiO_2 is the reason why it is extensively studied, although the formation and characterization of its defects are not fully understood yet. The explanation for the complexity of the quartz properties is the flexibility of the Si-O-Si angle (143.65° at room temperature) which easily causes lattice distortions and thus the defects. The Si-O bonds are near equal in length being the shorter bond of 1.607 \AA and the longer bond of 1.612 \AA , but their directions are inequivalent and responsible of the asymmetrical properties of SiO_2 . The conventional theoretical approach of studying charge transfer and geometries is thus not always appropriate in quartz defect characterization [6]. Notwithstanding, the application in archaeology and geology for dating purpose is possible since quartz acts as a natural dosimeter. This means that it is able to record the dose absorbed, because ionizing radiation passing through crystalline lattice produces a large

number of luminescence and paramagnetic centers. Even if not fully characterized, their quantification permits to reconstruct the accumulated radiation dose by the material after an event (such light exposure or heating) erasing previous signals. Traps in quartz lattice can be both thermally and optically stimulated, thus it is possible to perform both TL and OSL measurements. Paramagnetic defects with an uncoupled electron are always recognized in quartz, allowing also EPR spectra recording [7]. In particular the three techniques can be in principle applied to dating pottery since quartz is the most common temper used in ceramic production, either present in raw material or intentionally added to the clay.

2.5.1 TL emission spectra

Thermoluminescence signal is called glow curve and it is a plot of the luminescence emission as a function of the temperature. The glow curve has a particular shape and its intensity depends on the material, on the type of radiation and on the absorbed dose. In the simplest case, the luminescence signal will increase with the dose and thus the older is the sample, the more light is produced. The dose response is tested by comparison with a calibrated laboratory irradiation. In rising up temperature, the number of electron evicted from their traps increases until the TL intensity reaches its maximum. Then the signal decreases rapidly to zero because of the steady emptying of the traps and the subsequent reduction of recombination events. A growth curve is constructed as a plot of the luminescence intensity versus the absorbed dose.

The position of the peaks in the TL spectra depends on the experimental conditions, in particular on the heating rate of the sample. For this reason the peaks can be positioned at different temperatures. When the samples are heated from room temperature to 500°C with an heating rate of 20 °C/s, the identified emission peaks in quartz are at about 110°C, 230°C, 270°C, 325°C and 375°C (Figure 2.5). The lower temperature peaks are found only in artificially irradiated samples since electrons at shallow traps recombine in short time. From a physical point of view, the position of the peaks are due mainly to the trap depth and partially to the probability of eviction, which determines also the long term stability of the electrons in the traps.

The glow curve consists of a number of overlapping peaks since it is not possible to select different electron traps present in natural crystals. Consequently, from the glow curve the emission of each recombination centre cannot be distinguished. Measurements of the wavelength of TL emission of natural quartz show two main bands between 460- 480 nm (blue region) and 610-630 nm (orange region). Irradiated samples show another emission in

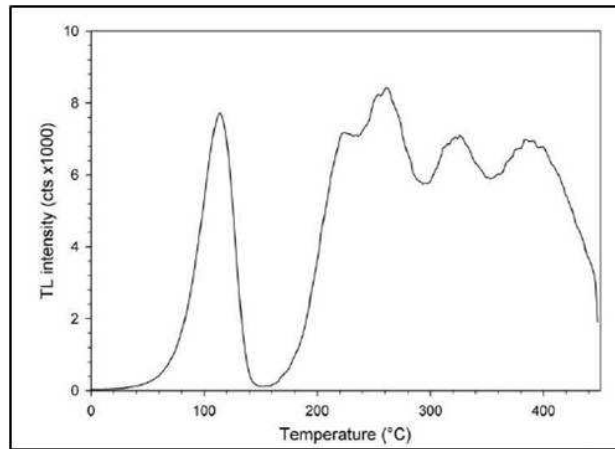


Figure 2.5: TL glow curve (heating rate $5^{\circ}\text{C}/\text{s}$) of quartz showing five peaks at 110° , 225° , 265° , 325° and 385°C [7].

the near UV-violet region between 360 and 420 nm [8, 7].

Only luminescence signals originating from stable traps can be used to calculate an age. For temperature above about 300°C , the signal could be affected by a leakage of charge during the timescale relevant to archaeology because shallow traps can be emptied even at room temperature. As artificial irradiation produces signals of unstable components, a preheating treatment is performed to remove unwanted components in the glow curve. In order to establish the range of temperatures in which the signal shows sufficient thermal stability, a plateau test [3] is performed. The shape of the natural glow curve is compared with the glow curve observed after the artificial irradiation. When this ratio reaches a plateau, the corresponding traps are deep enough for dating and the leakage of electrons is negligible. The plateau test helps to identify the appropriate temperature range for the integration of the luminescence signal. However, the growth of thermoluminescence intensity is not always linear. An initial supralinear rising is observed followed by a constant increase until the saturation is reached. This phenomenon of supralinearity is explained by the difference in sensitivity of TL at the beginning of the irradiation compared to higher doses. The saturation is reached when all traps are filled and the signal does not increase increasing the dose. The saturation is an essential parameter because it limits the dating range at samples of age of about 10000 years. It can occur also in samples with incomplete bleaching, where a geological signal is still present. For example, saturation is observed for pottery fired at temperatures too low for the complete resetting of the signal. Also a strong irradiation due to high concentration of radioactive

isotopes in the sample or in the environment can cause saturation, filling all the traps in times shorter than supposed. Another important phenomenon which causes loss of signal not dependent from temperature is the so called *anomalous fading*. It consists on a release of charges from the traps at a rate which is much faster than expected. Quartz is not known to suffer from anomalous fading of signal whereas K-feldspar usually does. Underestimation of sample age is possible if fading is not recognized. A special storage test is performed on samples in order to understand if they are affected by a significant degree of loss of signal. To evaluate this effect, some aliquots are irradiated with an additive dose and one is measured immediately, the others after a period of storage. If the signal decreases, the sample is affected by the anomalous fading. The phenomenon has been attributed to the effect of quantum mechanical tunneling [3]. A trapped electron has a small but finite probability of being found outside the energy barrier that retains it. If this probability overlaps that of a nearby recombination centre, a transition may occur. In these conditions an electron can escape, even at low temperature.

2.5.2 OSL emission spectra

In optical dating the recorded signal is a decay curve, called shine down curve. It is a plot of the luminescence signal versus the stimulation time. OSL of quartz is obtained with a blue-green stimulation and detection in the UV region. If a single type of electron trap was present, a simple exponential decay would be expected. However, there may be more than one light-sensitive trap and furthermore charges can be transferred during measurements. Hence different components can be distinguished in the shine down curve, called fast, medium and slow [9, 86] (Figure 2.6).

The eviction of the electrons from different traps is responsible of the three contributions which may vary significantly from sample to sample depending on the bleaching rates of their defects.

An exposure to light of few seconds is sufficient to reset the fast and the medium component whose light-sensitivity is suitable for dating applications. In the decay curve both components contribute to the initial part. The slow component refers to the depletion of less sensitive traps to light exposure and it is eliminated by the subtraction of the background signal. OSL signal decreases with the increasing of the stimulation time because the traps are emptied by progressive exposure to light. The area under the curve is proportional to the absorbed dose from the moment of the last optical bleaching to the time of the laboratory measurement. Growth curves are constructed similarly to TL data processing, providing artificial irradiation for the calibration. In dating archaeological objects, the natural signals are within the

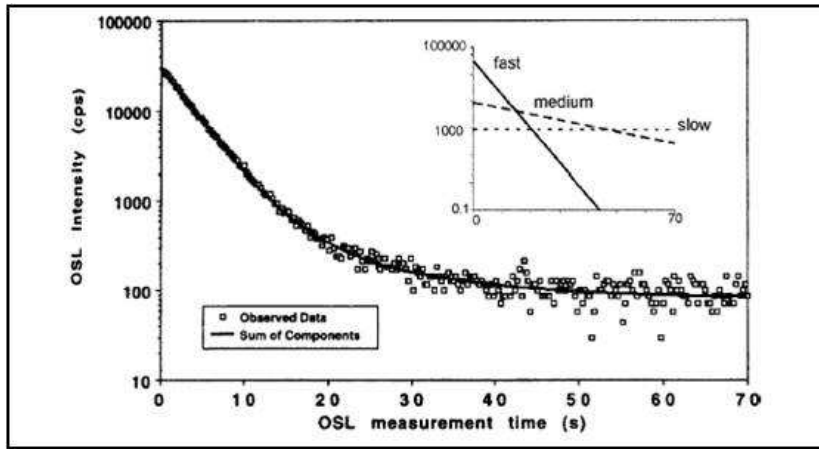


Figure 2.6: OSL shine down curve and its component.

linear range of the growth curves because they are relatively young in comparison with sediments. Thermally unstable components are eliminated by preheating the samples before the light stimulation. As for TL curves, from the OSL emission spectra is not possible the identification of electron traps and recombination centers.

2.5.3 EPR spectra

The EPR spectrum is the plot of the microwave absorption as a function of the magnetic field intensity. The spectrum may consist of one or more absorption lines which are characterized by some parameters. First of all, the magnetic field at which the absorption occurs defines the position of the signal. Line width and shape give information about the structure of the sample. When many lines are present, their number, separation and relative intensity give information about the spin system. Since spectra can be recorded at different frequencies, a parameter independent from the measurement conditions is needed for the identification of the species in the samples. The g factor is used for the distinction of the different lines in a spectrum because its value is determined only by the local environment within the material. The g factor for a free electron is 2.0023. Deviations from this value are due mainly to spin-orbit coupling between the ground state and excited states. The orientation of the molecular orbitals is responsible of the anisotropy of the g factor. In a crystal structure, the g factor changes rotating the sample in the spectrometer. In disordered samples, the orientation with respect to the external magnetic field is randomly distributed and

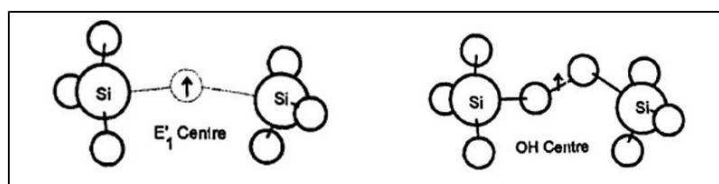


Figure 2.7: The E' centre in quartz with an unpaired electron at an oxygen vacancy and the peroxy centre, a trapped hole centre delocalized between two adjacent lattice-sited oxygens.

the anisotropy is averaged out. For this reason, in a powder spectrum, the signals arise from the superimposition of the single crystal spectra, each one corresponding to a specific orientation. The intensity of the EPR signal is related to the concentration of the paramagnetic species. It is represented by the integrated amplitude (i.e. the area beneath the absorption curve) that is proportional to the number of unpaired electrons in the sample.

EPR signals are more complex than luminescence glow curves and even if it is in principle possible to identify the paramagnetic center by its g factor, difficulties due to the overlapping of different lines may arise.

A great number of defects in natural and synthetic quartz are well characterized but not all of them are suitable for dating purposes [10]. Quartz is present in nature in metamorphic, sedimentary and igneous rocks. On the basis of the formation and the history of the quartz crystals, different paramagnetic centers could be recognized. For volcanic rocks and artificially heated materials as pottery, EPR dating is possible because the reset of previous paramagnetic centers is provided by the thermal annealing. In other conditions, for example in dating geological faults, the phenomenon of interest is the mechanical annealing of the defects due to the stresses during the formation of the fault plane [2]. The simplest point defect in quartz is the E' center, which is an unpaired electron localized at an oxygen vacancy (Figure 2.7). The mechanisms involved in the formation of this center are not fully established. The production by ionizing radiation of the E' center is influenced by interstitial alkali metal ions present as charge compensators when Si^{4+} is replaced by Al^{3+} . Also the temperature at which the irradiation occurs seems to play a role in the formation process, probably being responsible of the mobility of the interstitial alkali ions [11].

The growth of the E' EPR signal with γ irradiation suggests the possibility of its quantification for dating applications. However, a so called *counterfeit E'* was observed in artificially irradiated quartz samples [12] which overlaps the real E' signal. When E' must be used for dosimetry measurements, a

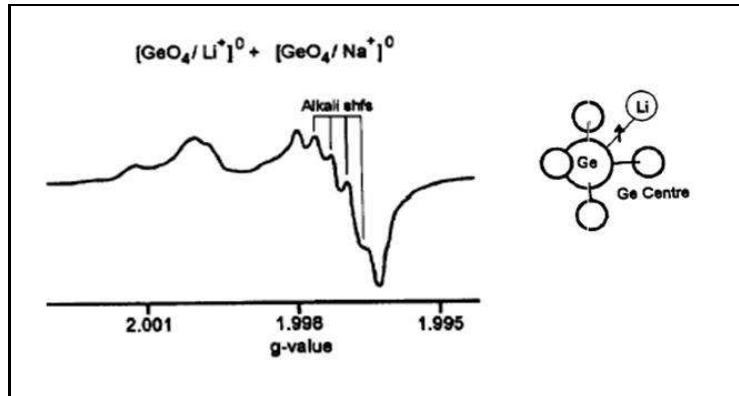
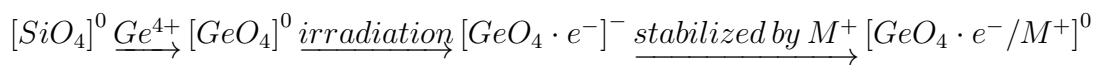


Figure 2.8: The EPR spectrum of the Ge centre in quartz and the schematic representation of the defect.

test for the presence of the counterfeit signal has to be performed. Another dose dependent intrinsic defect in quartz is the peroxy centre (Figure 2.7). It is an oxygen excess defect, in which two oxygens replace a single oxygen in the structure. It may be considered as a trapped hole, even if a model of its formation is not yet defined, the peroxy centre seems to form around dislocation [2]. Heated materials are dated mostly by impurity related defects. They are mainly due to the substitution of Si^{4+} by other metal ions. A model representing the production of this kind of defect is exemplified by the Ge center. Ge^{4+} substitutes for Si^{4+} site in the SiO_2 lattice. Compared to the silicon ion, germanium has a larger electron affinity which causes the trapping of a free electron produced by the passage of ionizing radiation through the crystal. The center has thus a negative charge, compensated by a monovalent cation (H^+ , Li^+ or Na^+) to form a stable system. (Figure 2.8)



An impurity-related defect is also the Al center. Al^{3+} occupies the Si^{4+} site with the association of a monovalent metal cation to give rise to a neutral center. When it traps a hole produced by ionizing irradiation, the charge compensator diffuses away.



It can be measured only at low temperatures.

Methods in Luminescence and EPR dating

3.1 Equivalent dose determination methods

3.1.1 Multiple Aliquot Additive Dose (MAAD)

The additive dose method is the protocol usually adopted in the TL dating of pottery. Many aliquots of the sample are used in order to obtain the growth curve, but each of them can only be measured once. The total radiation dose that has been deposited on the sample can be determined by comparing the signal from the sample in the natural state with that induced by exposure to an artificial source of irradiation. Natural TL is measured for 4 different aliquots while other subsamples are given different artificial calibrated doses which adds up to the natural signal. A growth curve is constructed by plotting the luminescence signals as a function of the delivered dose. The natural signal is the lowest point on this curve, which is then extrapolated back to zero to estimate the equivalent dose (ED in Figure 3.1). This method is based on the assumption that all the aliquots have the same luminescence response. If the reproducibility is low, a large error affects the equivalent dose estimation. The strength of the procedure is that the response to laboratory dose is not altered by any zeroing procedure. The equivalent dose is obtained independently from the experimental data set and depends upon the mathematical expression used [13, 8]. EPR dating employs the same protocol of TL, but several measurements can be performed on the same aliquot since the signal is not erased by the experimental procedure.

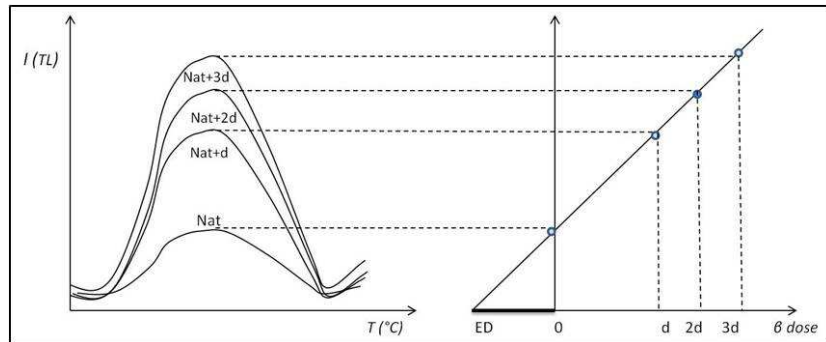


Figure 3.1: The extrapolation of the equivalent dose from the growth curve obtained with the MAAD protocol.

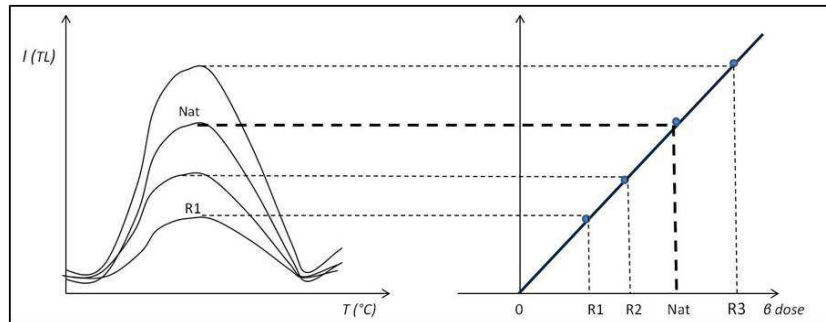


Figure 3.2: The interpolation of the equivalent dose from the growth curve obtained with the SAR protocol.

3.1.2 Single Aliquot Regenerative Dose Protocol (SAR)

The regeneration method measures the luminescence of the samples by using the same amount of material to record natural and artificial irradiated signals. The Single Aliquot Regenerative dose protocol (SAR) was first suggested by Huntley in 1985 and the developed and modified by Murray and Wintle (1998) to overcome the problem of sensitivity changes of the sample during the measurement cycle of the conventional regeneration method [14, 15]. In the SAR protocol artificial incremental irradiations are given to an aliquot that have been first measured for the natural signal and thus zeroed. Repeated measurements are conducted on the same subsample throughout the experiment. The regenerative dose has to be chosen to match the natural dose as closely as possible. The aim is the regeneration of the growth curve from zero and then the natural signal is fitted by interpolation (Figure 3.2)

The steps of the SAR protocol are:

1. Preheat
2. OSL (TL): L_0
3. Test Dose
4. Preheat
5. OSL (TL): T_0
6. Dose D_i
7. Preheat
8. OSL (TL): L_i
9. Test Dose
10. Preheat
11. OSL (TL): T_i
12. Repeat steps 6-11 with different D_i

The preheat treatment is able to remove the charge in the shallow traps. However, the subsequent heating after each irradiation of the sample changes the luminescence sensitivity. This means that different doses of artificial irradiation are needed to produce the same amount of luminescence. The rate of trap filling could change the luminescence efficiency and subsequent signals from the artificial irradiation are not comparable. To overcome the problem of sensitivity changes associated with repeated irradiations, preheat and stimulation, a correction is calculated on the basis of the test dose. It consists on a small irradiation (about 10% of the assumed natural signal), constant during all the sequence of the experiment, delivered to the sample after each luminescence measurement. The signal of the test dose has the same sensitivity as the preceding signal and thus it can be used as a correction to equalize the sensitivity of the natural and subsequent regenerated signal. The curves of the natural and irradiated signals are integrated in an appropriate time interval. In this way the L_0 value for the natural signal and the L_i values for the irradiation are calculated. Similarly the T_0 and the T_i values for the test dose are assessed. The ratio L_i/T_i is plotted as a function of the dose to construct the growth curve. The interpolation of the L_0/T_0 allows obtaining the equivalent dose. The so called *Recuperation Test*

is the measurement of a zero dose to check the presence of unwanted signals that the irradiation and the heating treatments could have produced. The measurements should give zero signals but transfer of charge from deeper traps can occur because of previous irradiation and stimulation. If a signal is recorded, it should not exceed 5% of the equivalent dose to be considered negligible. At the end of the cycle the first regeneration dose after the natural signal measurement is repeated to verify if the same curve is reproduced. This is called *Recycling Ratio Test*. Usually the first dose delivered to the aliquot is chosen because the sensitivity changes progressively. Thus the first and last measurements will give the maximum spread in sensitivity change. The ratio of the sensitivity corrected data $(L_i/T_i)/(L_1/T_1)$ should be unity but the range of acceptability ranges from 0.90 to 1.10 for experimental data [16]. Over the traditional multiple aliquot method, the normalization between measurements is not necessary because using only one aliquot of sample there are not variations in weight or mineralogy. The experiment is repeated over several aliquots of each sample, resulting in different equivalent dose estimations which are averaged. However, the number of aliquots required for SAR protocol is smaller than the one employed for the MAAD method. This is important in working on archaeological materials or when small-sized samples are available. Furthermore, less effort is needed for the minerals separation, if required. A great advantage of SAR protocol is also the elimination of the complication related to aliquot dependent variations in luminescence characteristics [8, 16]. The SAR protocol is usually applied in OSL dating of unheated material. The advantages of this approach over the traditional MAAD technique for potteries suggested the attempt to apply it also to heated materials. To date, few applications of SAR TL of pottery have been published [17, 18, 19] but the results are in agreement with those obtained by MAAD protocol. For EPR dating, SAR protocol can be applied only if an annealing treatment can be performed before the regenerative irradiation. In quartz dosimetric studies, artificial heating has proven to be the most efficient zeroing procedure [20].

3.2 Thermoluminescence (TL)

3.2.1 Fine grain and Quartz inclusion techniques

In luminescence dating, samples are divided in several aliquots for the measurement of the natural and artificially generated signal. There are two basic techniques for dating pottery, differing in sample preparation and minerals used for recording thermoluminescence. In the so called *fine grain technique*,

all the material is used without any mineralogical separation. The external layer is removed to avoid any contamination and then the inner portion is drilled. A grain size separation in acetone suspension is needed to collect the useful fraction of 4-11 microns. This grain size receives the full alpha dose since the diameter is smaller than the average alpha particle range in silicates ($\sim 20\mu\text{m}$). In the quartz inclusion technique both physical and chemical treatments of the sample are required in order to extract the sand-sized (coarse) grains of quartz from the pottery matrix. The grain size is between 80 and 150 microns thus only the outer part of the grains receives the alpha dose from the environment. It is therefore necessary the calculation of its contribution or its deletion by removing the external skin with a chemical etching. This is achievable because neither quartz nor feldspar has internal sources of alpha irradiation, thus all the alpha dose comes entirely from the surrounding soil. Coarse grain has the advantage of involving only one mineral with known luminescence properties. However, the coarse grain fraction in archaeology could be difficult to be exploited, since pottery not always presents abundant inclusions of the right size. Otherwise, for the mineral separation a quite large amount of ceramic is needed and this requirement is often not satisfied when working on archaeological findings.

3.3 Optically Stimulated Luminescence (OSL)

3.3.1 Principles of OSL dating

Many features of TL and OSL dating are very similar because the underlying principles of the two techniques are the same. The major difference is the energy used to empty the electron traps during the measurements. In OSL the stimulation is performed by light, for this reason the method is also called optical dating. The recombination between electrons evicted from the traps with holes emits a luminescence that can be collected and quantified. The resetting of the OSL signal is called bleaching; to avoid this phenomenon before measurement, the sampling and the preparation of the material are performed in subdued red light. OSL is suitable for dating purpose because it is possible to correlate the intensity of the recombination emission to the elapsed time since the last exposure to light. If the duration of the exposure is insufficient for full resetting (partial bleaching), the measured signal will not be an indication of the event to be dated. Unlike TL, it is not possible to distinguish shallow and deeper traps. A source of light of appropriate wavelength and intensity is chosen on the basis of the minerals present in the sample to induce the transition of the electrons from the traps to the

conduction band. The emission related to the recombination of electrons and holes is monitored as a function of the stimulation time. The integral of the luminescence signal is a measure of the radiation dose absorbed by the sample since it was last exposed to light. OSL includes stimulation not only from the visible region of the electromagnetic spectrum but also from IR and UV radiation. The rate of emptying of the traps is dependent from the rate of incident photons (lighting power). Unlike TL, it is possible to observe the luminescence from quartz and from feldspars separately because of their different range of emission. Quartz emits between 360 to 420 nm (near UV-Violet), while feldspars emit luminescence at 390-440 nm (Violet to Blue). As for TL, also in OSL measurements the phenomenon of anomalous fading has to be taken into account. The protocols to measure and correct the obtained ages are based on the comparison of luminescence intensities measured shortly after the irradiation with those measured after some time delay [21]. The approach adopted for OSL measurements is the SAR protocol (subsection 3.1.2), applied mainly to sediment dating, the field of the development of this method. Some recent studies have demonstrated that OSL SAR is suitable also for dating archaeological heated materials as pottery.

3.3.2 OSL of heated materials

OSL is a well established method for age estimation of sediments. Even if there are not conventional procedures for pottery dating by OSL, there are some examples of comparison of ages calculated with traditional MAAD and SAR protocols, both with TL and OSL. The quartz inclusion technique and SAR protocol (OSL and TL) were applied to late medieval bricks, whose calculated ages are in agreement with the architectural context [17, 22]. Attempts of optical dating of archaeological pottery by quartz inclusion were successfully made also by Barnett [23]. Fine grain samples were dated by Leung [24] and Oke [25]. In general the use of TL has been often supplemented by optical dating methods and in particular SAR OSL is a procedure more practicable when the TL sensitivity of the quartz grains is poor and the availability of datable material is limited [26]. In applying OSL for dating of pottery it is important to be sure of the complete bleaching of the signal during the manufacturing steps in order to avoid overestimation of the ages.

3.4 Electron Paramagnetic Resonance (EPR)

3.4.1 EPR dating

EPR is becoming an important tool in radiation science, an interdisciplinary field incorporating applications in medical physics, radiation dosimetry, geochronology and archaeology. Electron Spin Resonance (ESR) or Electron Paramagnetic Resonance (EPR) is a magnetic spectroscopy able to detect the absorption of microwaves by unpaired electrons under the effect of a strong magnetic field. Unpaired electrons are present in free radicals, in crystalline lattice defects and in transition metals ions: these species are in principle detectable by means of EPR. Dating through EPR like the luminescence technique belongs to the category of radiation induced defect dating since it quantifies the radiation effects accumulated in time. Radiation dose can be determined from the EPR signal intensity of radiation induced paramagnetic defects which is proportional to the number of lattice defects housing unpaired electrons. In many materials the traps are metastable, because, although the release of trapped charges is energetically favored, the activation energy is too high for a spontaneous release, resulting in the very long lifetime of defect centres. EPR spectroscopy is a non-interfering method allowing the measurement of the total dose absorbed by the sample. Differently from luminescence techniques, EPR is a magnetic spectroscopy dealing with the spin transitions between electron states of different energies. EPR measures directly the concentration of trapped charges in a specific trap, without the recombination of the electrons with the holes during measurements. EPR dating is possible since the signal intensity is proportional to the total dose to which the sample was exposed. The time elapsed from the last zeroing of the trapped charges can be calculated by dividing the total dose absorbed by the sample with the estimated annual dose. For radiation exposures considerably shorter than the lifetime of the trapped charges, the charge concentration in these traps will be directly related to the accumulated dose. Not all the signals satisfy the previous statements so the first step of EPR dating is the identification of the appropriate signal on the basis of its lifetime and its dependence on the radiation dose for the specific material. Since the signal is not erased by the measurements, the protocol usually applied for dating is the Multiple Aliquot Additive Dose (subsection 3.1.1) with the construction of a growth curve from which the total absorbed dose can be extrapolated. The time range covered by EPR dating depends on the sensitivity of the spectrometer and on the presence of interfering background signals. Trap emptying (bleaching - annealing) is less critical in EPR than in TL and OSL. EPR can rarely provide ages with uncertainties $<10\%$. The dated material

itself does not possess a particular intrinsic level of reliability but the burial context has a significant impact on the degree of the attainable accuracy or precision in the dating procedure, as in luminescence methods [2].

3.4.2 Principles of EPR

An electron can be considered as a tiny magnet since it is a negative charged sphere whose rotation produces a circulating current in the direction opposite to the rotation. The current produces in turn a magnetic field in the proximity of the electron. Generally the electrons are paired, with a neutralizing effect of the magnetic field. A magnetic moment is present when the electron is unpaired, as for example when it is trapped at lattice defect sites. The EPR spectroscopy is able to record the absorption of microwaves by an unpaired electron under an external magnetic field. In the absence of an external magnetic field (B_0), the energy states associated to the magnetic moments are degenerate. When a magnetic field is applied, they exhibit a splitting with an energy difference ΔE as a function of B_0 , called *Zeeman effect* (Figure 3.3). The spins tend to align to the external field. Since the energy states are quantized, only two directions of the orientation for an electron with spin = 1/2 are possible: parallel (lower energy, β) and antiparallel (higher energy, α). The spin moments are randomly distributed with an excess of population in the parallel state which is energetically favored. Since the energy is given by

$$E = -g\mu_B B_0 M \quad (3.1)$$

where g is the g factor (2.0023 for free electron) and μ_B is the Bohr magneton (unit of the electron magnetic moment $9.274 \cdot 10^{-24}$ J/T), B_0 is the applied magnetic field and M the magnetic quantum number (+1/2, -1/2), the difference between the two states becomes:

$$\Delta E = g\mu_B B_0 \quad (3.2)$$

In order to promote the transitions of spins between the two states it is necessary to cover the energy difference of the levels. When this condition is satisfied the resonance occurs:

$$\Delta h\nu = \Delta E = g\mu_B B_0 \quad (3.3)$$

The absorption of this energy by the unpaired electrons makes possible the transition between the states. The correspondent B_0 is called field of resonance (Figure 3.3). The promotion of such a transition requires an irradiation in the microwaves range and applied magnetic fields of the order of

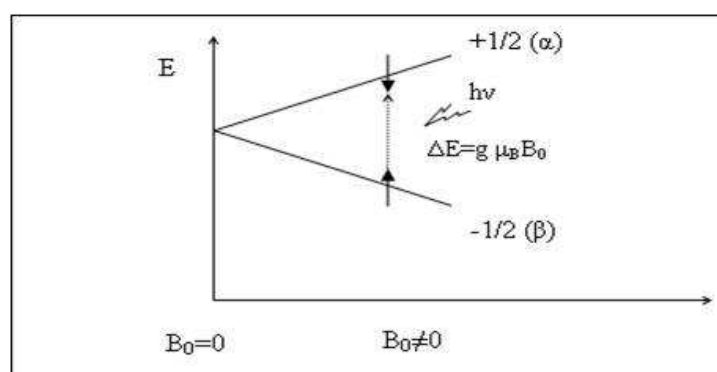


Figure 3.3: The EPR experiment.

100 mT-1000 mT. The acquisition of an EPR spectrum consists in the measurement of the energy absorbed by the paramagnetic system as a function of the amplitude of the applied magnetic field.

It is possible to gain the resonance conditions either sweeping the magnetic field and maintaining the microwave frequency constant or vice versa. Because of the difficulties in scanning microwave frequency, EPR spectrometers operate at constant electromagnetic frequency while sweeping the magnetic field.

The previous considerations are referred to isolated paramagnetic centers. However, the paramagnetic centers usually interact with the surrounding atoms. In many systems of interest in EPR studies, the unpaired electron is located near the atoms with a nuclear spin, which are responsible of a nuclear magnetic moment producing a local magnetic field. The interaction of the magnetic moment of the unpaired electron with those of the nearby nuclei is called hyperfine interaction. The magnetic field produced by the nuclei can add or oppose to the external applied magnetic field depending on the alignment of the moment of the nucleus. The hyperfine interaction causes the splitting of the EPR signal. For n equivalent nuclei with spin I one observes $2nI + 1$ lines in the EPR spectrum.

3.4.3 CW EPR and Echo Detected EPR

The continuous wave (CW) method is characterized by microwaves continuously irradiating the sample while sweeping the magnetic field. In the pulsed method, short pulses of high-power microwave radiation are sent to the sample. If the pulse is sufficiently short, a single pulse is able to promote all the transitions, covering all the frequencies at which they occur. All the

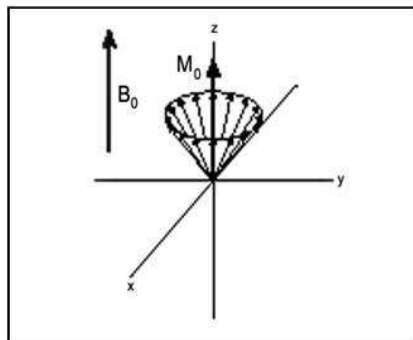


Figure 3.4: The precession of the magnetization around the z axis.

transitions are represented by the FID (Free Induction Decay) from which the spectrum is obtained by the Fourier transform. In this way the time of acquisition is considerably reduced. However, due to technical limitations in EPR spectroscopy, it is not possible to excite the whole spectrum by a single microwave pulse. During and a short time after the pulse, the detector must be protected from the high power and the signal recording is not possible. The short time that must pass after the last pulse before signal recording is called *instrumental dead time*. The dead time can be reduced by increasing the bandwidth of the resonator. The large bandwidth of the pulse EPR resonator is responsible for the lower sensitivity as compared to CW EPR. In order to circumvent the dead time problem, most experiments are based on the detection of electron spin echoes (ESE). Some principles of pulsed EPR are briefly explained below. The magnetization is the vector sum of all the magnetic moments in the sample. M_z is defined as the longitudinal magnetization, while M_x and M_y are the transverse magnetization. At thermal equilibrium M_z is constant (Figure 3.4).

Spin magnetic moments precess around the external magnetic field until the microwave pulse (90° or $\pi/2$) perturbs the system and a transverse magnetization is produced by rotating the magnetic moment from the z axis to the perpendicular xy plane. The frequency of the precession is called *Larmor frequency* (ω_L). It is proportional to the energy difference between the spin levels of the system:

$$\omega_L = (g\mu_B/\hbar)B_0 \quad (3.4)$$

The system tends to return to the thermal equilibrium, with a progressive reduction of the magnetization in the xy plane aligning to the z axis. In the pulsed experiment, only the xy component of the magnetization is recorded,

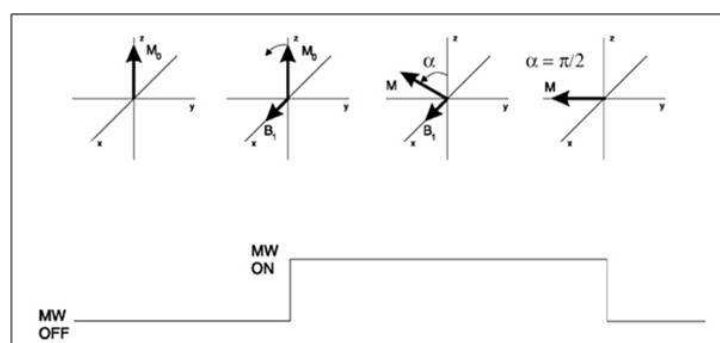
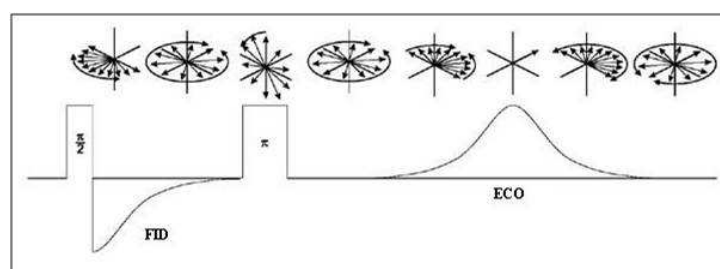
Figure 3.5: The effect of a 90° pulse.

Figure 3.6: The EDEPR experiment.

by dividing it in two vectors, one along x and the other along y direction. In Figure 3.5 the x component of the magnetization after a 90° pulse is shown.

If a second pulse of 180° (π) after a certain time τ is applied, part of the magnetization is aligned along y . The signal recorded after a time τ from the second pulse is called echo. After the 90° pulse, the spins are divided in groups rotating with different speed in the xy plane. The second pulse inverts the magnetization (Figure 3.6) and the spin groups with high speed get behind the others. The higher speed is responsible of the realignment of all the spin groups. However, due to the irreversible dephasing of each spin group, the signal will be lower.

After the pulses, the system returns to the equilibrium state with characteristic times. The process is called relaxation and brings back the magnetization from the xy plane to the z axis. The spin-lattice relaxation time T_1 is the time to orient the spins back to z direction (longitudinal relaxation) while the decay of the magnetization in the xy plane is called spin-spin or transverse relaxation with a time constant T_2 ($T_2 < T_1$). The relaxation process depends on the magnetic fields summing up to the applied magnetic

field. They are generated by nuclear magnetic moments nearby the spins. When they have components rotating at the Larmor frequency, they induce spin transitions responsible for the longitudinal relaxation. The components of lower frequency are responsible for the dephasing of the magnetization on the xy plane thus influencing the transverse relaxation. The relaxation times provide information about the structure of the sample, being characteristic parameters of the spin system. The Echo Detected EPR (EDEPR) experiment consists in applying a pulse sequence while sweeping the magnetic field. The echo intensity is recorded for each value of the magnetic field. The echo represents the transverse magnetization, therefore, in the absence of relaxation processes, its intensity as a function of the magnetic field should represent the magnetization along z in the same interval. However, the relaxations are responsible for the decay of the transverse magnetization which is thus lower than the thermal equilibrium magnetization. In such conditions the EDEPR spectrum is the same recorded by CWEPR but with lower intensity¹. The relaxation is different at different values of the magnetic field and the EDEPR spectrum is therefore different from the corresponding CW spectrum. This is due to the difference in relaxation times. For species characterized by very short relaxation times, the magnetization could be completely decayed during the pulse sequence and no contribution to the spin echo is recorded. This is a limiting factor because not all the species can be studied by EDEPR spectroscopy, but it could also be a powerful tool to separate overlapping signals according to their relaxation times.

3.5 Annual dose

The annual dose is the energy absorbed per mass unit by the sample from the environment and from the material itself in a year. The annual dose is an estimation because it is calculated on the basis of present data and it does not take into account possible variations occurred during the burial period. The environmental contribution to the annual dose can be determined directly, using thermoluminescence dosimeters which should be exposed in situ for at least one year to consider seasonal variations.

When this approach is not feasible, the concentration of the naturally occurring radionuclides in soil is evaluated. The annual dose is provided in

¹It is to note, however, that the EDEPR spectrum is recorded without a Lock-in system and no modulating field is applied (see section 6.6), and therefore looks like a *normal* absorption spectrum after the acquisition. In order to have a meaningful comparison between CW and ED EPR spectra one should therefore either digitally integrate the CWEPR spectra or digitally derive the EDEPR spectra.

roughly equal parts by potassium, thorium and uranium and for a few percent by cosmic rays. In general, the emission by radionuclides and the absorption of energy by the material are not equal. However, in dating of pottery it is possible to use the so called *infinite matrix assumption* which simplifies the determination of annual doses. When the volume is greater than the ranges of radiations, the rates of energy emission and absorption are the same. This is verified assuming that the matrix is uniform in radioactivity and absorption coefficients. For pottery this is a good approximation since its components (quartz, feldspars and clay minerals) have similar atomic weights and atomic numbers.

3.5.1 Effect of moisture

Because of its porous structure, which may vary from 5% for compact fabric to 25%, pottery absorbs water from the environment. Water acts as a screen because the energy producing luminescence does not entirely arrive to the material. The water absorption coefficient compared to minerals in pottery is 50% higher for alpha radiation, 25% for beta and 14% for gamma. It is necessary to take into account the effect of the moisture, introducing the saturation parameter in the annual dose estimation. The weight of a pottery sample is measured as it is, after drying and in saturation condition. The saturation level sets an upper limit to the effect of water on the calculated age.

3.5.2 Radioisotopes contribution

In order to determine the uranium and thorium content in samples and soils, an alpha counter can be used. The material is reduced to powder and a thick layer is placed on the top of a scintillation screen of zinc sulphide which is viewed from beneath by a photomultiplier, both held in a dark box to avoid external light interference. When an alpha particle from the sample strikes the screen, scintillation is produced. Photoelectrons from the photocathode of the photomultiplier are converted after amplification in one electrical pulse for each scintillation. A voltage threshold rejects pulses corresponding to beta particles and gamma rays and the suitable ones are read by a counter. Counts are recorded at regular intervals, for example every minute. With this method all the alpha emission from the sample is collected without distinguishing the single radioisotope emitting the particle. The concentration of radioisotopes in the sample is then calculated on the basis of thorium to uranium ratio (equal to 3.16 for ceramics). The concentration of radioisotopes has to be converted in the alpha, beta and gamma dose contribution [3].

The contribution to the annual dose of ^{40}K is deduced from the total concentration of K determined by means of flame photometry. This is an atomic emission technique which allows the direct measurement of alkali and alkaline earth metals as sodium and potassium. 500 mg of powdered sample is etched with hydrofluoric acid and perchloric acid in order to dissolve silicates and carbonates. The resultant solution is aspirated into the flame, where the evaporation of the matrix occurs followed by its atomization. The temperature of the flame is able to excite the atoms which emit radiation in returning to the ground state. These emissions have a definite wavelength depending on the energy level from which each atom drops. A specific filter is used in order to select the emission of the atom to be quantified. The intensity of the emission is then related to the concentration of the atom in the sample. The quantitative determination of potassium in the solutions is obtained by comparing the emission intensity of the sample with that of a standard solution with concentration covering the regions around the expected signals.

Pottery in archaeology

4.1 The role of pottery in archaeology

Ceramic is a crystalline artificial solid material obtained by thermal treatment of clays. Clays are formed by weathering of rocks and composed by the so called *clay minerals*. These are silicates of the phyllosilicate group, characterized by parallel sheets of silicate tetrahedra. This particular structure is responsible for the plasticity, one of the most important properties for which clay is used in manufacturing of pottery. It is due to the water absorbed between mineral sheets and bonded to the surfaces of the crystals. This is possible since clay minerals exhibit a very large surface area per unit weight. The plasticity allows pottery being shaped at room temperature. During the heating treatment the loss of water causes the hardening of the pottery which maintains its form. At about 600°C clay minerals undergo the release of the chemically bonded water and the changes in the structure are irreversible. After the firing, the material acquires some characteristics that may vary on the basis of raw materials and manufacturing process.

Ceramics can be hard, water resistant, brittle, insulating and chemically stable. All these properties explain why pottery is often the most abundant material found in archaeological excavations. Ceramics are almost inert and so they are easily preserved in quantity at the archaeological sites. Ceramic is suitable for many different applications such tools, vessels, ornaments and building material and it was exploited since prehistoric times. It is so diffused that the archaeological interpretation of a site is often based on the study of ceramic findings. The study of ancient pottery is both archaeological and technical, with the support of archaeometric analysis. Different information could be deduced from the material, not only of production, use and chemical-physical features but also related to people involved [27].

Pottery production needs the knowledge of choosing and manipulating

clay for forming objects and the use of fire for hardening. Even if it could seem an easy task, the selection and processing of raw materials and their firing to obtain a ceramic which satisfies the strength, resistance, permeability requirements in use, is not so simple. In providing clay for pottery production, a primary condition is to ensure a sufficient plasticity for forming. At the same time its drying shrinkage must not be great to avoid cracking. Non-plastic materials (sand, grog, chaff, fragments of rocks) must be added to the clay if not yet included, to achieve these conditions. Even in presence of a suitable raw material, the firing procedures are critical steps in the productive process. The knowledge of the treatment of clays with high temperature can be recognized early in human history, probably as a consequence of the daily use of fire and the observation of its effect on the ground soil. At the present time it is possible to reconstruct the firing processes by observing the color and by mineralogical analysis of shards. Black potteries are indicators of a reducing atmosphere while red ceramics are produced in oxidizing conditions. In order to determine the temperatures reached during firing, changes in mineralogy and in the microstructure of the material (as porosity and vitrification) are checked.

The surface treatments are also an important technological and cultural indicator, because they could be just decorative or have a practical meaning, for example reducing permeability to liquids. The treatments as slips and glazes can be of different nature and decorations can be applied to the surface, impressed by means of tools and painted.

From a more general point of view, the study of pottery permits to reconstruct the organization of the production, involving the craft skills, the level of technologies, the permanent facilities and the degree of standardization. These are all technical data regarding the production but also socio-economical indicators. The knowledge of the processes involved from the choice of the raw material to the use of ceramic objects needs to take into account the technological development, the specific cultural context and their relation to the economical context. The advantages of pottery technology compared to the difficulties in achieving a good material are demonstrated by its extensive use from prehistoric times to the present day. The quite simple basic procedure of pottery production and the availability of non expansive clay are the main reasons of the wide diffusion of this versatile material.

Pottery is one of the few materials used in the course of history in very different fields, as food preparation and conservation, transport, building materials, art and ornaments. Hence, the study of this material involved many aspects of ancient society: economy, daily life, culture, trades. It is clear why pottery is so important in the archaeological interpretation not only of a site, but of regions and periods. Different archaeometric studies were developed in

order to understand the production technology (raw materials, surface treatments, firing conditions), the provenance (locally produced or imported), the age and the different uses (storage, food preparation, tools, and ritual). Improvements in pottery manufacturing are indicator of the technological development of mankind. In many cases pottery contains also an artistic expression and it is the product of the creativity, not only of the ability of the craftsmen. Technological aspects, archaeological interpretation, functional details must be integrated in view of a complete archaeological interpretation of finding as well as dating. In summary, pottery is so important in archaeology because it is the only material at the same time frequent, dated, with functional values and thus able to reconstruct local history. Ceramic allows also establishing comparisons between different periods and geographical areas.

4.2 Origin of pottery

Ceramic is the first synthetic material and it is among the oldest and most significant technological innovation in the history of human achievement. The complexity of the processes necessary for a good pottery production indicates that many experimentations and errors have been made during a quite long period of development. Critical analysis on the origin of pottery is not the purpose of this work but it is interesting to point out some aspects, because African desert ceramic plays an important role in deciphering this theme. At the beginning of XIX century, pottery was considered in European prehistoric studies, as the sign of the passage from Paleolithic to Neolithic, corresponding to the transition to farming. At the present time it is possible to affirm that it was a simplified interpretation of the archaeological findings, which is not true in all the cultures. A distinction between pottery with symbolic significance and pottery with utilitarian functions must be made. This is important since the circumstances of pottery manufacture are not always clear. The first pottery production is found to be linked to ritual and social spheres and not to economic or subsistence dynamics. Moreover, the oldest vessels occur before the introduction of agricultural practices, proving that pottery containers were produced among hunter-gatherer groups [28]. The most ancient ceramic findings in Europe (site of Dolní Vestonice, Czechoslovakia, Figure 4.1), dating to about 26,000 BP are anthropomorphic and zoomorphic figurines [29]. These materials suggest that the fired clay technology was applied with a symbolic meaning and may have had a ritual function not related to the daily life functional use of objects.

In Asia, fired clay containers were found in Japan dating back to ca

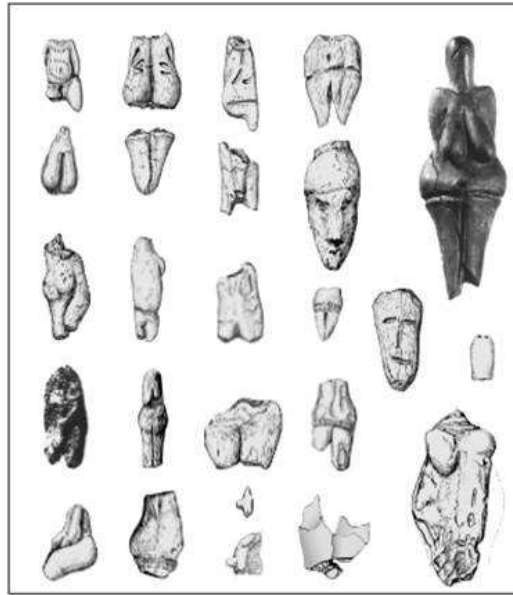


Figure 4.1: Anthropomorphic and zoomorphic ceramic figurines from the Upper Palaeolithic Pavlovian sites Dolní Vestonice, Pavlov and Predmosti (from [30]).

12,700-10,000 BP. They belong to the so called Jomon pottery. A pottery production of about 20,000 years ago was found in China. It is associated to hunter-gatherers population using this technology for very long times before they became sedentary and began cultivating plants [31]. These recent studies of East Asian ceramic refute the idea that the beginning of pottery production was associated in that area with the transition to agriculture.

In the African continent, the production of the first pottery is probably to be placed between North Africa and the middle Nile Valley about 10,000 years BP [42]. The Sahara region at that time was not a desert and the Nile Valley was a rich habitat. Sites at which pottery was found are associated to semi-sedentary groups living on use of riverine resources. The ceramic found in this region is the so called Khartoum Mesolithic pottery. It is in general well formed and fired at high temperatures. Shards of this period are a very common finding in the Nile valley and it is clear that there was a diffuse use of pottery technology. It is thus reasonable to think about a more ancient fired clay material as the first step in the development of shapes, decoration and in general of technology of pottery production. No correlation with food production of shards belonging to hunter-gatherer population with seasonally occupation of riverine settlements has been recognized. Fur-

thermore, considering that the first Neolithic settlements in the Levant and Upper Mesopotamia (Pre-Pottery Neolithic A, B, C: 8,500-5,500 BC) bear no evidence of pottery production the *Neolithic revolution* is not sufficient to explain the reasons of the origin of pottery. The *Neolithic revolution* is thus not sufficient to explain the reasons of the origin of pottery. The invention of ceramic is a technological advancement for many cultures. It helped nomadic societies for a more sedentary lifestyle allowing the storage of food for long periods. But it is also true that pottery making would have required long time to permit the finding and the selection of suitable clay and possible tempers to obtain appropriate recipes and to improve the manufacturing process. From this point of view the pottery production seems to be possible only in sedentary societies. The technological choices are influenced by the natural environment for the availability of raw materials and by the skills in producing and using tools and controlling firing conditions. Moreover the technological developments must be considered as a long-term process, during which the technical improvements are adapted to economical and cultural changes. For all these reasons it is not appropriate to think about pottery production as the result of systematic experiments since the technological choices come from a mix of environmental, economic, ideological factors. It is instead reasonable to think about an invention of pottery in different places independently and adopted for different functions [32]. Last of all, it is important to point out that it was not possible until now to reconstruct a full sequence of the development of pottery manufacture. On the basis of the findings available at the present time it is possible to affirm that early pottery appeared in environments rich in food resources and water, which do not require food production. It is reasonable that the new material was first used as a social distinction in communal feast before a use in cooking or in storage food [28].

4.3 Dating pottery

As described in the previous paragraphs, pottery is an important material in archaeology due to its ability in providing information on many aspects of the past, including chronology. The plasticity of clay enables to create a great variety of shapes with a wide range of surface treatments and decorations using different combinations of paste and temper. The shapes and the decoration of pottery and the clay mix composition are subjected to many variation in time, thus chronological frameworks often rest on the development of these features. The stylistic examination of shapes, surface treatments and decorations, is the first and the oldest method employed for

direct dating of pottery. Recognizing stylistic changes through time or other attributes detecting variation trends is useful mainly for establishing relative chronology of the artifacts. This approach based on similarities in shapes, technology or style is empirically derived and does not provide by itself absolute ages. It is possible to use correlation and differences between areas and phases of archaeological sites to define chronological sequences which have to be fixed using absolute dating method. Moreover, in order to create reliable association of materials, site formation processes have to be understood and a stratigraphy, where artifacts are arranged in chronological sequence, is necessary. Different approaches to the chronological topic are possible and they are functional for dating specific moments of the lifetime of a ceramic object, as the manufacture, the use or the burial. The choice of an absolute dating technique is related to the archaeological event for which an age is required and to the availability of the type and quantity of material suitable for the specific analysis. The application of radiocarbon dating on pottery is possible only in few cases. Radiocarbon ages can be obtained only in presence of organic residues, as food or charcoal. However, pottery rarely has an organic content that can be exploited as a basis for radiocarbon dating. Even in the case of suitable material, there is always the risk of contamination by the substances from the soil and displacement of residues through the stratigraphic units. Especially for buried artifacts, the migration of older or younger organic matter is a complication for radiocarbon age determination. Even if some sample treatments as the purification of the organic matter could help in resolving this problem, the best approach is to date only the materials unequivocally linked to the artifact. Surface residues or matter absorbed within the fabric are suitable for radiocarbon dating. In particular lipids are often preserved in ceramic in sufficient quantities. The radiocarbon dating of individual compounds isolated from lipids from potteries from the Neolithic to the Medieval periods is in good agreement with the independent calculated ages of these materials [33].

In the absence of associated datable carbon containing organic matter, pottery can be directly dated by other methods. A new approach is based upon the rehydroxylation [34]. This process is the slow recombination of the material with the environmental moisture. A first measurement of the mass of the sample is representative of the sum of the original mass of the as-fired material and the mass of water that has chemically combined with it over its lifetime. The sample is then heated to determine its lifetime water mass gain. The exposure to water vapor is then performed to measure the mass gain rate and calculate its kinetic constant. The age of the sample is established by extrapolating the mass data to find the time needed to regain the mass lost during heating. This is possible by estimating the sample mean

lifetime temperature provided by a regional meteorological record.

A different physical phenomenon is at the basis of the well established technique of pottery dating of Thermoluminescence (TL), which has been described in Chapter 2. In general, radiation effect dating is useful only in presence of quartz and this assumption is nearly always satisfied for pottery. TL is able to date the event of firing that can be usually associated to the manufacturing of the object. In some cases a heating over 400°C after the production as incidentally or deliberately action may occur and TL ages are thus referred to these events. Post-depositional heating is a rare event and in general is not a problem in dating procedure. Over radiocarbon, TL expresses a calendar age in years without needing any calibration [35].

The traditional dating methods and the new ones are in continuous updating, in order to reach a better precision and to provide an important tool to archaeology. Dating groups of ceramic shards from the same site (also with different techniques) will give information about duration of use, will distinguish phases of occupation and in some case could be the only chronological reference for an excavation. This is true especially for the prehistoric times for which pottery is often the basis of chronological frameworks.

The *El Salha Archaeological Project: rescue excavation in central Sudan*

The pottery shards for dating studies come from archaeological excavations in the Central Sudan. The *El Salha archaeological project* (from the name of the region, south of Omdurman along the western bank of the White Nile) started in November 2000 and it is directed by the archaeologists Donatella Usai and Sandro Salvatori. The project is promoted by the Istituto Italiano per l’Africa e l’Oriente (IsIAO) and the Centro Studi Sudanesi e Sub-Sahariani with the financial support of the Italian Ministry of Foreign Affairs, the Michela Shiff Giorgini Foundation, the Centro Veneto per gli Studi Classici e Orientali and GASID of Torino. From the archaeological point of view, the interest on the Sudanese region is relatively recent, because of the proximity of Egypt, which has been a preferred subject of research in the last two centuries. The study of central Sudan prehistory began in the mid twentieth century with the archaeological surveys and excavations of J. Arkell (1947, 1949, 1953, 1972). Since then, many activities have been performed but there are still some gaps in the prehistoric reconstruction of the area [36]. The Italian archaeological mission acts in this contest with two different projects. One of them is now concluded and it investigated in detail and with a multidisciplinary approach a Neolithic cemetery (V millennium B.C.) in the north of Sudan (site R12) [37]. The second project is located in the central area of Sudan, south of the capital Khartoum. The knowledge of the northern region is nowadays more complete for the Neolithic period than the one of the central area thanks to the Italian mission. For central Sudan prehistory there is a lack of information because of the obsolete methods adopted in previous excavations and their un-systematic publication. A common problem in

studying this area is the age determination of sites of uncertain attribution. Even if chronological data are available for some archaeological excavations, they do not cover the entire cultural sequence of interest. The specific scientific topic of the Italian project is primarily the transition from Mesolithic hunter-gatherer-fishers to Neolithic pastoral and agricultural societies, a key stage in human history of Sudan [38]. The main feature of the Mesolithic of Sudan is its pottery production, usually more typical of Neolithic societies [38]. Clay workmanship in some contexts dates back to 26.000 years ago (Gravettian) but just for human and animal figurines [29]. However, first attempts of vessels production occurred in hunter-gatherer cultures in Eurasia during the Late Pleistocene/Holocene transition (e.g., [39]). During the Early Holocene there are two cultures of hunters, gatherers and fishers important for their pottery production: Early Jomon culture in the north of Japan [40, 41] and the Mesolithic in the Nile valley/Saharan regions [42, 43]. Pottery technology implies effects on economy, resource management, mobility and organization of hunter-gatherer populations. The study of Sudanese pottery highlights that at the beginning of the seventh millennium B.C. the technology of production was already developed and it is thus reasonable to expect that there was a previous long lasted phase of testing. At the moment there are not firm archaeological evidences of such a stage in the area of concern. The antiquity of pottery production along the Nile Valley and in the Sahara region has been a recurring theme of research in the last years but it is not fully understood yet [42, 43]. The Italian mission made headways in studying the Khartoum Mesolithic, especially thanks to the location and excavation of the site called Al Khiday 1, at about 25 km south of Omdurman [36, 44, 45, 46, 38, 47, 48, 49, 50, 51].

The first structural remains, mud structures of Mesolithic period have been found there together with big fireplaces and pits, never attested before. In this context, the first stratigraphic sequences of the Khartoum Mesolithic emerge from excavation that allow following the evolutionary process of pottery and other materials production technology along two millennia (VII and VI millennium B.C.). It is very difficult to find such condition in sites along the Nile because of a strong erosion, that affects all arid environments, and of the action of anthropic and animal post-depositional events typical of the Sudanese Nile Valley. Nile floods, wind and water erosion, and human and natural disturbances altered the matrix of the soil in powdered deposits without cohesion in which archaeological finds can be more easily displaced. For this reason the original context of deposition is often lost. The main anthropic post-depositional disturbance is due to Post-Meroitic cemeteries built along the Nile. Even if it is usually possible to partially reconstruct the cultural sequence of sites that were reused for different purposes along

history, in this case the construction of Post-Meroitic tumulus graves caused the destruction of the prehistoric deposits. The construction of tumulus-like graves using hearth gathered all around was a common practice from the fourth to the sixth century AD. In this way all the Mesolithic and Neolithic materials were mixed and their primary stratigraphic setting fully disrupted. In some cases archaeological excavations are not possible also because of the presence of modern and contemporary cemeteries [38]. The situation is different at site Al Khiday 1 and it is clear that there are many important reasons to enhance the study of the archaeological material from Al Khiday 1. The archaeological investigation proved the presence of undisturbed archaeological layers that provide unique information to the understanding past events of the entire Nile Valley. Unfortunately, the new international airport of the capital will be built in the next years in this area so that many archaeological sites, both prehistoric and historic, along the west bank of the White Nile will be destroyed and evidences of such an important heritage will be erased.

Since its beginning, the Italian mission was characterized by a multidisciplinary approach, involving different skills for specific material analysis and for palaeoenvironment reconstruction. An important goal of the archaeological mission was the reconstruction of a model for site formation processes along the Nile. The poor preservation of sites induced archaeologists in the past to adopt excavation methods based on arbitrary cuts and the El Sahla project was the first to test the stratigraphic method in such conditions. This approach led to the description of deposition processes of natural and anthropic origin and to the understanding of post depositional events. Several Mesolithic sites were located along the White Nile river bank. The investigated sites show high density distribution of archaeological materials: pottery shards, lithics, bone tools and faunal remains. Neolithic materials are less numerous, probably due to an increase of the mobility that, consequently, makes the sites characterized by less anthropic deposits. Among the Neolithic and Mesolithic sites the best preserved were selected for stratigraphic excavation (10-X-6, 10-W-4, 16 D-5, 16D-4, 16D-4b, Figure 5.1 [36, 38]). The study of neolithisation of the Nile Valley is supported by the palaeoenvironmental reconstruction, because it is well known that climate and natural surroundings played an important role in the determination of human behavior.

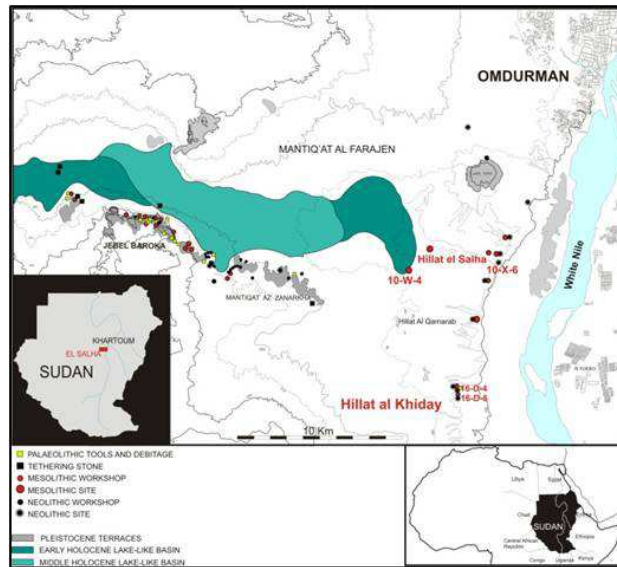


Figure 5.1: Prehistoric archaeological sites distribution in the el Salha region.

5.1 Actual environment and palaeoenvironment along the White Nile

The current climate of the region is arid with average annual temperatures of approximately 30°C and annual average precipitations of 100 mm. Conditions vary seasonally with precipitations concentrated in summer. Past conditions were very different, being characterized by different climate changes occurred in the course of time. The Nile basin during the early Holocene (10.000 BP to 8.000 BP) was characterized by humid conditions and floods along the river. A reduction of humidity and a decrease in floods are attested between 8000 and 7000 BP, but some seasonal floods are still recorded. This period is interpreted as a dry interval occurring during the general humid conditions lasted until mid Holocene. A semi-desert climate trend started about 8000 BP but this was more humid if compared to the present days [52]. A real arid-to hyper arid climate started about 4000 BP (Figure 5.2). Studies on sediments and associated radiocarbon dates of shells and fish bones establish intervals when the river levels were high. These intervals are: around 14.7-13.1 ka, 9.7-9.0 ka, 7.9-7.6 ka, 6.3 ka and 3.2-2.8 ka. Overall, other indication of humidity is the presence of small lakes during the periods of high Nile flow, also in agreement with radiocarbon ages. Palaeoenvironmental reconstruction of Nile basin is of primarily importance in order to

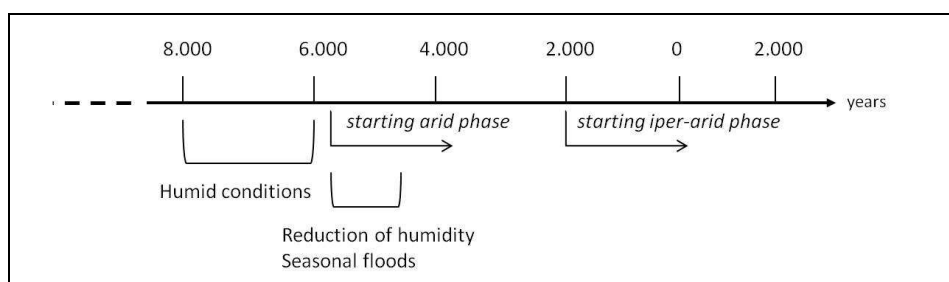


Figure 5.2: Schematic representation of climatic changes of the Nile Valley.

interpret the transition from Mesolithic to Neolithic, which has some specific features in central Sudan. This general issue, that is not the purpose of this work, is a key argument in Nile Valley prehistoric studies and not yet fully understood.

Understanding why and how human population started farming and herding after millennia of hunting wild animals and gathering plants is one of the big challenge for prehistorians and a single explanation is deemed to be unsatisfactory. This may be the case for Cohen's idea that the growth of population required to start food production [53]. This requirement is not realized in the Nile valley, where, on the opposite, agriculture seems to be the cause of the increase of population. The domestication of plants and animals started in the Near East and in the Eastern Sahara and it did not occur at the same time also in the Nile Valley. One possible hypothesis is the lack of farmland due to the persistence of swamps and thus the cultivation started only when the land was physically available. While it is hard to believe that the birth of agricultural societies in the Nile Valley can be directly linked to a previous population growth the hypothesis here mentioned makes it clear that palaeoenvironmental studies are essential to support archaeological interpretation of human behavior. In central Sudan there are not bones of domesticated animals till the appearance of a Neolithic economy around 5000 BC, while in the North of Africa and in the Sudanese Nubia food production is attested already from the beginning of the 6th millennium BC. Although the transition from hunting-gathering-fishing to a farming-herding economy is influenced by different kinds of pressure, demographic being one of them, climate changes seem to be a key factor in the evolution towards food production. The increase of aridity started from the North of Africa and arrived in central Sudan during the second half of the sixth millennium BC, when domesticated species are attested and a Neolithic transformation rapidly took place [45, 54, 55]. It seems appropriate, therefore, to state that

while food producing economies were already developing in Upper Nubia and in Eastern and Western Egyptian desert, Central Sudan prehistoric societies were still having a hunter-gatherer-fisher way of life. Moreover, while in the North a food production economy was achieved through a long period of animal control practices, no evidences of systematic effort to domesticate animals have been found in Central Sudan [56, 57, 58].

5.1.1 El Salha

Sites of archaeological interest are located in the western bank of the White Nile. Most of the sites located in the area surveyed by the Italian project revealed a total absence of stratified deposits and structures than only few sites with a better state of preservation were selected for excavation. They are located on the top of hillocks, placed in elevated position as observed in general for prehistoric settlements and cemeteries in Sudanese territory. Sites are roughly parallel to the river course at a distance between 2.5 and 4 km from the present course of the Nile. Their distribution at the western limit of a dark belt corresponds to the limit of alluvial silt deposited by the flooding of the White Nile. The place where the prehistoric sites are located corresponds to the older fluvial terrace as evidenced by palaeochannels attesting the higher level of the river in the past [59, 60, 61, 62]. The ridges where the archaeological materials are found are characterized by sandy layers with lenses of gravel. On the other hand, the river terrace consists of sand rich in organic matter with calcium carbonate cement. It is difficult to recognize accurately their limits because of the strong erosion affecting this environment. Sediments found in the surveyed area are typical of a climate with alternating wet and arid seasons. During the wet one, the flooding of the Nile enriches the soil in organic matter. The subsequent arid season causes a high and rapid loss of the water as attested by the structure of the sediments: polyedric aggregates, blocky microstructure, desiccation cracks are the consequence of strong evaporation, dissolution and recrystallization of calcite. Related to seasons are also the swamps, an important feature of the territory during prehistoric times because they are strongly connected to human exploitation of natural resources. It is known that during the period between 7800-5900 BC there was a high availability of water in correspondence to high flood level. In general, large Mesolithic possibly permanent settlements are located along the banks of the Nile and seasonal specialized and opportunistic settlements are attested, for example along the inner lagoons, always related to river dynamics [51].

5.2 The excavation at site 16-D-5, Al Khiday 1

The site 16-D-5 is located in the west bank of the Nile; it is a 3.5 m high mound of about 2 hectares. From a more general point of view it is possible to place 16-D-5 in the group of settlements and cemeteries located along an old Nile bank which is higher than the actual Nile flood plain. A modern cemetery is present not far from the 16-D-5 site but fortunately it does not insist on the prehistoric sites under investigation. When discovered, Mesolithic and Neolithic materials were found all over the mound site surface. In 2004, a test trench was opened on the north-western slope because the domed morphology of the top of the mound was surely indicative of post Meroitic earthen tumuli. The surface cleaning attested the presence of inconsistent soil as found in other similar situation (10-X-6 site; [50]). At about 50 cm under the surface, the top of a pit filled with a mix of pottery shards, grinding stones and pestles were found. This turned to be the fill of a post Meroitic pit-grave excavated into the colluvial deposit from a post-Meroitic tumulus responsible of the destruction of the prehistoric deposits. Nevertheless, below the post Meroitic pit grave, shells, lithics and pottery were found, dated 7050-6820 cal. BC. In cleaning the layer a fireplace was identified, the first Mesolithic one recognized in central Sudan with pottery types never attested before. It produced also a pebble with the representation of a boat [63]. After this important result, during the following field season, the colluvial deposit was removed excavating it by artificial cuts and then the stratigraphic method was applied. The evidence of mud structures, identified as the remnants of low walls made with a light brown clay, provided the evidence of a well structured Mesolithic compound (Figure 5.3). The distribution of anthropic materials allowed distinguishing different areas, probably diversified on the basis of special functions. The interpretation of the archaeological data is supported by geoarchaeological analysis aiming at understanding the stratigraphic local context, but also at studying the distribution of settlements in the past in relation to the climate and landscape changes. The geoarchaeological approach has confirmed the archaeological interpretation of the stratigraphy [51]. Mud structures are located in the eastern side and are made of light brown clay while the soil is characterized by a gray silty deposit. A number of materials were found associated to the fireplaces. In the western side the soil is dark gray and it is interpreted as an open space between the structures and the hump at the western limit of the site [36].



Figure 5.3: Structural Mesolithic remains at 16-D-5 site.

5.2.1 Pottery assemblages at 16-D-5

The pottery sequence excavated at site 16-D-5 is representative of the Early and Middle Khartoum Mesolithic Culture covering the years from 7000 to 6200 BC approximately. The most ancient stratigraphic units date back to the beginning of the seventh millennium BC with potsherds belonging to the Wavy Line pottery assemblage. From the same levels new decoration types were found associated to Wavy Line pottery. For the first time pottery shards decorated with *Lunula shaped* motifs and impressed deep dots or drops characterized by a red or yellow slips were discovered providing a first insight in the Khartoum Mesolithic pottery production. New motifs (Rocker Stamp Dotted Zigzag, Rocker Stamp Plain Zigzag and Rocker Stamp Drops motifs) are introduced during the second Mesolithic phase identified at the site, dated to the second quarter of the seventh millennium BC, when Lunula-shaped motifs are no more attested while Wavy Line continues to be present. Around the mid of the millennium new decorations in fan-like patterns occurred, realized by means of combs with different sized teeth which becomes thinner with time. The changing trend in pottery decoration types and temper recipes is consistent with what is known about pottery assemblages of the Late Mesolithic period of the sixth millennium BC. The trend of decoration motifs at 16-D-5 shows an increasing of Rocker Stamp Drops and Rocker Stamp Plain Zigzag patterns, the disappearing of the Lunula-shaped motif and a gradual decreasing of Wavy Line pottery. Temper variability is very large, probably as a result of a household production. Impressed Wavy Line pottery is usually tempered with feldspar and quartz grains with angular

edges (>2 mm), while in the second phase of the sequence it is more often tempered with fine feldspar and quartz grains with angular edges (<1 mm). A similar trend is present in the temper variability of pottery decorated with a rocker stamp dotted zigzag motif. Lunula-type decoration, rocker stamp drops, rocker stamp plain zigzag and scraped potsherds are mostly characterized by sandy tempers in various admixtures with ochre, calcareous grains and vegetal elements. Dotted Wavy Line sherds are mainly tempered with sandy recipes (73.34 %) and to a lesser extent with feldspars and quartz grains with angular edges (26.66 %) [36].

Materials and Methods

Luminescence methods have proven to be a suitable tool for dating archaeological pottery but some limitations are still present, especially for very ancient materials for which the natural signal could be close to saturation. For this reason, different techniques (TL and OSL) are applied, testing different protocols in order to assess the better approach to date prehistoric pottery. On the other hand, archaeological pottery is a recent material for EPR dating compared to rocks and sediments for which the method is well developed. The application of EPR for the dating of pottery is quite a challenging due to the low amount of paramagnetic radiation induced signals per unit of absorbed dose. Furthermore, a strong iron background in Continuous Wave (CW) EPR spectra hides the signal of radiation induced defect centers. Echo Detected EPR was here applied instead of the Continuous Wave method to circumvent this problem. OSL, TL and EDEPR measurements on different pottery shards were intercompared to verify their potential application to measurements of radiation induced defects. A chronological framework of materials was provided by radiocarbon dating of the archaeological stratigraphic unit of provenance and by stylistic features of surface decorations.

6.1 Description of the samples

Twelve pottery shards from Al Khiday 1, 16-D-5 site were selected on the basis of the dimension and the presumed quartz grain temper (Table 6.1). For dosimetric dating, samples have to be thick enough to permit the extraction of the inner portion of material and the amount has to be sufficient not only for the equivalent dose determination but also for the annual dose assessment. In the specific case, a considerable amount of pottery was required because of the application of different techniques (TL, OSL and EPR) and approaches

Table 6.1: Pottery samples with their stratigraphic unit of provenance and related radiocarbon age.

Sample ID	SU	^{14}C dating of SU (BC 2σ cal)	Period
1			
24			
36	5	4708-4487	Neolithic
47			
49			
50			
67			
74	455	7032-6690	Early Mesolithic
75		6814-6572	
82	452		Middle Mesolithic
86			
193	6	7050-6750	Early Mesolithic

(MAAD and SAR) other than petrographic analysis. The quartz content was the second parameter considered because this is the mineral showing the dosimetric properties. The choice was made by observing each potsherd along the cutting surface. These fragments are thought to be the best choice for EPR measurements, which requires very ancient material in order to identify signals that are sufficiently intense for dosimetry. It is important to note that some of them come from the most ancient levels of the site (SU 6 and 455).

Samples of soils were also collected in situ for annual doses determination. The geoarchaeological investigation of the site permits to select a sample of soil representative of all the SU of provenance of the chosen potteries. In Figure 6.1 macroscopic images of Neolithic potsherds are reported. All potteries present a polished surface with decoration, except for the sample 1. A Rocker Stamp motif characterizes four samples: 24 and 36 showing the variant *unevenly spaced dots*, 47 and 49 with the dotted zig-zag pattern. The last sherd (50) has a dotted lines decoration motif.

Mesolithic potteries are shown in Figure 6.2. The sample 67 is a typical Wavy Line pottery while 193 has a Lunula decoration type. The other potsherds show a Rocker Stamp motif with some variants. Samples 74 and 86 are decorated with very deep drops, 75 with Rocker Stamp Drops Fan and 82 with Plain zig-zag motif.



Figure 6.1: The Neolithic potsherds.

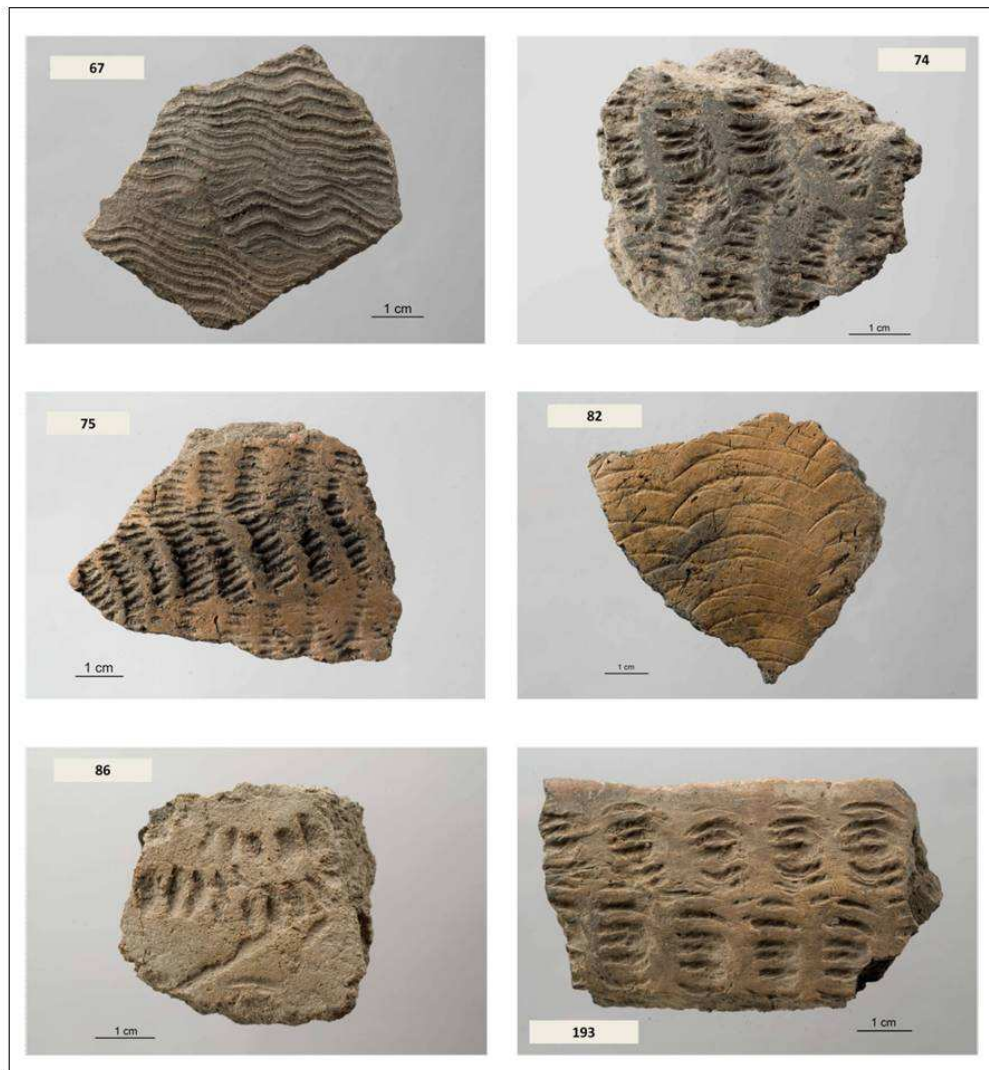


Figure 6.2: The Mesolithic potsherds.

6.2 Annual dose determination

As described in the previous chapters, the water content plays an important role in radiation dosimetry. The first step to determine the effect of moisture was weighing each sample. Potsherds were then soaked in cold water for 24 hours and weighed (weight wet: maximum possible water intake). Potteries were put in an oven at 50°C for drying and a further weight measurement was taken (weight dry). The value of saturation was obtained by the equation:

$$saturation = \frac{weight_{WET} - weight_{DRY}}{weight_{DRY}} \quad (6.1)$$

Alpha dose rate was derived from the total alpha counting using ZnS scintillators discs. The U and Th concentration of potteries and soil were estimated assuming the Th/U ratio equal to 3.16 [3]. The beta contribution to annual dose due to ⁴⁰K content was deduced from the total concentration of K obtained by means of flame photometer (Sherwood Scientific Model 410).

6.3 Samples preparation

6.3.1 Fine grain

The samples were prepared under red light of wavelength >600 nm using the standard procedures. For TL samples preparation, reduced light levels are needed because it was verified that ambient light decreases the signal. For OSL preparation red light is necessary because any other optical stimulation is responsible of the bleaching of the signal. All the samples were prepared following the fine grain technique (subsection 3.2.1).

6.3.2 EPR

For EPR measurement, after the removal of the surfaces, potteries were gently crushed in an agate mortar in order to break the matrix without damaging quartz inclusions. Then the samples were sieved to select the fraction with the grain size of quartz inclusion for each potsherd, determined by the petrographic analysis (section 7.5). For EPR measurements about 0.05 g of material is needed for each aliquot.

6.3.3 Quartz separation

In order to perform a better characterization of the samples and their dosimetric properties, two of them were subjected to a quartz separation. No chemical treatments were adopted but mechanical and magnetic methods of separation were applied. When the grain size was large enough, the pottery was gently crushed in an agate mortar and sieved. Then the minerals of interest were selected by hand-picking under a stereomicroscope. For small-sized tempered sample, the procedure described above was not possible. A hand magnet was used to check the presence and remove magnetic minerals. A Frantz separator allowed collecting the non-magnetic fraction, which consists of almost pure quartz.

6.4 TL measurements and artificial irradiation

TL measurements are performed with an instrumentation allowing the heating of the sample and the collection of its light emission at the same time. The system (Figure 6.3) apt to record the thermoluminescence must provide for:

1. the heating of the sample
2. the detection of the light emission
3. the signal processing

The heating system consists of a chamber of anodized aluminum, containing a stainless steel strip where the disc with the sample is placed. The strip is connected to a thermocouple recording the temperature. The heating must be performed in inert atmosphere by extracting the air from the chamber by means of a vacuum pump and releasing nitrogen. This is necessary since oxygen is responsible of light emission and thus of spurious TL signals. A red rejection color filter is applied to reduce the thermal signal. A photomultiplier tube (PMT) allows the detection of the emitted light and the glow curve is plotted in real time. A BG 12 filter is used in order to select only the wavelengths of emission of quartz and to eliminate the unwanted IR components. Although it could seem a simple experimental equipment, there are two aspects complicating the instrumental system: the low level of the signal and the controlling of the heating rate. The recording of TL is possible thanks to the introduction of the photomultiplier, which is a very sensitive light detector permitting the collection of the weak light emitted by the recombination of electrons and holes. The heating has to be regular and

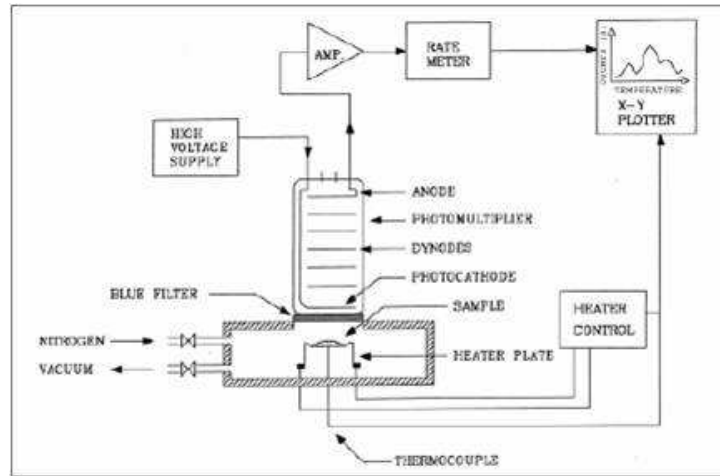


Figure 6.3: The TL system.

fast. The intensity of TL emission is proportional to the heating rate, while the noise and the thermal radiation are independent. However, the heating rate cannot be too high because of the delay in heating between the strip and the sample: the best rate is established between 10° and $20^\circ\text{C}/\text{sec}$. TL glow curves were recorded using a lab designed TL reader based on a photo counting technique with a photomultiplier tube (EMI 9235 QB) coupled to a Corning BG12 blue filter. The samples were heated from 50 to 480°C at the rate of $15^\circ\text{C}/\text{s}$. A preheat treatment of 20s at 200°C was applied. The artificial irradiations were administrated with a calibrated $1.85\text{ GBq }^{90}\text{Sr}/^{90}\text{Y}$ beta source providing $4.40 \pm 0.1\text{ Gy}/\text{min}$ and a $37\text{ MBq }^{241}\text{Am}$ alpha source providing $14.8 \pm 0.1\text{ Gy}/\text{min}$. The data collected were elaborated using the software Cronos 1.3 (Coretech Scientific).

6.5 OSL measurements

The OSL measurements were performed using an automated luminescence system (RisøTL-DA-20, Figure 6.4), equipped with a beta source ($^{90}\text{Sr}/^{90}\text{Y}$) for the artificial irradiation and light emitting diodes (LEDs) for the optical stimulation. The quartz OSL was stimulated by an array of blue LEDs ($470 \pm 30\text{ nm}$) at 125°C for 100s with a constant stimulation power of $54\text{ mW}/\text{cm}^2$. The absence of feldspars was checked using an IR diode array ($830 \pm 10\text{ nm}$) with a stimulation power of $360\text{ mW}/\text{cm}^2$. Samples are deposited on stainless steel discs and loaded onto a sample carousel placed in the measurement chamber where it is possible to create a nitrogen atmo-

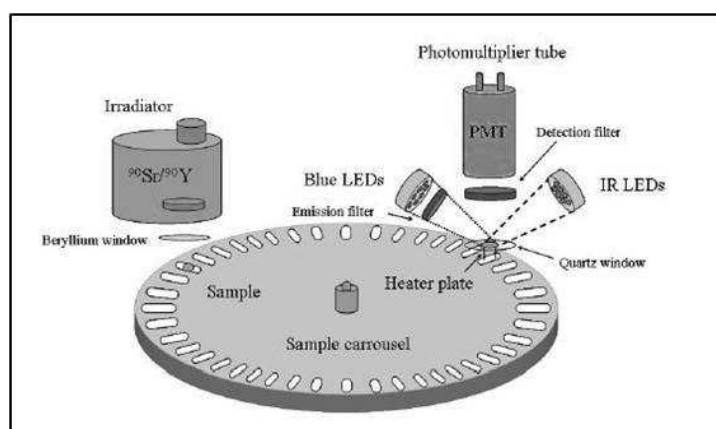


Figure 6.4: Schematic drawing of the OSL reader.

sphere. A heating system provides temperatures from room temperature up to 700°C. The preheat treatment was performed at 200°C for 10 s. Photons were detected by a bialkali photomultiplier tube (EMI 9235QB) coupled to a 7.5 mm Hoya U-340 filter to define the spectral detection window and to prevent scattered stimulation light from reaching the PMT. The intensity of the emitted luminescence is many orders of magnitude smaller than the intensity of the stimulation light and the two wavelengths must be separated in order to permit the collecting of the emitted light.

The test dose suitable for pottery samples was estimated in 20 s of irradiation, corresponding to a dose of 4.6 Gy. The integration range for the equivalent dose estimation was selected in the dose dependent part of the decay curve (first five channels), while the signal integration of the last section of the curve was used for background subtraction. RisøAnalyst software was used for the elaboration of OSL data.

6.6 EPR measurements

In Figure 6.5 the general layout of a typical EPR spectrometer composed by the electromagnet, the microwave bridge containing the source and the detector, the resonant cavity and the console is shown.

Microwaves are produced in the microwave bridge and led by a wave-guide to the resonant cavity in the static magnetic field produced by the electromagnet. The resonant cavity amplifies the incident radiation and the weak radiation from the sample. The amplification is possible since the radiation is reflected several times on the internal side of the cavity. The constructive

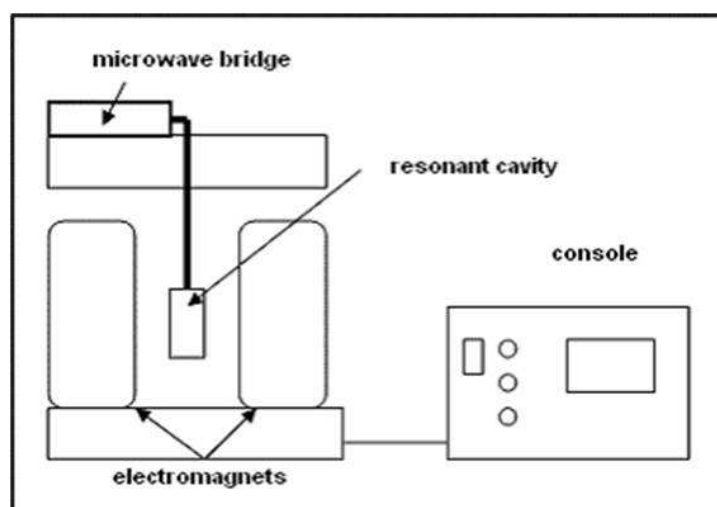


Figure 6.5: Schematic drawing of the EPR spectrometer.

interference generates a wave with amplitude even 100 times higher than the one of the incident radiation. The sample is placed into the resonant cavity in a quartz tube with diameter between 3 and 5 mm. At the resonance frequency, microwaves remain inside the cavity and are not reflected back. Cavities are designed to provide optimal placement of the sample, in correspondence to the minimum microwave electric field and the maximum microwave magnetic field. In such conditions the strongest signals and the highest sensitivity are achieved. The sweeping of the magnetic field is performed by changing the current in the electromagnet coil. When the spin transition occurs, the sample absorbs the radiation, generating a reflected wave reaching the microwaves bridge through the wave-guide. The detector is able to convert the radiation in a proportional electrical signal. In order to obtain a better signal/noise ratio, the modulation of the signal is performed. Spectra are usually collected by superimposing an oscillating (usually at 100 KHz) magnetic field between 0.01 mT and 1 mT to the applied magnetic field. During the spin transition, the intensity of the reflected wave oscillates with the same frequency of the modulation field. A specific filter, called Lock-in filters out all the frequencies different from 100 kHz that are not in phase with the modulation field. In this way, the electrical noise is strongly reduced and the signal/noise ratio is improved. As a consequence of the modulation method of CWEPR acquisition, the CWEPR signals coming out of the Lock-in looks like the first derivative of the absorption spectrum. The *normal* absorption spectrum could be recovered by digital integration of the

Lock-In CWEPR spectrum, but it is praxis in the EPR community to show the CWEPR spectrum as it results experimentally. The console contains signal processing, control electronics and a computer. The computer is used for analyzing data as well as coordinating all the units for acquiring a spectrum. Both CW and Pulsed EPR measurements were made on an ELEXYS Bruker spectrometer equipped with a dielectric resonator and Oxford CF 935 flow cryostat. The Echo detected spectra are obtained by the acquisition of the two pulse Electron Spin Echo while sweeping the magnetic field. The echo intensity is recorded as a function of the magnetic field. The typical Hahn sequence ($\pi/2$ - τ - π - τ -echo) was used. The artificial irradiations were administrated with a calibrated $^{90}\text{Sr}/^{90}\text{Y}$ beta source (dose rate 0.14 Gy/s).

6.7 XRF analysis

The bulk chemistry of the samples was determined by X Ray Fluorescence spectroscopy [64, 65]. The external surface of each shard was cleaned from possible alteration with a micro-drill and then ground in powder in an agate mortar. A known amount of powders (nearly 1.5 g) was heated in a furnace at 860°C for about 20 minutes and then at 980°C for about 2 hours for the determination of loss on ignition (L.O.I.). The L.O.I. can be affected by the volatile elements present: hydrogen, oxygen and carbon that are not determined by XRF and are related to the organic matter and the water of primary phases or anions, such as CO_3 , originally present. Samples was then prepared as glass beads mixing 0.65 g of the calcined powder and the flux di-lithium tetraborate $\text{Li}_2\text{B}_4\text{O}_7$ with a dilution ratio of 1:10 and melted with a fluxer Claisse Fluxy (1150°C). The samples analysis were carried out on a WDS sequential Philips PW2400 spectrometer, operating under vacuum conditions equipped with an 3kW Rh tube, five analyzing crystals (LiF220, LiF200, Ge, PE, TlAP), two detectors (flow counter and scintillator), three collimators (150 μm , 300 μm and 700 μm) and four filters (Al 200 μm , Brass 100 μm , Pb 1000 μm and Brass 300 μm). The quantitative and qualitative analyses were performed with the software package SuperQ, the concentration of the major and minor elements expressed as percentage of their oxides (SiO_2 , TiO_2 , Al_2O_3 , Fe_2O_3 , MnO , MgO , CaO , Na_2O , K_2O , P_2O_5) and of trace elements expressed in ppm (Sc, V, Cr, Co, Ni, Cu, Zn, Ga, Rb, Sr, Y, Zr, Nb, Ba, La, Ce, Nd, Pb, Th, and U) were detected with a precision within 0.6% relative for major and minor elements, and within 3% relative for trace elements. The concentrations were obtained using a calibration line performed with International geological standards [66].

Results and discussion

7.1 Annual doses

In Table 7.1 the parameters used for dose rate calculation of pottery samples and surrounding soil are summarized.

In the light of the available information on the humidity of the site, the pottery was assumed to have been in saturation for 50% of the time. It should be noted that all the annual doses calculated are in the range of the typical values observed in pottery with the exception of the sample 67. For this sherd, a high dose rate is obtained due to the high potassium content. The petrographic analysis of the sample revealed a considerable amount of K-feldspar in the temper (unlike the other sherds containing only quartz) responsible of the high value of internal dose rate. ^{40}K is concentrated in feldspar grains where it forms part of the lattice structure while in quartz is present only as an impurity. The a-value, which takes into account the different efficiency of alpha particles in inducing TL, was calculated for each sample. It varies between 0.098 and 0.34 and it is in accordance with reported a-value for polymineral fine grain pottery samples, being the range from 0.05 to 0.5.

7.2 TL

7.2.1 TL MAAD

The MAAD glow curves in Figure 7.1 are representative of the behavior of all the samples. Different aliquots were used for measuring the natural signal and the artificial irradiation induced signal (different from sample to sample). Low temperature peaks are not present since aliquots were preheated for 10 s to 200°C. Both natural and irradiated aliquots show a broad peak centered

Table 7.1: Annual dose estimation of the potsherds.

Sample ID	Water content H ₂ O sat % (± 10%)	%K ₂ O (± 3%)	ppm U (± 5%)	ppm Th (± 5%)	Annual dose (mGy/y)
1	9.7	1.2	1.01	3.20	2.82±0.13
24	13.9	1.57	1.42	4.48	3.46±0.17
36	9.6	1.29	1.10	3.48	2.97±0.14
47	6.7	0.56	1.80	5.70	2.23±0.11
49	11.2	1.13	1.81	5.72	3.62±0.17
50	9.6	1.05	1.84	5.81	2.99±0.14
67	7.8	4.00	3.72	11.77	8.90±0.4
74	11.1	1.24	0.92	2.91	2.44±0.12
75	12.0	0.83	1.33	4.20	2.77±0.13
82	8.5	0.29	1.17	3.68	2.86±0.14
86	11.2	0.89	1.53	4.85	3.19±0.15
193	10.0	1.52	1.61	5.08	2.54±0.12
soil		0.47	1.50	4.75	

around 350°C. Based on the plateau test that allows to identify the thermally stable portion of the curves [3], the TL signals were integrated between 350 and 400°C.

In order to calculate the equivalent dose, a growth curve was constructed as reported in Figure 7.1 where luminescence counts are plotted versus the additive dose. The equivalent dose is calculated by extrapolation. It was not possible to apply the MAAD protocol to the sample 67 because of the saturation of the TL signal due to the high annual dose value. A similar behavior of saturation was observed also for the sample 193. Potteries for which the protocol was successfully applied are reported in Table 7.2 with their equivalent doses.

7.2.2 TL SAR

The equivalent doses obtained for the TL SAR protocol are calculated as averages values obtained from multiple sub-sample (minimum 3 maximum 7) for each potsherd. The samples did not show any change in sensitivity and TL emissions were therefore not corrected for the test dose. The steps of the SAR protocol were thus the following:

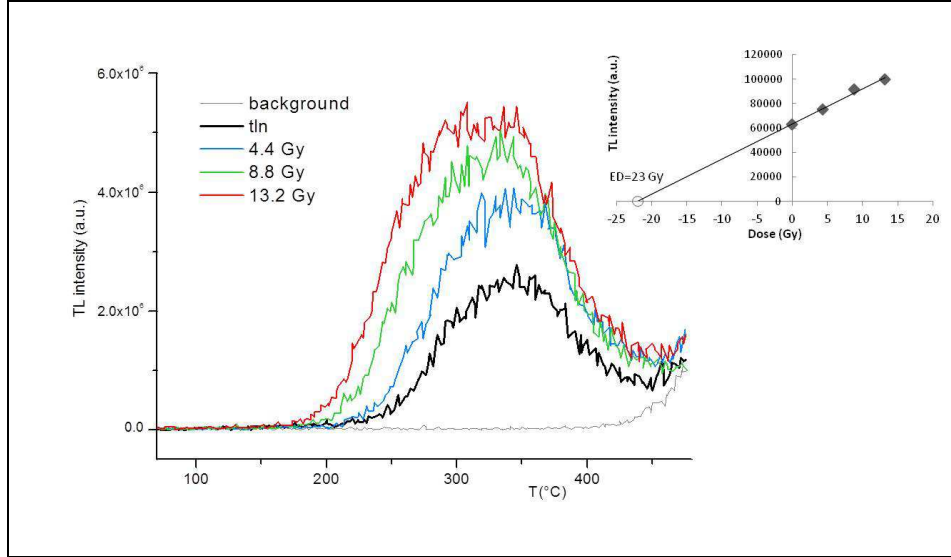


Figure 7.1: TL MAAD glow curves (left) and related growth curve (right) of sample 49.

Table 7.2: Equivalent doses estimated with the TL MAAD protocol.

Sample ID	Equivalent dose (Gy)
1	22.0 ± 2.0
24	26.0 ± 3.0
36	32.0 ± 2.1
47	18.0 ± 1.6
49	22.0 ± 2.1
50	18.3 ± 1.7
74	16.2 ± 1.6
75	25.0 ± 2.3
82	24.8 ± 2.6
86	26.0 ± 2.3

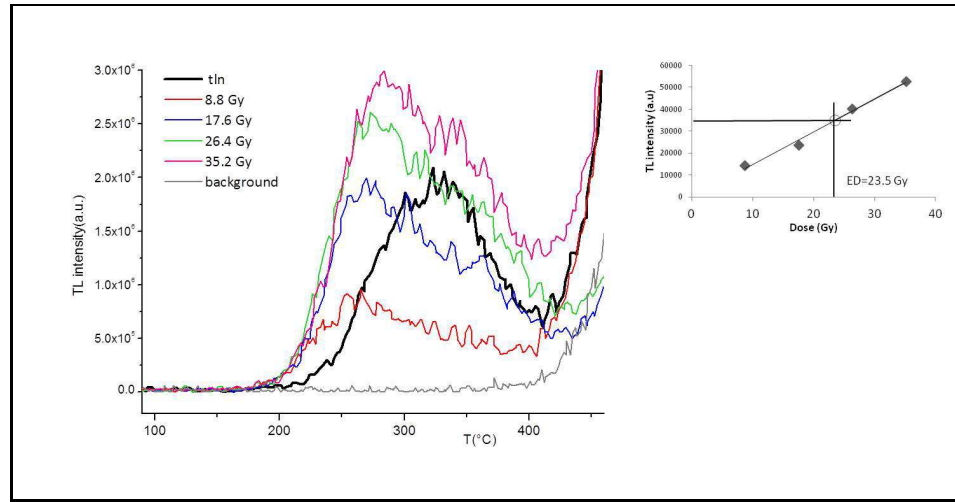


Figure 7.2: TL SAR glow curves (left) and related growth curve (right) of sample 49.

1. TL : L_0
2. Dose D_i
3. Preheat (200°C 10 s)
4. TL: L_i
5. Repeat steps 2-4 with different D_i

In Figure 7.2 an example of SAR TL emission curves and related growth curve as a function of the artificial dose is shown. Unlike the MAAD protocol, this method interpolates the natural signal onto the growth curve for each aliquot of the same sample and the equivalent doses obtained are then averaged out.

Two different shapes of regenerative peaks can be observed in pottery samples. The artificial irradiated signals of the samples 1, 24, 36, 49, 50, 74 and 193, exhibit a dominant peak at about 270°C with a shoulder at 340°C (Figure 7.2). The other samples are characterized by a broaden peak between 260° and 340°C as observed in Figure 7.3. As will be discussed later on, the distinction of the two groups is due to the difference in granulometry and distribution of the quartz temper in the potteries. The samples showing two well distinct peaks in the glow curve have an average grain size of quartz inclusions under $300\ \mu\text{m}$. The others are characterized by a broaden peak

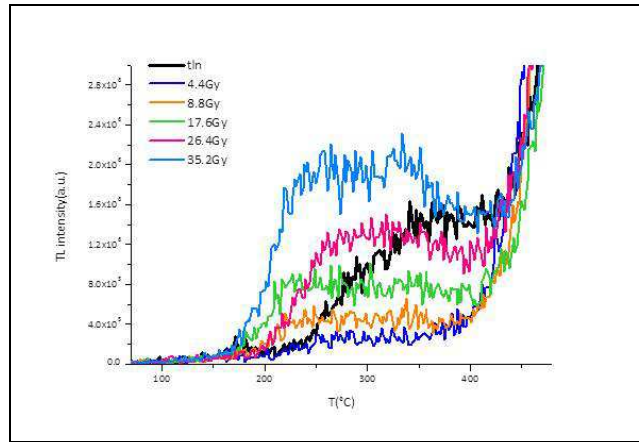


Figure 7.3: TL SAR glow curves of sample 82 showing the broadening of the peaks between 260°C and 340°C.

between the two main quartz TL emission including samples with larger grain size. The poor resolution of the peaks could be related to the quartz shortage in the aliquot. The sample preparation procedure for the fine grain technique selects only the fraction between 4-11 microns which is present only in small amount in potsherds characterized by large grain size temper.

The mean values of equivalent doses with their errors obtained for the samples are listed in Table 7.3. For sample 86 there was not enough material for the application of the SAR protocol.

7.3 OSL

The SAR protocol was adopted also for the estimation of the equivalent dose by means of OSL. On the basis of the potsherd size, a number between 5 and 21 of aliquots were measured for each sample. The small sample size precluded the measurement of potsherds 24 and 50. A typical shine-down curve and related growth curve used for the interpolation of the equivalent dose are reported in Figure 7.4.

The steps of the SAR protocol (subsection 3.2.1) were the following:

1. Preheat (200°C 10s)
2. OSL : L_o
3. Test Dose

Table 7.3: Equivalent doses estimated with the TL SAR protocol.

Sample ID	Equivalent dose (Gy)
1	22.0 ± 1.0
24	23.0 ± 0.5
36	31.4 ± 0.9
47	14.8 ± 0.1
49	21.5 ± 0.6
50	18.2 ± 0.3
67	52.6 ± 3.5
74	28.7 ± 0.9
75	27.1 ± 0.8
82	26.1 ± 0.8
193	24.2 ± 0.6

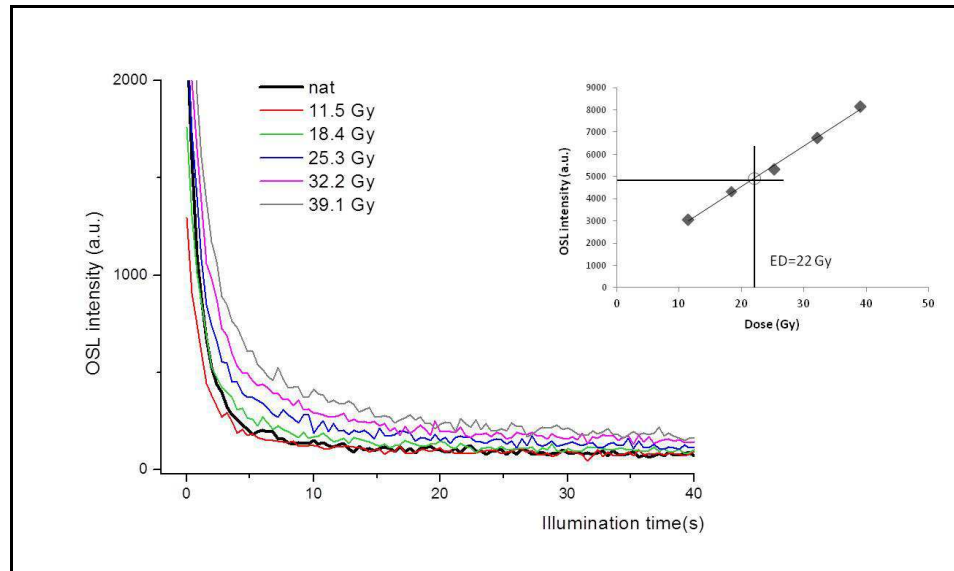


Figure 7.4: OSL SAR shine-down curves (left) and related growth curve (right) of sample 49.

4. Preheat (180°C 10s)
5. OSL: T_0
6. Dose D_i
7. Preheat
8. OSL: L_i
9. Test Dose
10. Preheat
11. OSL: T_i
12. Repeat steps 6-11 with different D_i

The integration range used to obtain the OSL growth curves dose was selected in the first part of the curves (the first five channels corresponding to the first 1.6 t seconds of acquisition were considered). The last section of the curve is considered to be independent from the dose and used as background (last 20 s of acquisition). Quartz and feldspars react differently to the wavelength of light stimulation. Pottery selected for dating are characterized by quartz inclusion but at the end of the SAR sequence an irradiation in the IR range was performed in order to verify any contribution by feldspar to the OSL signal of the mixed minerals aliquots of the samples. An IRSL contribution was recorded for samples 49, 67, 74, and 193. The recycling ratios and the recuperation tests results indicate that the OSL SAR is suitable for dating these samples. The fading rate (rate of luminescence loss in absence of a source of stimulation) was measured for all the samples [21]. The equivalent doses were calculated taking into account the effect of fading, however a general underestimation affects the results. Fading is critical for the OSL emission of sample 67. As previously described, this sample has a temper characterized by a considerable amount of feldspar, a mineral affected more than quartz by the anomalous fading. The SAR OSL mean values of equivalent doses are listed in Table 7.4.

7.4 Comparison between luminescence ages

The ages obtained with each procedure of luminescence dating (TL MAAD, TL SAR and OSL SAR) are shown in Table 7.5. The ages express the years passed since the firing of the potteries and are obtained by dividing the

Table 7.4: Equivalent doses estimated with the OSL SAR protocol.

Sample ID	Aliquots	Equivalent dose (Gy)
1	13	16.0 ± 0.5
36	7	17.3 ± 0.4
47	21	15.1 ± 0.7
49	5	20.0 ± 0.5
67	15	29.9 ± 0.7
74	20	28.7 ± 0.9
75	10	25.1 ± 0.4
82	20	25.2 ± 0.5
86	10	23.1 ± 0.3
193	20	20.8 ± 0.9

equivalent dose by the corresponding annual dose rate. Errors, calculated following the standard procedures [3], ranged from 5 to 15%.

The results obtained with MAAD technique had, as expected, the highest errors, being the extrapolation procedure intrinsically less precise than interpolation. For only 7 over 12 samples the equivalent doses estimated by the different protocols are in agreement within 1σ . In the remaining cases, high discrepancies are observed without any systematic trend. The statistic treatment of data allows getting a thorough analysis of the results. The samples were not individually considered but grouped in the two periods Mesolithic and Neolithic. The 15 data obtained for the Mesolithic samples and the 16 for the Neolithic ones were separately considered. To establish if some results were likely to be spurious, the Chauvenet criterion for deletion of outlier data was applied, assuming that the experimental data were normally distributed. Thus the following data were rejected: 67 SAR OSL, 36 MAAD TL and 36 SAR TL. For the two groups of samples (Mesolithic and Neolithic) and for the sub-classes based on techniques and protocols (TL MAAD, TL SAR and OSL SAR) mean, standard error, weighted mean and error of the mean have been evaluated as reported in Table 7.6.

The mean attributed the samples to the correct period, but with a high standard error (about 20% in some cases). The attribution to Mesolithic and Neolithic period is not distinguishable if the confidence level is $\pm 2\sigma$. However, the weighted mean allows a better distinction of the groups with an error noticeably reduced. A visual representation of the distribution and precision of the data is given in Figure 7.5.

Luminescence techniques correctly dated the set of prehistoric potteries.

Table 7.5: Ages of pottery samples obtained with the luminescence techniques expressed in years BP. The first group (samples 1-50) comes from Neolithic layers, US radiocarbon dating 6240-6460 BP cal 2σ ; the second group (samples 67-193) from Mesolithic layers, US radiocarbon dating 8510-9060 BP cal 2σ .

Sample ID	TL MAAD	TL SAR	OSL SAR
1	7810±790	7800±500	5680±310
24	7510±940	6640±350	
36	10760±870	10560±580	5830±300
47	8070±820	6640±330	6760±460
49	6070±620	5940±320	5520±290
50	6120±630	6080±300	
67		5930±480	4760±170
74	6650±730	11770±690	10280±530
75	9030±930	9780±540	7730±390
82	8680±1000	9140±530	8830±460
86	8160±810		7240±350
193		9510±500	8160±520

Table 7.6: Statistical treatment of the ages divided for periods (Mesolithic, first group; Neolithic, second group) and methods (TL MAAD, TL SAR and OSL SAR).

	#	Mean age	St. dev.	Weighted mean age	Weighted calendar age (BC)	Error (1σ)	Error (%)
All	14	8630	1510	8600	6590	220	2.6
MAAD	4	8130	1050	7900	5890	360	4.6
SAR TL	5	9230	1770	9150	7140	240	2.6
SAR OSL	5	8450	1180	8050	6040	200	2.5
All	14	6600	860	6100	4090	100	1.6
MAAD	5	7710	1720	7350	5340	620	8.2
SAR TL	5	7280	1740	6550	4540	1060	2.4
SAR OSL	4	5950	560	5750	3740	160	2.8

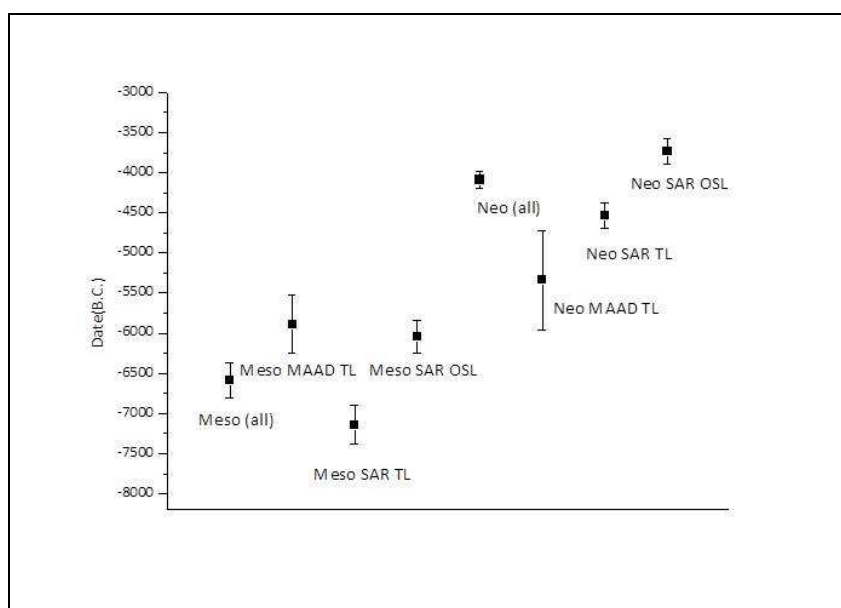


Figure 7.5: Distribution of the ages.

The correlation between luminescence ages (accepting the error limit) and the stratigraphic unit chronology is higher for Neolithic samples and less precise for the Mesolithic ones. For both the groups, the less precise and more spread results are given by the additive dose protocol, while the single aliquot regenerative dose protocol was systematically more precise and accurate. The blue stimulated OSL emission of polymineral fine grain samples gives good results even in absence of quartz separation from the matrix. This is due to the richness in quartz characterizing the temper of these samples.

7.5 Petrographic analysis

7.5.1 Optical Microscopy

The Optical Microscopy is a powerful tool in archaeometry since it is possible to collect in relatively short time different kind of information about the sample. Potteries are prepared in thin section (thickness of $30\ \mu\text{m}$) and studied under a transmitted light microscope in order to describe them in terms of minero-petrographic and microstructural features following the method proposed by Whitbread [67]. It is mainly based on the characterization of matrix, voids and inclusion in pottery thin sections. Particular attention was paid here for the analysis of the size and the size-distribution of the quartz

inclusions.

Matrix

The pottery matrix is defined as the fine-grained groundmass of the clay minerals, fine silt and possible glassy material formed during the firing process. The particles size is less than 10 μm . The matrix is described in terms of homogeneity, orientation and optical state. The homogeneity considers the spatial distribution of textural elements of the ceramic body; heterogeneities may occur with respect of the types of the voids and their distributions, the nature of inclusions and their concentration. The orientation refers to the arrangement in a preferential direction of micas, clay minerals and pores; matrix can be oriented or isotropic. The optical state is the optical activity observed upon rotation of the thin section under crossed polars. In the groundmass, clay minerals can be parallel aligned forming units called domains. If they display interference colors and extinction, the groundmass is optically active. Otherwise, if no changes in rotating the thin section are observed, the matrix is optically inactive. The optical activity depends on the firing temperature, as well as on the grain-size of the clay minerals flakes and aplastic inclusions forming the matrix, on the quantity of the organic matter and opaque minerals.

Voids

The voids in the ceramic body are classified as primary and secondary. The first term is referred to pores formed during the processing of raw materials caused for example by an excessive speed in working the clay. Secondary voids are instead due to the shrinkage of the clay and the decomposition of clay minerals, carbonate phases and organic remains during the firing process. The amount of pores is estimated as a percentage, by comparing the field of view at the microscope with the chart reported in Figure 7.6.

The voids shape description is based on the classification of the pores in four different types (Figure 7.7):

- planar voids: they are linear in thin section but planar in three dimensions, width is variable, frequent and sub-angular changes in direction may be noted
- channels: they may be linear in thin section, they are cylindrical in the three dimensions
- vughs: they are relatively large and irregular voids
- vesicles: they are regular in shape with smooth surfaces

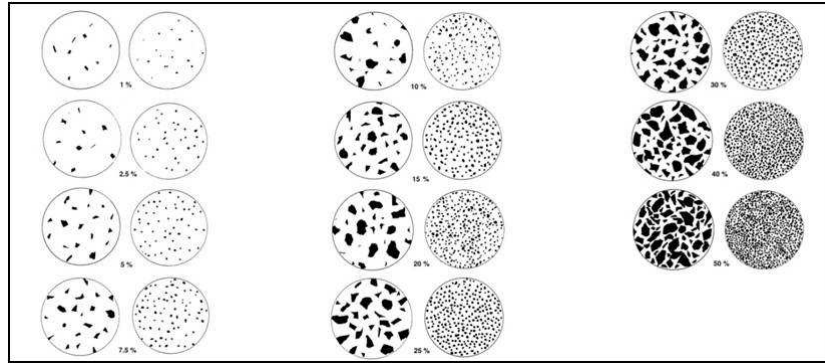


Figure 7.6: Diagram for the visual estimation of the percentage composition of the textural elements [68].

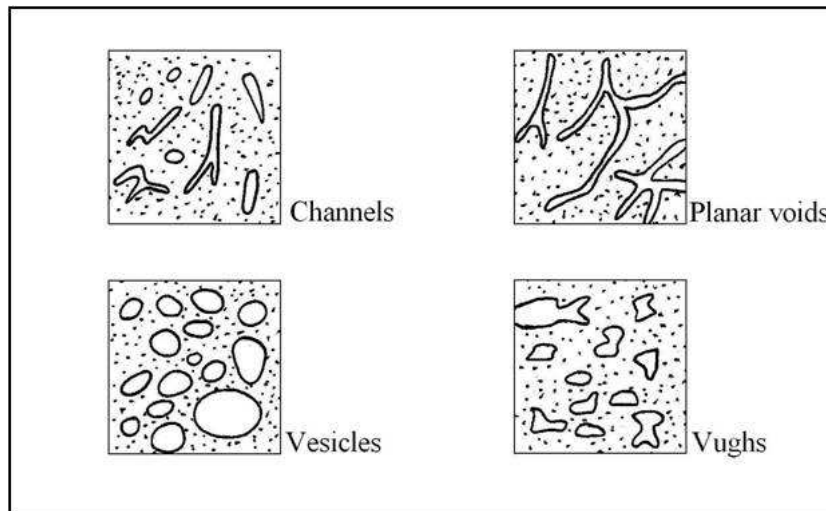


Figure 7.7: Voids shape in thin section [69].

The voids size is measured at the microscope they are classified by average diameter size [69] in mega (>2 mm), macro (0.5-2 mm), meso (50 μm -0.5 mm) and micro (<50 μm).

Inclusions

Minerals and rock fragments with size above 10 μm are defined as inclusions. They are responsible of the reduction of the plasticity, determining a lower shrinkage of the artifact in the drying period. Inclusions play also an important role in the leaking of gases and water vapor during the firing process, thus leading to a general improvement of the quality of the finished product. They can be naturally mixed to the clay or deliberately added by the potter (in this case called temper). The amount of inclusions is defined by the estimation of the c:f ratio that represents the relative proportion of the coarse (c) and fine (f) components of the fabric on the basis of their size larger or smaller than 10 μm . The c:f ratio is expressed as a percentage, without estimating the voids areas; when they are considered the c:f:v ratio is used. The approximate measure of the packing of inclusions within a fabric is defined as the c:f related distribution. Most of the ceramics shows a porphyritic related distribution in which the coarse particles (c) occur in a dense groundmass (f). The c:f related distribution can be:

- close-spaced: grains have points of contact;
- single-spaced: the distance between grains is equal to their mean diameters;
- double-spaced: the distance between grains is equal to double their mean diameters;
- open-spaced: the distance between grains is more than double their mean diameters.

The description of the inclusions is performed by visual comparison of the chart in Figure 7.8, where the different types of roundness are reported. Roundness is the degree of rounding of edges and corners of a grain: angular (A), sub-angular (SA), sub-rounded (SR), rounded (R), well-rounded (WR).

In the inclusions characterization, maximum, average size and grain-size distribution are indicated. Finally, minero-petrographic analysis allow studying shape and habit, colour and pleochroism, cleavage, relief and possible twinning, zoning and alterations of the crystals in plane-polarized light, and interference colors with crossed polar; the examination of microstructures and mineralogical associations leads to the definition of rock-type.

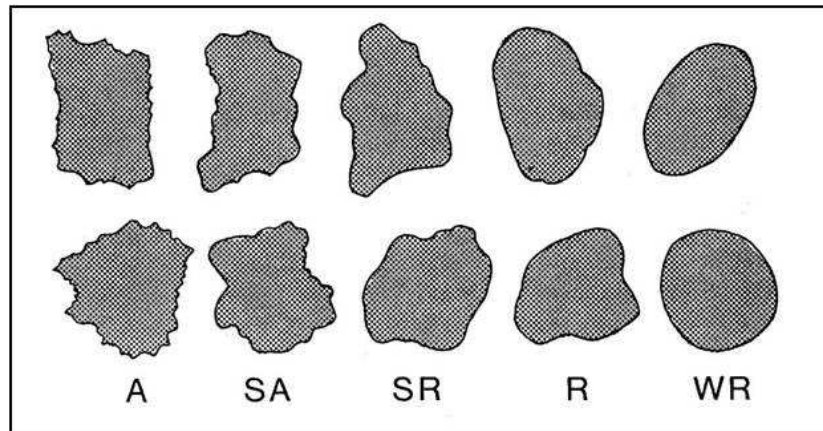


Figure 7.8: Main roundness classes [70].

The potsherds from Al Khiday, analysed in thin section under the transmission light microscope, were divided into two petrographic groups:

- *Feldspar-rich potsherd* (sample 67, Figure 7.9): it is characterized by a homogeneous and optically inactive groundmass. Voids (Table 7.7) are the 20% of the total area, with irregular (vughs) and elongated (channels and planar voids) shapes. Inclusions are abundant (c:f = 60:40), with a seriate grain-size distribution, maximum and average size of 1300 and 450 μm , respectively. They are angular shaped and composed of dominant alkali feldspar (microclin-perthite), subordinated quartz, and rare crystals of plagioclase, biotite, amphibole, pyroxene, chlorite and opaque minerals (Tables 7.8, 7.9, 7.10).

- *Quartz-rich potsherds* (samples 1, 24, 36, 47, 49, 50, 74, 75, 82, 86 and 193, Figure 7.10). Most of the samples belong to this group, which is characterised by potsherds with a homogeneous groundmass, in some cases showing an optical activity (samples 49, 74 and 86). Voids (Table 7.7) are between 15% and 30% of the total area, mainly with elongated shapes, such as planar voids and channels, and occasionally vughs. In many cases the presence of a reduced matrix surrounding some large voids, indicates that they derive from the decomposition for combustion of chaff (samples 50, 67, 74, 75, 82, 86). Inclusions (Tables 7.8, 7.9, 7.10) are predominantly quartz with sub-angular shape and occurring as single crystals, polycrystalline quartz, chert and sandstone fragments. Rare alkali feldspar (microcline and perthite), plagioclase, biotite, chlorite, white mica, amphibole, pyroxene and opaque minerals are also present, occasionally associated to ARF (argillaceous rock fragment) and ochre fragments.

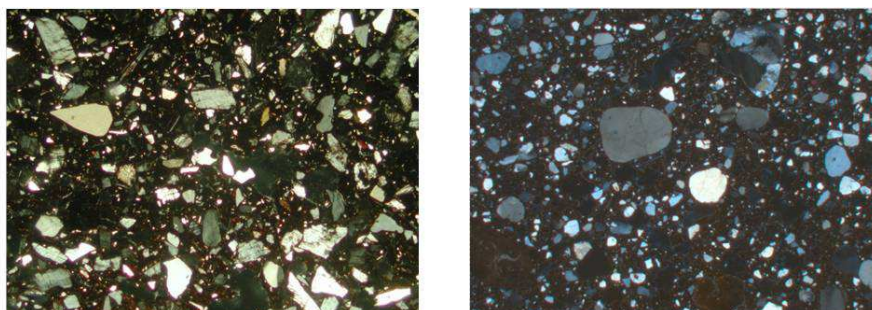


Figure 7.9: Microphotograph of the feldspar-rich sample (67, left) and of a quartz-rich sample (75, right); cross polars, image width: 8 mm.

Table 7.7: Structural features of pottery samples analyzed under optical microscope: voids. Abbreviations: PV: planar voids, Ch: channels, Vu: vugh, Chaff: voids derived from chaff decomposition.

Sample ID	%	PV	Ch	Vu	Chaff
1	20	•		•	
24	15			•	
36	20			•	
47	20	•	•		
49	20	•		•	
50	25	•	•		•
67	20	•	•	•	•
74	30	•	•		•
75	25	•	•		•
82	20	•	•	•	•
86	25	•	•		•
193	15		•	•	

Table 7.8: Structural features of pottery samples analyzed under optical microscope: inclusions. Abbreviations: Distribution: SE: seriate BI: bimodal IA: iatal.

Sample ID	c:f ratio	Max size (μm)	Average size (μm)	Distr
1	25:75	800	250	SE
24	25:75	350	100	SE
36	50:50	300	150	SE
47	50:50	1800	350/100	SE/IA
49	25:75	600	200/80	IA
50	50:50	600	300	SE
67	60:40	1300	450	SE
74	50:50	1100	400/150	BI
75	60:40	2000	800/350	BI
82	60:40	1400	700/200	BI
86	50:50	900	350	SE
193	40:60	200	80	SE

Table 7.9: Structural features of pottery samples analyzed under optical microscope: inclusions. Abbreviations: Shape: A: angular, SA: sub-angular, SR: sub-rounded, R: rounded, W: well-rounded; c:f RD: c:f related distribution : Cs: close spaced, Ss: single-spaced, Ds: double-spaced, Os: open-spaced.

Sample ID	A	SA	SR	R	W	Cs	Ss	Ds	Os
1		•	•				•		
24		•	•					•	
36		•				•			
47		•		•		•			
49		•	•					•	
50		•	•			•			
67	•	•		•		•			
74		•	•				•		
75		•		•		•			
82		•		•			•		
86			•	•			•		
193	•	•					•		

Table 7.10: Composition of inclusions: qtz: single crystals of quartz, qtzp: polycrystalline quartz, qtzm: chert, AR: sandstone fragments, Kfs: alkali feldspar, Pert: perthite, Pl: plagioclase, Ms: muscovite, Bt: biotite, CS: sparitic calcite, CM: micrite, An: amphibole, Pyr: pyroxene, Rt: rutile, Chl: chlorite, Oliv: olivine, ARF: argillaceous rock fragment, Ochr: ochre fragment, granite. Abundance of mineral phases: xxxx: predominant (>70%), xxx: dominant (50-70%), xx: frequent (30-50%), x: common (10-30%), +: few (2-10%), -: rare (<2%).

ID	qtz	qtzp	qtzm	AR	Kfs	Pert	Pl	Ms	Bt	CS	CM	An	Pyr	Rt	Chl	Oliv	ARF	Ochr	Gran
1	xxxx	xx	-					-					-			-			
24	xxxx	-		-	-		-	-				-	-						
36	xxxx	x	x	xx	-		-	-				-	-		-	-	-		
47	xxxx	x	-	xx	-		-						-						+
49	xxxx	-		+			-	-					-	-			-		-
50	xxxx	x	-	x	-		-	-				-	-		-		-		
67	xxx	x	+	+	xx	xx	-	-	-			-	-						-
74	xxxx			-	-		+	-				+	+						
75	xxx	xx	-	x			-				x	-	-			-			
82	xxxx	x	-	+	-		-	-				-	-						-
86	xxxx	-		+	-		-	-				-	-						-
193	xxxx				-		-	-				-	-		-	-			-

Abundance and grain-size distribution of inclusions is very variable, and different situations can be defined. More in detail, c:f ratio are: 25:75 (samples: 1, 24, 49), 40:60 (sample 193), 50:50 (samples 36, 47, 50, 74, 86), 60:40 (samples 75, 82). Two different grain-size distributions can be observed in the samples: seriate unimodal (samples 1, 24, 36, 50, 86, 193) and bimodal (samples 47, 49, 74, 75, 82). The inclusions different from quartz were considered negligible for dating purpose due to their rarity. The active matrix observed for three samples could be an indication of low firing temperatures. Even not very high, the temperature reached during firing was sufficient to reset the geological signal of the raw materials. As attested by TL glow curves, the emissions are not affected by partial bleaching of the signal, a phenomenon observed when a residual luminescence is present.

7.5.2 Digital Image Analysis (DIA)

Since quartz-rich samples are highly dissimilar in terms of grain-size distribution (Table 7.8), it is not possible to distinguish homogeneous groups. Therefore, in order to describe properly the grain-size distribution, a quantitative approach had to be carried out through digital image analysis (DIA). DIA was traditionally gained by visual estimation, a method relatively fast but with low accuracy and reproducibility, or by point counting, a method that has higher accuracy but very time consuming ([71, 72, 73, 74]). Here, computerized analysis of digital images was performed representing a considerable saving in time and increasing the precision and reproducibility of the work. The following protocol was adopted for DIA of quartz-rich potsherds. A set of about 5-6 images, covering all the sample section, were taken for each sample under optical microscope at cross polars. The images were then processed using the graphical software package ImageJ (1.44p National Institute of Health, USA). Each image was converted into 8-bit grey-scale, and a series of pre-processing steps were done to improve the quality of the image before being segmented. In particular, the brightness and contrast were enhanced and the noises were reduced and smoothed with a median filter. The noise reduction was performed removing the outliers through an algorithm which replaces a pixel by the median of the pixels in the surrounding, if it deviates from the median by more than a certain value (chosen by the operator). This procedure was also useful to correct faulty pixels. The files were saved as TIFF type (Tagged Image File Format), an uncompressed file format that prevents the loss of image quality. Then, the segmentation was carried out through an unsupervised classification mode, using MultiSpec (version 3.3, Purdue Research Foundation). The image segmentation is the process of partitioning a digital image into several segments, or sets

of pixels, in order to simplify its representation in a second image that is more meaningful and easier to analyze. Partition usually defines homogeneous regions which cover the entire image, without intersections. Every pixel is assigned to one segment. In the unsupervised classification (clustering), the grey tones were assigned to a set of 25 arbitrary classes, covering all the range of grey values of the image (from black to white, 0-255). Different mineral phases or textural features may not correspond to a single class, but could be described by more classes. In this case study, since the DIA was performed on images obtained under the optical microscopy in cross polars, quartz inclusions display a variable interference colour. This is due to the orientation of the optical axes of the minerals with respect to the polars, showing all the grey tones from the white (maximum birefringence when parallel to the optical axes) to the black (perpendicular to the optical axes or in extinction position). Quartz inclusions were assigned by the operator, grouping successive classes (between 10 and 12) using ImageJ, and converted to a binary image. This method allows obtaining a segmented representative image (binary image), in which the selected quartz grains do not suffer of problems connected with extinction. An ongoing research (Maritan, personal communication) on the degree of similarity between the particles distribution of a sample as detected using different acquisition methods (cross polars optical microscopy, back-scattered scanning electron microscopy SEM-BSE, and microchemical mapping under scanning electron microscopy) indicates that the results achieved by the approach here adopted are reliable. After the segmentation, further manual treatment of binary images is required in order to reduce disturbances and obtain a more correct representation of the analysed phase. Particle analysis on the binary images allowed extracting the Minimum Feret diameter (MinFeret) of quartz grains. Min Feret is defined as the shortest distance between any two points along the selected grain boundary, which corresponds to the minimum size of quartz inclusion. The use of MinFeret diameter to describe the particles size was chosen for their similarity with parameters used in sedimentology researches, in particular to grain size obtained by sieving method (the most used method to define grain-size curve in sedimentology). More in detail, grain-size distributions were described by means of frequency distribution diagrams of the MinFeret vs. the particle percentage area, using Statgraphics Centurion XVI. The size distribution of the quartz inclusions of the pottery samples were expressed in the form of box plot which is a graphical description of the distribution of a variable through five-number summaries (Figure 7.10):

- Q0: the smallest observation (sample minimum);
- Q1: lower quartile: 25% of the cumulative frequency;

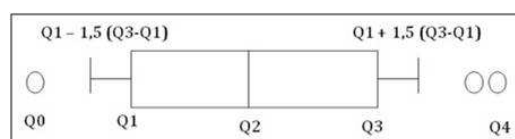


Figure 7.10: Structure of the box plot.

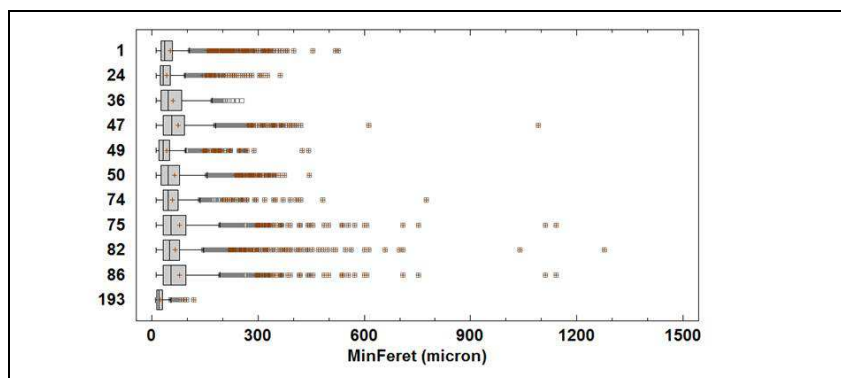


Figure 7.11: Box plot of potteries of the quartz-rich group.

- Q2: median: 50% of the cumulative frequency;
- Q3: upper quartile: 75% of the cumulative frequency;
- Q4: largest observation (sample maximum).

This approach allows also distinguishing the outliers (observation numerically distant from the rest of the data) by identifying data external to the interval defined by $Q1 - 1,5 (Q3 - Q1)$ — $Q1 + 1,5 (Q3 - Q1)$. In Figure 7.11 is shown the box plots referred to the pottery samples of the quartz-rich group. It is possible to identify a similarity between samples 24 and 49 in the distribution of particles, both in the box plot size and in the position and distribution of outliers. Affinities are also recognized between samples 47, 75 and 86 but with less outlier data for the 47. The narrowest interval is observed for sample 193. Apparent discrepancies between the maximum value defined through DIA with respect to the maximum size measured by optical microscopy (as reported in Table 7.8) are due to the choice of the MinFeret as diameter in DIA for comparison with sieving method.

In Figure 7.12 the mean of the MinFeret for each quartz-rich sample is reported. The numbers above on right of the diagram represent the number of particles analyzed for each sample. As previously observed, the potsherds

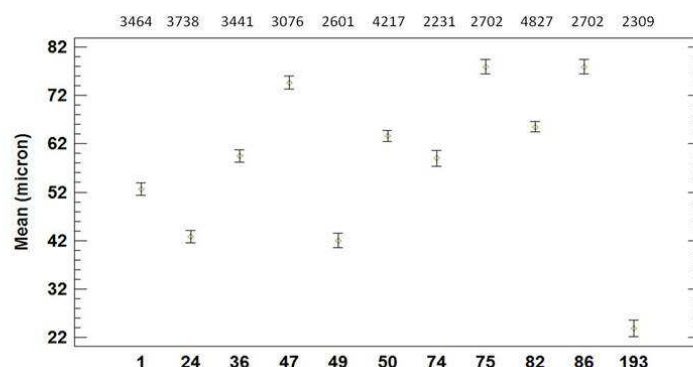


Figure 7.12: Mean of MinFeret for samples of the quartz-rich group with the number of particles analyzed.

show very different grain sizes, preventing from the possibility of distinguish homogeneous groups. It is important to note that the petrographic features observed under the optical microscopy were only qualitative, while by the DIA it was possible to quantify them. Moreover, by the DIA approach it is possible to process a number of particles not achievable by the standard microscopic analysis.

Grain-size distribution was also determined in terms of area percentage as shown in Figure 7.13.

When comparing the size distribution of quartz inclusions vs. their area % for all the studied samples, important differences arise among them (Figure 7.14). More in detail, samples 24, 36, 47 and 193 show a unimodal grain-size distribution, with an asymmetric tail to the largest size for sample 24, and the presence of a unique large crystal about 1100 μm in size in sample 47. All the other samples have a bimodal or polymodal grain-size distribution, and can be divided into two main groups, one comprising samples with an average value of the coarser modes around 500-600 μm (samples 74, 75, 82 and 86) but reaching maximum size around 1 mm, and the other one formed of samples with a general smaller grain-size distribution, with grains always smaller than 600 μm (samples: 1, 49 and 50). Despite these differences, all the samples show at least a mode for values less than 200-300 μm , representing the finer grain-size fraction of quartz, naturally present in the base clay.

Differences in the grain-size distribution are more difficult to detect in the cumulative curves of reported in Figure 7.15, despite the fact that this type of representation largely used in sedimentology and in the grain-size analysis of loose materials.

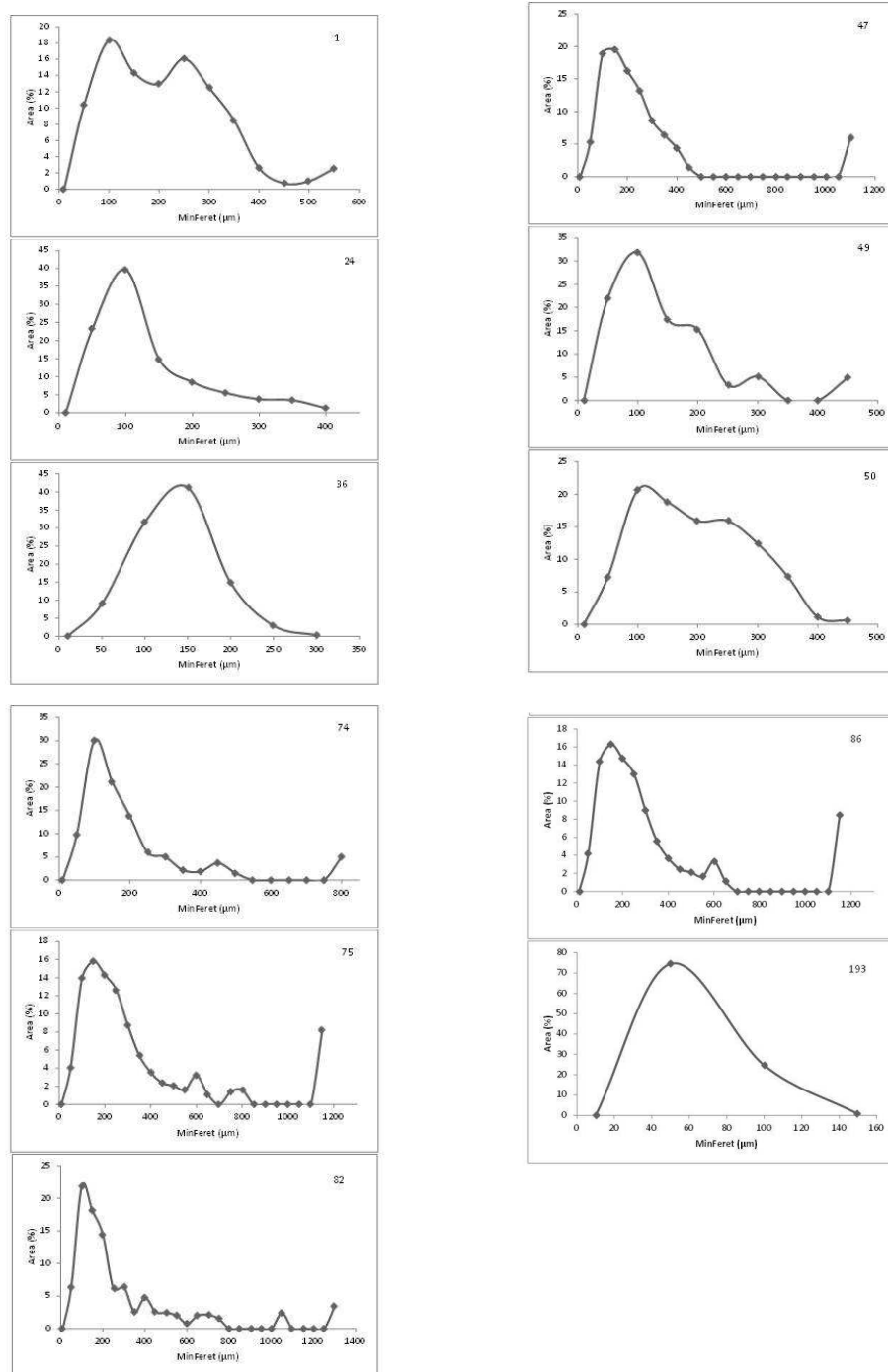


Figure 7.13: Grain size distribution in terms of area percentage for each quartz-rich sample.

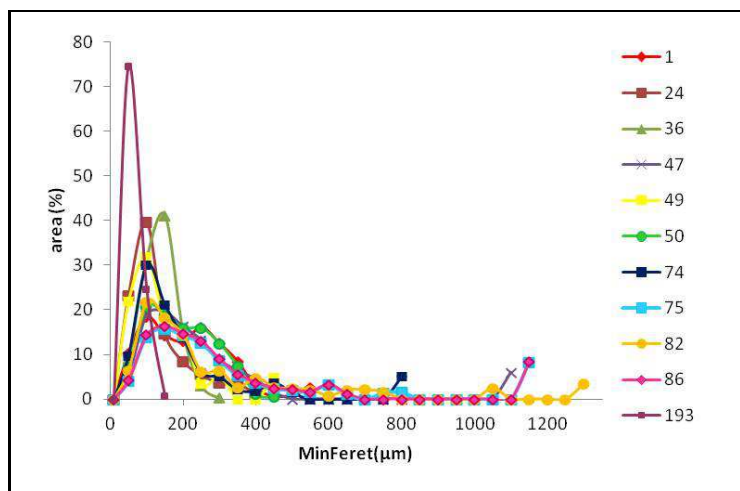


Figure 7.14: Comparison between the grain size distributions in terms of area percentage of quartz-rich samples.

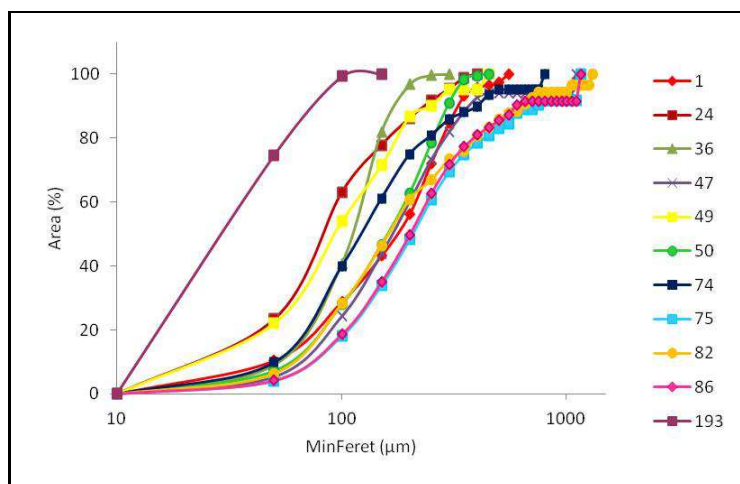


Figure 7.15: Cumulative curves of grain size distributions vs area %.

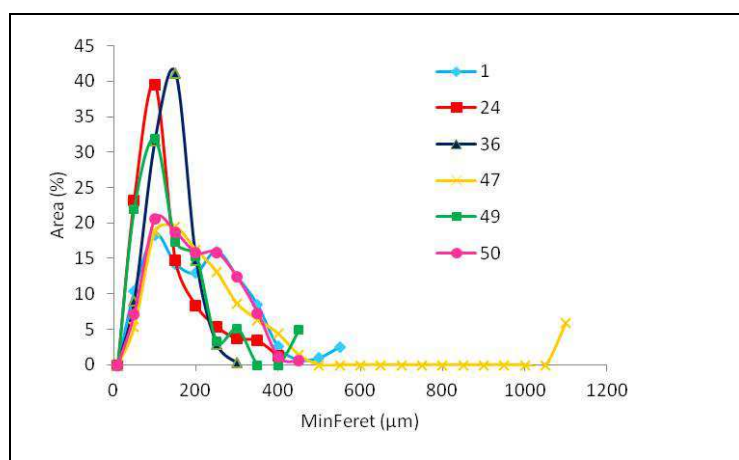


Figure 7.16: Grain size distribution vs area % of Neolithic potsherds.

In general it has been observed that Mesolithic samples have quartz inclusion larger in size than Neolithic ones (Figures 7.16, 7.17). The Neolithic potsherds are characterized by quartz inclusions smaller than $600 \mu\text{m}$ (with the exception of sample 47). Mesolithic samples have inclusions reaching $800 \mu\text{m}$ with some grains exceeding also the mm. Moreover, the Neolithic materials appear more homogeneous than the Mesolithic ones in the distribution of the grain size.

In respect to the data obtained by optical microscopy, the DIA results are in agreement for the majority of the samples (24, 36, 47, 49, 74, 75, 82, and 193). Discrepancies are observed for samples 1, 50 and 86, the grain-size distribution of which was defined as seriate by microscopic analysis and bimodal by DIA.

7.6 EPR

7.6.1 CWEPR

The CWEPR spectra of all the samples were recorded at room temperature. A typical spectrum of pottery is shown in Figure 7.18 where only a large line due to Fe(III) at $g \sim 2$ can be recognized. Iron is always present in pottery but it is not dependent on radiation effect. The broad signal of Fe(III) is thus not useful for dating purpose and its superimposition to the weak lines of radiation induced defects prevents the CWEPR studies on paramagnetic radiation induced defects in ceramic.

Some chemical treatments are proposed with the aim of remove iron from

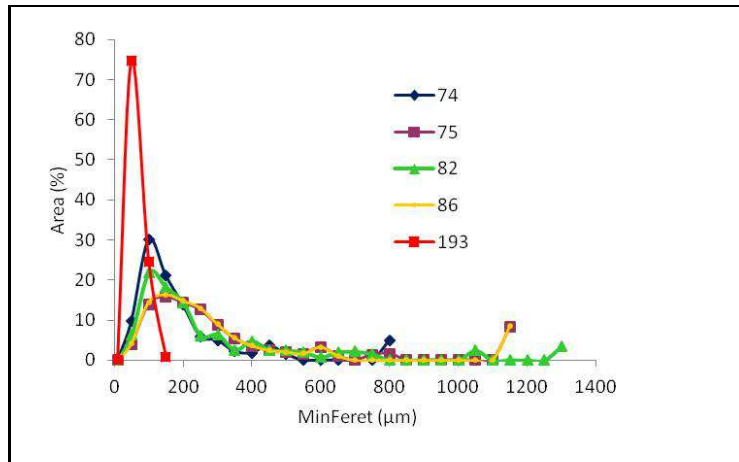


Figure 7.17: Grain size distribution vs area % of Mesolithic potsherds.

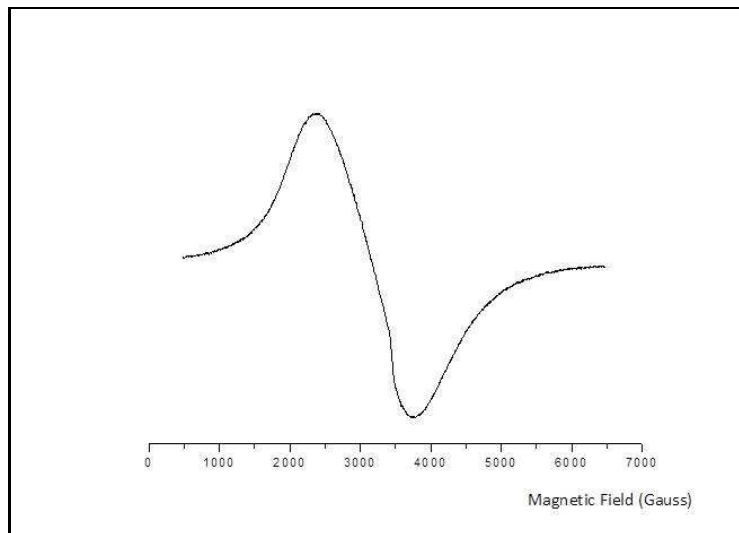


Figure 7.18: CWEPR spectrum of pottery.

pottery [75, 76, 77, 78], but even if reduced, an iron background is always recorded because of the sensitivity of EPR even to small amounts of this ion. The method proposed by Watanabe [79] was applied to sample 67, in order to check if the reduction in iron content would be sufficient. 700 mg of sample were immersed in 37% HCl for 40 minutes then washed with distilled water. Not all the iron oxide reacts with the acid to form iron chloride. For this reason 65% HNO₃ was added and H₂O₂ was used to eliminate soluble compounds generated during the chemical treatment. The sample was washed in distilled water to remove acid matrixes. Although the procedure is simple, cheap and quick in comparison to other methods as heavy liquids separation, it was not sufficiently effective. The CW EPR spectrum of the sample after the treatment shows a reduction of the iron background but it is still strong enough to prevent the identification of other signals of interest. Moreover, a considerable amount of sample is required for the treatment and this is a limiting factor for archaeological applications.

7.6.2 Echo Detected EPR

The pulsed technique called EDEPR allows recording the signal due to of the electron spin echo (ESE) as a function of the magnetic field. The resulting spectrum is similar to the one obtained with the CW method but it is possible to record the signals of species with relaxation times long enough for the acquisition of the ESE. In this way, the contribution of species characterized by short relaxation times, whose ESE decays to zero before the acquisition, is eliminated. The radiation induced defects, with their long relaxation times, are thus observed while the signals of transition metal ions having short relaxation times are eliminated. Ikeya [80] suggested to eliminate the disturbing transition metal ions signals in geological samples using EDEPR. The limit of the detectable dose depends on the sensitivity of the spectrometer and the sensitivity of pulse EPR spectrometer is lower than CW spectrometer. For this reason the technique is usually applied in geological dating, where the doses absorbed by the samples are of several orders of magnitude higher than the ones of archaeological material. The method was here tested on ceramic by recording the EDEPR spectra of all the Sudanese samples, which are among the most ancient ceramic found at archaeological excavations. The procedure was successfully applied for the iron background removal from the spectra. A natural signal attributed to radiation induced defect centres was identified in seven samples (1, 24, 36, 47, 49, 50 and 193). These samples were then artificial irradiated, in order to check the dependence of the signal from the dose, which is the first requirement for dating application. Five aliquots for each sample were collected by crushing the sample and sieving

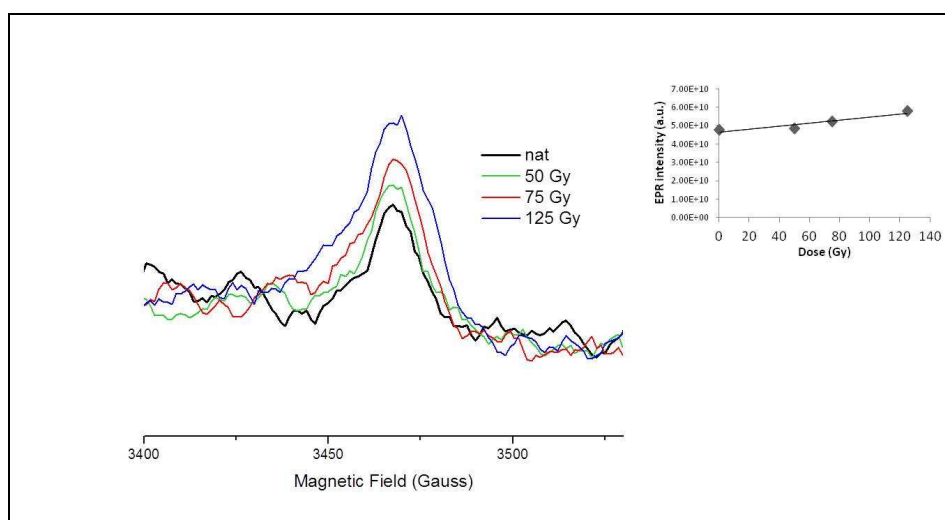


Figure 7.19: EDEPR of natural and beta irradiated aliquots of sample 1 (left) and growth curve (right).

the fraction corresponding to the quartz grain size established on the basis of the petrographic analysis. The doses provided for each samples were of 25, 50, 75, 100 and 125 Gy with a beta $^{90}\text{Sr}/^{90}\text{Y}$ source (dose rate of 0.14 Gy/sec). In Figure 7.19 an example of the EDEPR spectra recorded for natural and irradiated aliquots is reported. For each spectrum, the intensity was calculated as the integral under the EDEPR spectrum, after baseline correction. The EDEPR intensity increases linearly with the dose, as it is shown in the growth curve.

However, the extrapolation provides equivalent doses not in agreement with those estimated by luminescence techniques. A strong overestimation was observed, with results not compatible with dating. Possible causes of the phenomenon observed were taken into account. First of all, the presence of a paramagnetic background was checked, in order to verify if the radiation induced signal was superimposed to lines of different nature. An annealing test was performed, heating a small amount of a sample up to 450°C for 15 minutes. The EDEPR spectrum recorded after this treatment does not show any signal, proving that the overestimation of the equivalent dose is not due to a paramagnetic background. The disappearance of the signal excluded the possibility of a contribution by paramagnetic defects not dose dependent. Another test was performed in order to verify the possible influence of crushing in producing surface paramagnetic defects summing up to the radiation induced centers. The natural and the artificial irradiated aliquots

of the sample 1 were subjected to a chemical etching with HCl. EDEPR spectra were then recorded and compared to the ones collected before the treatment. Changes in the intensity of the signals were not observed and the possibility of paramagnetic centres produced by the mechanical sample preparation procedure was ruled out. The attention was then focused on the irradiation source. A radiation response model for EPR dating is not well developed because of the similarity with the luminescence techniques [81]. Usually the same models are applied, even if the efficiency of radiation sources is different in producing luminescence and paramagnetic centres. For this reason samples were gamma irradiated with the same doses of beta artificial irradiation. As it can be seen in Figure 7.20, a behavior similar to the beta irradiated samples is observed. The gamma and the beta artificial irradiation induce the same type of defect centre. The equivalent doses obtained by extrapolation from the growth curve are not reliable for dating the potsherds. These results show that the EDEPR equivalent dose is overestimated not depending on the type of irradiation, leading to an overestimation of the age. This is not completely unexpected, since in literature [82] it has been shown that OSL measurements on sand-sized quartz (63-90 μm) lead to 20-70% age overestimation with respect to OSL measurements on the fine fraction (4-11 μm). This discrepancy is not understood, since the SAR protocol was proven to be suitable for both the fractions. Constantin analyzed the OSL properties of different grain sizes of quartz, observing different saturation characteristics [83]. The saturation doses of the fine grain fraction were found to be higher than the ones of the coarser material. The equivalent doses obtained for each fraction are consistent and the behavior reported by Timar is not observed in these samples. Even if the phenomenon is not completely understood, it seems that the grain size plays an important role in dosimetric studies. The EDEPR spectra were acquired on a granulometric selection according to petrographic analysis (Table 7.8, samples 1 and 50: $> 200 \mu\text{m}$, samples 24 and 36: 80-150 μm , sample 49: 80-200 μm , sample 74: 100-200 μm , sample 193: 75-125 μm) and this coarse selection could be well responsible for the strong overestimation of the equivalent dose.

The identification of defects in TL studies is not possible since the only characteristic of an emission peak is its temperature, related to the trap depth and not to the type of the centre. EPR is in principle a suitable tool for the identification of point defect in quartz even if the correlation with the luminescence centres could be difficult. The origin of the radiation-induced defects observed in Echo Detected EPR is not completely clear. We have proven that the center(s) occur(s) in quartz (see section 2.5.3). A good simulation of the EDEPR (Figure 7.21, red line) is obtained combining the simulation of a peroxy center (blue line) with two centers E1': the standard E' (green line)

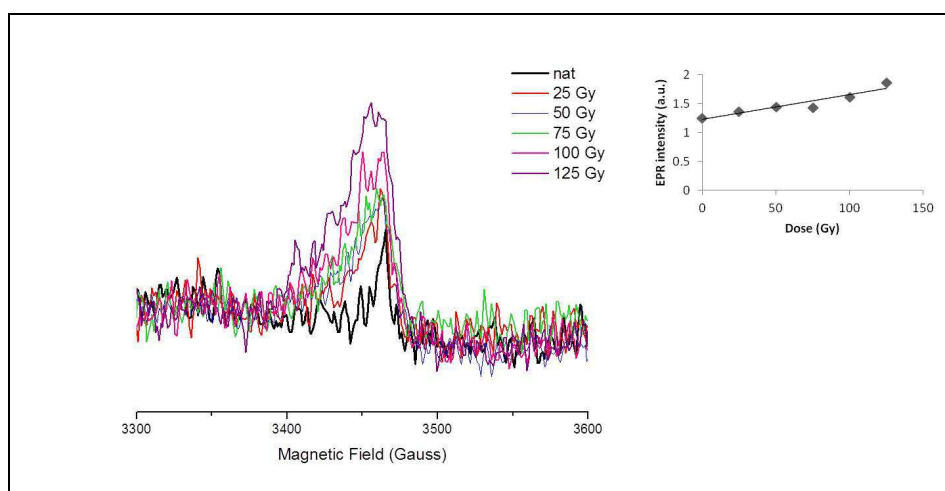


Figure 7.20: EDEPR of natural and gamma irradiated aliquots of sample 1 (left) and growth curve (right).

and the E'1-Ge(III) center (olive line). The ratio is 10:1:1, i.e. about 10 peroxy centers are combined with one standard E'1 center and one E'1-Ge(III) center. The presence of peroxy and E'1 centers is reasonable, because these centers are produced together during irradiation. Although the simulation is good, it is more likely that many slightly different E'1 centers are produced, not only two, and therefore the true signal is probably the combination of peroxy centers with a distribution of E'1 perturbed centers. Furthermore, the simulation does not match well the low-field part of the EDEPR spectrum. However, the low-field part changes a lot from sample to sample, whereas the high-field part is pretty well conserved. This suggests that the low-field part is contributed by minor paramagnetic radiation-induced species that are different in the different samples. Although the simulation is good, more investigations are necessary to establish on a firm ground the origin of the EDEPR signal.

7.7 Comparison between EDEPR spectra and petrographic analysis

The EDEPR signal was detected only in some of the studied samples. Considering the data reported in Table 7.11, it arises that the presence of a natural EDEPR signal is not direct related to the age, as expected. Instead, it is possible to find a relationship between the grain size and the EPR signals,

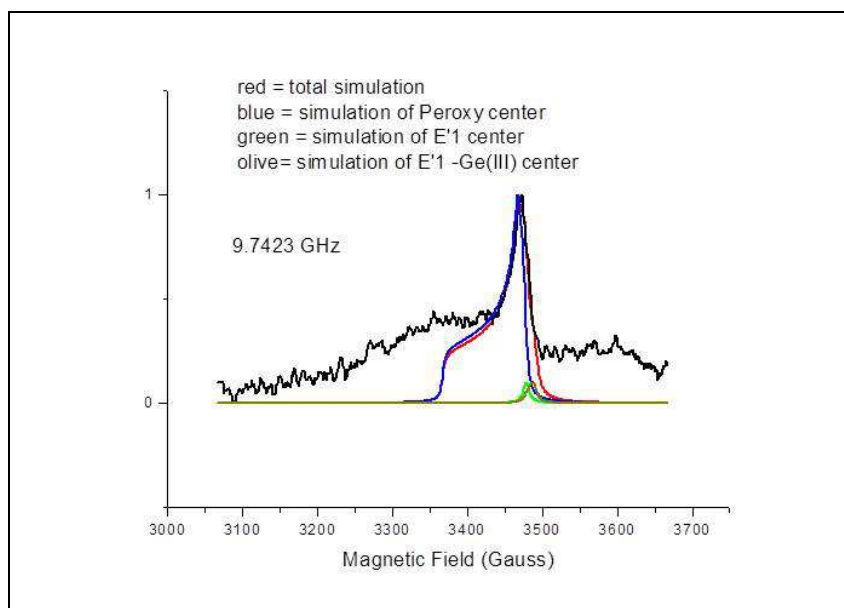


Figure 7.21: Simulation of EDEPR spectrum of sample 1, irradiated beta 125 Gy.

which were recorded just for potteries with a small size of quartz inclusions.

The correlation between natural EDEPR signal and quartz grain size was proven also by sieving two samples without natural signal (82 and 86) and selecting the fine fraction. In Figure 7.22 the spectra obtained measuring the whole samples in the magnetic field region in which the signal is expected do not show any line. In the spectra collected only on the fine grain size fraction (lower than $300\ \mu\text{m}$) of the same samples, it is possible to record natural EDEPR signal, as in the case of the other potsherds characterized by fine-grained quartz inclusions.

This difference in the palaeodose between fine and coarse fraction is known in literature and a theory was proposed to explain the difference [84]. The theory has been revised for adapting it to Monte-Carlo simulations on inclusions [85]. According to the theory, assuming that the quartz grain does not contain radionuclides, the palaeodose is related to the grain size by the relation:

$$D = (1 - \phi) \cdot D_m \quad (7.1)$$

where D_m is the infinite-medium dose of the matrix, D is the dose received by the quartz grain (the inclusion), and ϕ is the ratio between the average beta-dose in the inclusion D_i and the beta-dose which the grain would receive if it were infinite-size (D_{inf}). This ratio ϕ depends on the grain size, rang-

Table 7.11: Presence of the EDEPR signal related to quartz grain size. First group: Neolithic samples (1-50), second group Mesolithic samples (67-193).

Sample ID	Max grain size (μm)	Mean grain size (μm)	MinFert (mean) (μm)	EDEPR signal
1	800	200	53	•
24	350	100	43	•
36	300	100	59	•
47	1800	350-1000	75	
49	600	80-200	42	•
50	600	300	64	•
67	1300	450		
74	1100	150-400	59	•
75	2000	350-800	78	
82	1400	200-700	65	
86	900	350	78	
193	200	80	24	•

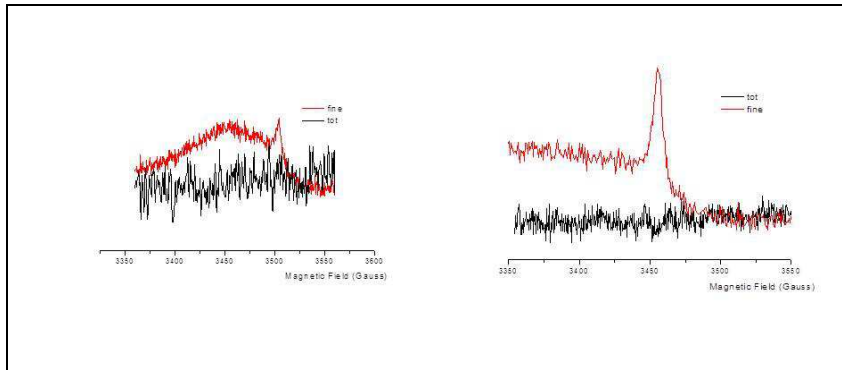


Figure 7.22: EDEPR spectra of samples 82 (left) and 86 (right) of the whole material and the fine fraction.

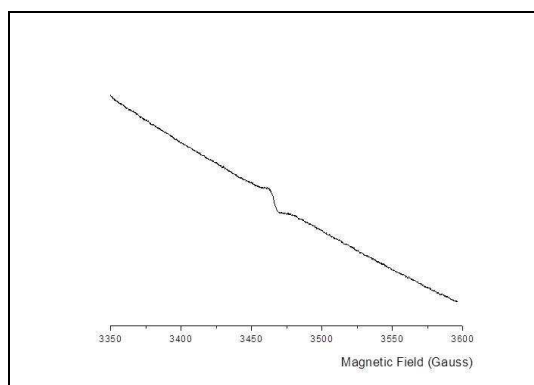


Figure 7.23: CWEPR spectrum of sample 193.

ing from 0 (zero-size inclusion) up to 1 (infinite-size inclusion). The above relationship shows that small grains tend to receive a larger palaeodose than bigger grains, and this is in agreement with our observations. The sample 193 is the only one showing a CWEPR signal and it is the one with the smallest grain size temper (Figure 7.23).

XRF analyses were performed for all the potsherds in order to verify if differences in the bulk composition could have a role in the generation of the EDEPR signal. The chemical composition of the samples (Table 7.12) does not justify the distinction between samples with and without EDEPR signal which can be thus related only to the quartz grain size.

7.8 Quartz extracted from pottery matrix

The separation of quartz either for luminescence and EPR dating is a time consuming procedure and it is not always feasible when working on archaeological objects. The procedures of separation are borrowed from geology, where the amount of starting material is not a critical factor. For archaeological studies an amount of material of tents of grams for a mineral extraction may not be available. Moreover it is a destructive approach, which is also a limiting factor. Usually the heavy liquid separation is performed in OSL dating, based on the different density of minerals. For quartz extraction, sodium polytungstate is used, but this substance is expensive and hazardous to human health and environment [79]. It is important to note that for OSL application the mineral separation has to be done in subdued red light to avoid bleaching effects, complicating the whole procedure of sample preparation. In this work, two samples were selected for quartz extraction. The

Table 7.12: Chemical composition of potsherds determined by XRF analysis.

	1	24	36	47	49	50	67	74	75	82	86	193
SiO ₂	65.18	64.97	73.12	76.61	63.70	71.82	64.26	70.64	76.70	74.64	75.58	68.61
TiO ₂	1.48	1.59	1.46	1.03	1.55	1.24	0.76	1.24	0.97	1.04	1.00	1.36
Al ₂ O ₃	16.49	17.02	13.51	13.12	17.67	13.16	19.93	13.35	11.07	11.24	11.57	14.43
Fe ₂ O ₃	9.85	9.58	6.38	4.82	10.10	8.61	5.78	7.35	4.87	8.41	6.08	7.52
MO	0.23	0.14	0.20	0.04	0.22	0.22	0.17	0.15	0.09	0.13	0.15	0.11
MgO	1.18	1.35	0.86	0.73	1.19	0.83	0.80	1.25	1.31	0.83	1.08	1.19
CaO	2.42	1.99	1.81	1.93	2.08	1.59	1.30	2.31	2.32	1.07	1.32	2.82
Na ₂ O	0.72	0.79	0.64	0.24	1.66	0.62	0.87	1.45	1.02	1.20	1.28	1.06
K ₂ O	1.59	1.53	1.41	0.60	1.40	1.08	4.52	1.43	0.90	0.44	1.05	1.84
P ₂ O ₅	0.31	0.23	0.21	0.06	0.25	0.30	0.23	0.18	0.12	0.33	0.22	0.09
tot	99.45	99.19	99.60	99.18	99.82	99.47	98.62	99.35	99.37	99.33	99.33	99.08

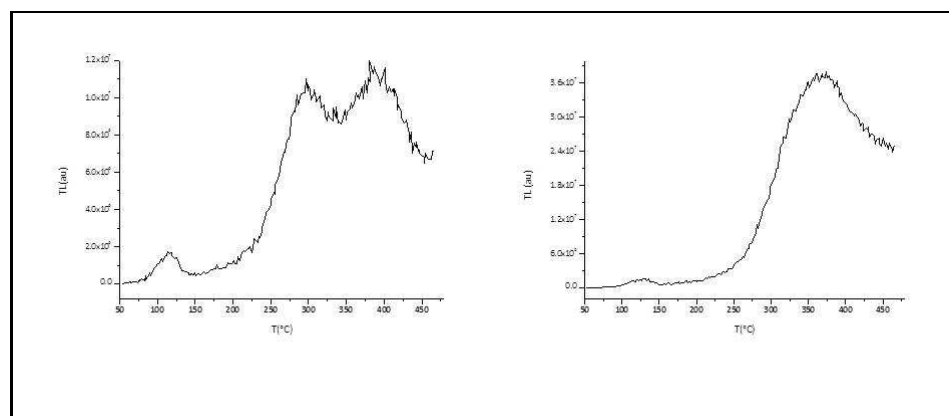


Figure 7.24: TL glow curves of quartz extracted from pottery 82 (left) and 24 (right).

amount of the separated mineral was not sufficient for applying the complete dating protocol but measurements were performed with the aim of a better comprehension of phenomena involved in the generation of EPR and luminescence signals. The surface of the sample 82, representing the group of pottery with larger quartz grains, was removed by means of a drill and the bulk was crashed to induce the mechanical separation between the matrix and the inclusions. The quartz separation was performed by hand-picking under a stereo microscope. The sample 24 was treated as the previous one, but the small quartz grain size prevented from the hand-picking separation. The powdered sample was washed in order to remove the very thin fraction and sieved to concentrate the quartz inclusions. A Frantz magnetic separator allowed the division of the quartz from the matrix according to their different magnetic susceptibility. In Figure 7.24 natural TL glow curve of the quartz extracted from sample 82 is shown. The grains were distributed in a monolayer onto a stainless steel disc without any grain size selection. The typical peaks of quartz at 110°C, 270°C and 375°C can be recognized, while in the natural TL of the fine grain correspondent sample it was not possible.

Because of the difficulty of extraction of quartz from the sample 24, the TL glow curve in Figure 7.24 is related to a fraction of sample with a high concentration of the mineral but with a residual fraction of the matrix. Here it can be identified only the main peak at 375°C while other peaks are not resolved probably due to spurious signals interfering with quartz emission. In the CWEPR spectra of the fractions extracted from the two samples only the iron signal is recognized and the separation was not sufficient to eliminate the background. The EDEPR spectra of quartz concentration of these two

samples do not show significant difference from the one of the whole pottery, proving that the clay matrix and the minerals of the temper do not influence the EPR signal of radiation induced defect in quartz. This is important since the quartz separation is thus not necessary, reducing the amount of material required for measurements and the time of sample preparation.

Conclusions

A comparative study of dosimetric dating techniques applied to archaeological pottery has been carried out. The selection of samples of known age characterized by quartz temper was a necessary premise for the dating approach. Three techniques (TL, OSL and EPR) were tested by applying two protocols (MAAD and SAR). Luminescence techniques allowed obtaining ages of the two groups of potsherds from Mesolithic and Neolithic periods in accordance with the radiocarbon dating of the layer of provenance. The additive procedure was the less satisfying and it is not recommended for dating prehistoric materials. The potential of the SAR protocol over the conventional MAAD was proven. Although the achievable accuracy needs more experimental testing, the SAR protocol is promising for those cases where the amount of sample is restricted. In particular, OSL can be used for dating heated materials as potteries, when they are characterized by a quartz-rich temper, without needing any mineral separation. This is an important result since, differently from geology, the availability of dating material in archaeology is very limited. EDEPR appeared to be a valid tool in spotting radiation induced defects in ceramic without any chemical treatment of the sample and with the possibility of performing several measurements on the same aliquot of material. A natural signal was isolated from potsherds characterized by quartz temper with a fine grain size and not, as expected, from the Mesolithic ones. The dose dependence of the signal was proven by beta and gamma irradiation but it was not possible to obtain meaningful equivalent doses for dating purposes. However, this was the first attempt to date archaeological pottery by means of EDEPR and even if further investigations are needed, these results are encouraging, also because the extraction of quartz from the matrix is not necessary. The dosimetric dating methods are a powerful tool despite the low precision in all the cases of absence of suitable materials for radiocarbon dating which is the most widely used technique. They are able

to give information about the ceramic itself and not about the related materials, improving the chronological framework of the samples. The approach adopted in this work could be a first step of a research project concerning the chronological studies of prehistoric pottery.

Bibliography

- [1] Wagner, G.A. 1998, Age determination of young rocks and artifacts – Physical and chemical clocks in Quaternary Geology and Archaeology, Springer, Berlin
- [2] Ikeya, M. 1993, New Applications of Electron Spin Resonance - Dating, Dosimetry and Microscopy, World Scientific, Singapore
- [3] Aitken, M. J. 1985, Thermoluminescence Dating, London: Academic
- [4] Galloway, R.B., 2001. Luminescence dating: Limitation to accuracy attainable, *Journal of Radioanalytical and Nuclear Chemistry* (247-3) 679-683
- [5] Zink, A.J.C. et al., 2011. Direct OSL dating of Iron Age pottery from South Africa – Preliminary dosimetry investigations, *Quaternary Geochronology* (8) 1-9.
- [6] Rudra, J.K. Beall Fowler, W., 1986. Oxygen vacancy and the E'1 center in crystalline SiO₂, *Physical Review B* (35-15) 8223-8230
- [7] Preusser, F. et al., 2009. Quartz as a natural luminescence dosimeter, *Earth-Science Reviews* (97) 184–214
- [8] Wintle, A.G. 1997. Luminescence dating: laboratory procedures and protocols , *Radiation Measurements* (27) 769-817
- [9] Bailey, R.M. et al., 1997. Partial bleaching and the decay form characteristics of quartz osl, *Radiation Measurements* (27- 2) 123-136
- [10] Rink, W.J., 1997. Electron Spin Resonance (ESR) dating and ESR applications in Quaternary science and archaeometry, *Radiation Measurements* (27- 5) 975-1025

- [11] Jani, M.G. et al., 1982. Further characterization of the E'1 center in crystalline SiO₂, *Physical Review B* (27-4) 2285-2293
- [12] Toyoda, S., Schwarz, H.P., 1997. Counterfeit E'1 signal in quartz. *Radiation Measurements* (27) 59-66
- [13] Feathers J. K., 2003, Use of luminescence dating in archaeology *Meas. Sci. Technol.* (14) 1493–1509
- [14] Huntley, D.J., et al., 1985 . Optical dating of sediments. *Nature* (313) 105-7
- [15] Murray, A.S., Wintle, A.G., 1998. Factors controlling the shape of the OSL decay curve in quartz. *Radiat. Meas.* (29) 65-79
- [16] Wintle, A.G., Murray, A.S., 2006. A review of quartz optically stimulated luminescence characteristics and their relevance in single-aliquot regeneration dating protocols, *Radiation Measurements* (41) 369-391
- [17] Bailiff, I.K., Holland, N., 2000. Dating bricks of the last two millennia from Newcastle upon Tyne: a preliminary study, *Radiation Measurements* (32) 615-619
- [18] Michael, C.T., Zacharias, N., 2006. Equivalent dose (palaeodose) estimation in thermoluminescence dating using a single aliquot of polymineral fine grains. *Radiation Protection Dosimetry* (119) 458-461
- [19] Hong , D.G. et al., 2006. Equivalent dose determination of single aliquot regenerative-dose (SAR) protocol using thermoluminescence on heated quartz, *Nuclear Instruments and Methods in Physics Research B* (243) 174-178
- [20] Shelmann G. et al. 2008. Electron spin resonance (ESR) dating of Quaternary materials, *Eiszeitalter und Gegenwart Quaternary Science Journal* (57/1-2) 150-178
- [21] Huntley, D.J., Lamothe, M., 2001. Ubiquity of anomalous fading in K-feldspar and the measurements and corrections for it in optical dating. *Can.J.Earth Sci.* (38) 1093-1106
- [22] Bailiff, I.K., 2007. Methodological developments in the luminescence dating of brick from English late-medieval and post-medieval buildings, *Archaeometry* (49) 827-851

- [23] Barnett, S.M., 2000. Luminescence dating of pottery from later prehistoric Britain, *Archaeometry* (42-2) 431-457
- [24] Leung, P.L. et al., 2005. The preliminary application of OSL in comparison with TL for authentication of ancient Chinese bricks, *Radiation Measurements* (40) 1- 4
- [25] Oke, G., Yurdatapan E., 2000. Optically stimulated luminescence dating of pottery from Turkey, *Talanta* (53) 115-119
- [26] Thomas, P.J. et al., 2008. Optically stimulated luminescence dating of heated materials using single-aliquot regenerative-dose procedure: a feasibility study using archaeological artefacts from India, *Journal of Archaeological Science* (35) 781-790
- [27] Tite, M.S., 2008. Ceramic production, provenance and use - a review, *Archaeometry* (50) 216-231
- [28] Rice, P.M., 1999. On the Origins of Pottery, *Journal of Archaeological Method and Theory* (6-1) 1-54
- [29] Budja, M. 2006. The transition to farming and the ceramic trajectories in Western Eurasia: from ceramic figurines to vessels. *Documenta Praehistorica* (XXXIII) 183-201
- [30] Verpoorte, 2001. Places of Art, traces of Fire. *Archaeological Studies Leiden University* 8 (*Dolnì Vestonice Studies* 6).
- [31] Wu, X. et al., 2012. Early Pottery at 20,000 years ago in Xianrendong Cave, China, *Science* (336) 1696-1700
- [32] Shelach, G., 2012. On the invention of Pottery, *Science* (336) 1644-1655
- [33] Stott, A.W., et al., 2003. Direct dating of archaeological pottery by compound-specific ^{14}C analysis of preserved lipids. *Anal.Chem.* (75) 5037-5045
- [34] Wilson, M.A. et al., 2009. Dating fired-clay ceramics using long-term power law rehydroxylation kinetics, *Proc. R. Soc.* (465) 2407-2415
- [35] Bonsall, C. et al., 2002. Direct dating of Neolithic pottery: progress and prospects. *Documenta Praehistorica* (XXIX, Issue: Neolithic Studies 9) 47-59

- [36] Salvatori, S., 2012. Disclosing Archaeological Complexity of the Khartoum Mesolithic: New Data at the Site and Regional Level, *African Archaeological Review* (29-4) 399-472
- [37] Salvatori, S., Usai, D. 2008. R12 and the Neolithic of Sudan. New perspectives in S. Salvatori and D. Usai (Eds.), *A Neolithic cemetery in the northern Dongola Reach (Sudan): Excavation at Site R12 (9-18)*. London: The Sudan Archaeological Research Society Publications.
- [38] Usai, D., 2005. The Mesolithic and Neolithic periods in the Sudanese Nile valley: problems and perspectives, *Africa* (LX,3-4) 544-554
- [39] Kuzmin, Y.V., 2006. Chronology of the earliest pottery in East Asia: progress and pitfalls, *Antiquity* (80) 362-371
- [40] Aikens, C. M. (1995). First in the world: The Jomon pottery of early Japan In W. Barnett and J. Hopes (Eds.), *The emergence of pottery. Technology and innovations in ancient societies (11-22)*. Washington: Smithsonian Institution Press.
- [41] Harris, V. (1997). Jomon pottery in ancient Japan in I. Freestone and D. Gaimster (Eds.), *Pottery in the making (world ceramic traditions) (20-25)*. London: British Museum.
- [42] Jesse, F., 2010. Early pottery in Northern Africa, *Journal of African Archaeology* (8) 219-238
- [43] Usai, D., 2004. Early Khartoum and related groups. In T. Kendall (Ed) *Proceedings of the Ninth International Conference of Nubian Studies, Museum of Fine Arts and Northeastern University, Boston, August 20-26, 1998 (419-435)*. Department of African-American Studies Northeastern University Boston.
- [44] Salvatori, S. et al., 2011. Mesolithic site formation and palaeoenvironment along the White Nile (Central Sudan), *African Archaeological Review* (28-3) 177-211
- [45] Salvatori, S. and Usai, D., 2008. El Salha Project 2005: New Khartoum Mesolithic sites from Central Sudan, *Kush* (19) 87-96
- [46] Usai, D. (2003). The Is.I.A.O. El Salha Project. *Kush*, 18, 173-182
- [47] Usai, D., 2006. The El Salha project, Sudan in *Actes of the XIVth Congress of the U.I.S.P.P., Liege, Belgium, 28 September 2001, general Sessions and Posters (207-212)*. Oxford: BAR International Series 1522

- [48] Usai, D., in press. Recent advances in understanding the Prehistory of Central Sudan in J. R. Anderson and D. A. Welsby (Eds.), *Proceedings of the 12th International Conference of Nubian Studies*. Leuven: Peeter
- [49] Usai, D., Salvatori, S., 2002. The IsIAO El-Salha archaeological project, Sudan and Nubia (6) 67-72
- [50] Usai, D. Salvatori, S., 2005. The IsIAO Archaeological Project in the El Salha area (Omdurman South, Sudan): results and perspectives, *Africa* (LX,3-4) 474-493
- [51] Zerboni, A. 2011. Micromorphology reveals in situ Mesolithic living floors and archaeological features in multiphase sites in Central Sudan, *Geoarchaeology: an international journal* (26-3) 365-391
- [52] Lario, J. et al., 1997. Palaeoenvironmental evolution of the Blue Nile (Central Sudan) during the early and mid-Holocene (Mesolithic-Neolithic transition), *Quat. Sci. Rev.* (16) 583-588
- [53] Cohen, M.N., 1977. *The Food Crisis in Prehistory. Overpopulation and the Origins of Agriculture*. Yale University Press, New Haven
- [54] Usai, D., 2006b. Early and Middle Holocene cultural change in the Nile Valley (Egypt and Sudan) in *Actes of the XIVth Congress of the U.I.S.P.P., Liege, Belgium, 2-8 September 2001, general Sessions and Posters* (93-99). Oxford: BAR International Series 1522
- [55] Usai, D., 2007. Geographic Overviews, Africa (North): Nubia (49-56) in D.M. Pearsall (Ed.) *Encyclopedia of Archaeology*. New York: Academic Press
- [56] Gautier, A., 1983. Animal life along the prehistoric Nile: the evidence from Saggai 1 and Geili (Sudan), *Orini* (12) 50-115
- [57] Gautier, A., 2007. Animal domestication in North Africa in M. Bollig, O. Bubenzer, R. Voelsang and H. P. Wotzka, (Eds.), *Aridity, change and conflict in Africa* (75-89). Koln: Heinrich-Barth-Institute
- [58] Gautier, A., 2007. Animal domestication in North Africa in M. Bollig, O. Bubenzer, R. Vogelsang and H. P. Wotzka, (Eds.), *Aridity, change and conflict in Africa* (75-89). Koln: Heinrich-Barth-Institute
- [59] Williams, M., 2009. Late Pleistocene and Holocene environments in the Nile basin, *Global and Planetary Change* (69) 115

- [60] Williams, M. A. J., 2012. River sediments, *Phil. Trans. R. Soc. A* (370) 2093-2122
- [61] Williams, M. A. J., Talbot, M.R., 2009. Late Quaternary Environments in the Nile basin in H. J. Dumont (Ed), *The Nile. Origin, Environments, Limnology and Human Use* (Monographiae Biologicae, Volume 89)(61-72). Dordrecht: Springer
- [62] Williams M.A.J., Williams, F.M., Duller, G.A.T., Munro, R.N., El Tome, O.A.M., Barrows, T.T., Macklin, M., Woodward, J., Talbot, M.R., Haberlah, D. and Fluin, J. 2010. Late Quaternary floods and droughts in the Nile valley, Sudan: new evidence from optically stimulated luminescence and AMS radiocarbon dating, *Quaternary Science Reviews* (29) 1116-1137
- [63] Salvatori, S., Usai, D., 2007. The oldest representation of a Nile boat, *Antiquity* (81,314). <http://www.antiquity.ac.uk/projgall/usai/index.html>
- [64] Rice, M.P., 1987. Pottery analysis. 2005 edn. USA: The University of Chicago Press
- [65] Veniale, F., 1990. Modern techniques of analysis applied to ancient ceramics, Advanced Workshop, Analytical Methodologies for the Investigation of Damaged Stones, Pavia (Italy), 14-12 September 1990
- [66] Govindaraju, K., 1994, 1994 compilation of working values and sample description for 383 geostandards , *Geostandards Newsletter* (18) 1-158
- [67] Whitbread, I.K., 1995. Greek Transport Amphorae: A Petrological and Archaeological Study, Fitch Laboratory Occasional Paper (4) British School at Athens.
- [68] Baccelle, L., Bosellini, A., 1965. Diagrammi per la stima visiva della composizione percentuale nelle rocce sedimentarie. *Ann. Univ. Ferrara* (N.S.) (9) 59-62.
- [69] Kemp R.A., 1985. Soil micromorphology and the Quaternary. *Quaternary Research Association Guide* (2) Cambridge.
- [70] Muller, G., 1964. Methoden der Sediment-Untersuchung. *Sedimentologie*, Teil I.E. Schweizerbart'sche Verlagsbuchhandlung, Stuttgart 303
- [71] Middleton, A.P., et al., 1985. Textural analysis of ceramic thin sections: evaluation of grain sampling procedures. *Archaeometry*, 27(1) 64-74.

- [72] Reedy, C.L., 2008. Thin-section petrography of stone and ceramic cultural materials. London: Archetype Publications Ltd.
- [73] Reedy, C.L., 2006. Review of digital image analysis of petrographic thin sections in conservation research. *Journal of*
- [74] Stoltman, J.B., 1989. A quantitative approach to the petrographic analysis of ceramic thin sections. *American Antiquity*, 54(1) 147-160
- [75] Dobosz, B., Krzyminiewsky, R., 2007. Linear transformation of EPR spectra as a method proposed for improving identification of paramagnetic species in ceramic. *Appl. Radiat. Isot.* (65) 392-396
- [76] Bartoll, J., Ikeya, M., 1997. ESR dating of pottery: a trial. *Appl. Radiat. Isot.* 48, 981-984
- [77] Bensimon, Y. et al., 2000. Nature and thermal stability of paramagnetic defects in natural clay: a study by electron spin resonance. *J.Phys. Chem. Solids* 61, 1623-1632
- [78] Campos, S.S. et al., 2011. Proposal for a new method to extract quartz from materials used for retrospective dosimetry and dating. *Radiat. Measur.* 46, 1509-1513
- [79] Watanabe, S. et al. 2008. Chemical process to separate iron oxides particles in pottery sample for EPR dating. *Spectrochim. Acta Part A: Mol. Biomol. Spectros.* 71(4) 1261-1265
- [80] Ikeya, M., 2004, ESR Dating, Dosimetry and Microscopy for Terrestrial and Planetary Materials, *Electron Paramagnetic Resonance* (19) The Royal Society of Chemistry
- [81] Jonas, M., 1997, Concepts and methods of ESR dating, *Radiat. Meas.* (27) 943-973
- [82] Timar-Gabor, A., Vandenberghe, D.A.G., Vasiliniuc, S., Panaoitu, C.E., Panaiotu, C.G., Dimofte, D., Cosma, C., 2011. Optical dating of Romanian loess a comparison between silt-sized and sand-sized quartz. *Quaternary International* 240, 62e70.
- [83] Constantin, D. et al., 2012. SAR-OSL dating of different grain-sized quartz from a sedimentary section in southern Romania interbedding the Campanian Ignimbrite /Y5 ash layer. *Quat. Geoch.*(10) 81-86

- [84] Mejdahl, V., 1979. Thermoluminescence dating: beta dose attenuation in quartz grains. *Archaeometry* (21) 61-73
- [85] Fain, J. et al., 1999. Luminescence and ESR dating Beta-dose attenuation for various grain shapes calculated by a Monte-Carlo method. *Quat. Geoch.*(18) 231-234
- [86] Wintle, A.G.,2008. Luminescence dating: where it has been and where it is going, *Boreas* (37) 471-482.